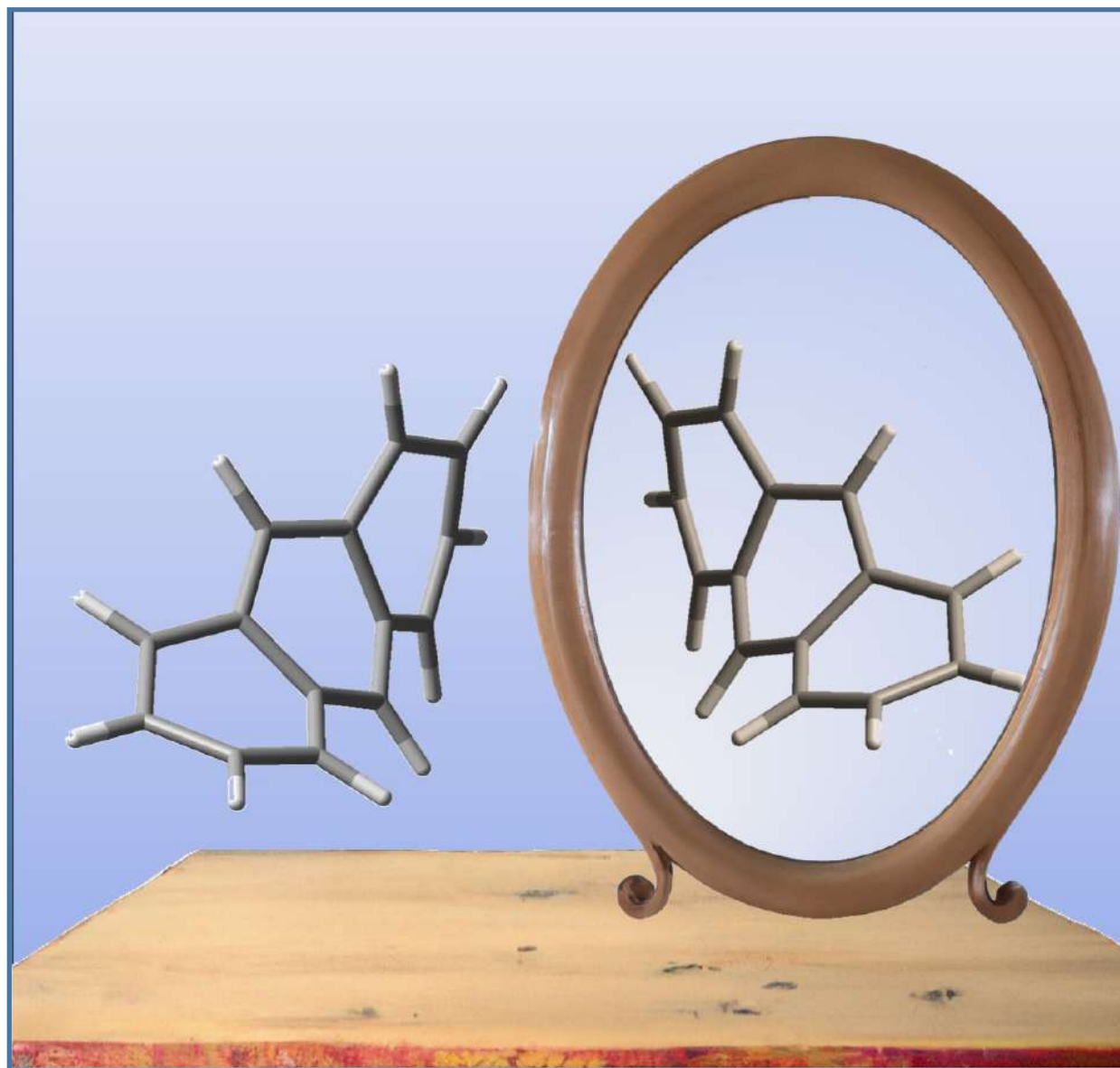


Issue 10 · September 2024 · Elul 5784

# The Israel Chemist and Chemical Engineer

# ICE

<https://doi.org/10.51167/ice00000>



The Israel Chemical Society  
(ICS: [www.chemistry.org.il](http://www.chemistry.org.il))



## Editorials

---

- 4 Letter from the Editor**  
Arlene D. Wilson-Gordon
- 5 Letter from President of ICS**  
Ehud Keinan

## Scientific Articles

---

- 6 Magnetic Resonance – from spectroscopic tools to practical technological devices**  
Aharon Blank
- 14 Aromatic materials – a twisted tale**  
Ori Gidron
- 23 Slippery science**  
Oded Hod
- 33 Additive manufacturing: from 2D to 4D printing**  
Doron Kam, May Yam Moshkovitz, Ouriel Bliah, Alexander Kamyshny, and Shlomo Magdassi
- 43 The chiral-induced spin selectivity effect**  
Ron Naaman

## History of Chemistry Article

---

- 48 Eugene Rabinowitch (1898-1973): A Voice of Conscience for the Atomic Age**  
Bob Weintraub

## Careers

---

- 53 Being a Patent Attorney (in Israel)**  
Temira Sklarz

## Profile

---

- 55 Interview with Ron Naaman**  
Arlene D Wilson-Gordon

## Reports

---

- 57 Report on the 87<sup>th</sup> Annual Meeting of the Israel Chemical Society**  
Ehud Keinan

**Front cover:** Ori Gidron “Mirror images”

The contents of this issue of ICE are published under license CC-BY-SA.



*Dear Readers,*

Despite all the major traumatic events in recent months, we welcome you to the tenth issue of the Israel Chemist and Engineer (ICE) online magazine, a publication of the Israel Chemical Society (ICS). We hope you will find the magazine interesting and will be inspired to contribute to future issues.

We present five scientific reports on diverse topics from recent ICS prize winners: Aharon Blank, the recipient of the 2022 ICS–Adama Prize for Technological Innovation, has contributed a report on “Magnetic Resonance – from spectroscopic tools to practical technological devices”; Ori Gidron, the recipient of the 2022 ICS Excellent Young Scientist Prize has written on “Aromatic materials – a twisted tale”; Oded Hod, the recipient of the 2022 ICS Tenne Family Prize for Nanoscale Sciences, has contributed an article entitled “Slippery science”; Shlomo Magdassi, the recipient of the 2022 ICS Excellent Scientist Prize, and his coworkers, have written on “Additive manufacturing: from 2D to 4D printing” and Ron Naaman, the recipient of the 2022 ICS Gold Medal, reviews his work on “The chiral-induced spin selectivity effect.” I also had the pleasure of interviewing Ron for this issue of the ICE magazine.

Bob Weintraub continues to inform us about the history of science, this time with a timely article entitled “Eugene Rabinowitch (1898-1973): A Voice of Conscience for the Atomic Age.”

In this issue, we introduce a new feature on potential careers for chemistry graduates, beginning with Temira Sklarz on “Being a patent attorney (in Israel).”

If you have suggestions for future issues, comments on the current issue, or would like to contribute an article, please contact me at [gordon@biu.ac.il](mailto:gordon@biu.ac.il).

### **Arlene D. Wilson-Gordon**

Professor Emerita

Chemistry Department, Bar-Ilan University

ICE Editor



*Dear Colleagues,*

Before October 7, 2023, we all naively assumed that the COVID-19 pandemic had created the worst possible disruption of our traditional activities. Indeed, the ICS Annual Meeting of 2021 fell victim to the global pandemic, forcing a gap of 2.5 years between the 85th Meeting of February 2020 in Jerusalem and the 86th Meeting of September 2022 in Tel Aviv. Unfortunately, the horrendous massacre of October 7 and the consequential war in Gaza and other fronts forced us to postpone the 87th meeting several times until we finally reduced it to a single day on April 3, 2024 (see my conference report in this issue).

With much hope to get back on track, we scheduled the 88th Annual Meeting for February 18-19, 2025, at the Jerusalem Conference Center, under the leadership of co-chairs Professors Hagay Shpaisman and Gerardo Byk of Bar-Ilan University. We are preparing to host a significant delegation from Taiwan to that event, including ten professors and 20 graduate students.

Nevertheless, we should also remember the many good things that occurred during these tumultuous times. We have signed an agreement with the German Chemical Society on the Richard Willstätter Lectureship. A unique feature of this scientists' exchange program is that the traveling scientists will take with them an excellent graduate student. We plan to apply this unprecedented principle to other exchange programs we are planning now with Taiwan and Japan.

On January 10, 2024, I signed an MOU agreement with the Chemical Society of Japan, and we intend to create another scientist exchange program between Japan and Israel. This agreement adds to five other collaboration agreements we signed earlier with the USA, Germany, Spain, the Netherlands, and the Czech Republic. I hope to sign the seventh agreement with Taiwan soon, supported by an endowment fund of \$100,000.

Another exciting development is the establishment of two new Sections of the ICS. The Bioinorganic Chemistry Section under the leadership of Graham de Ruiter, Omer Yehezkeli,

and Amir Mizrachi, and the Organic Chemistry Section under the leadership of Doron Pappo, Mark Gandelman, and Elad Shabtai. The establishment of the latter is associated with other exciting news. We have established an international prize and lectureship in memory of the late Prof. Richard Lerner, previous President of The Scripps Research Institute (TSRI). This achievement is a result of a global collaboration, with six of Lerner's friends collectively contributing an endowment of \$100,000 to support this annual Prize: Professors Phil Baran, Benjamin F. Cravatt, Jeff W. Kelly, Chi-Huey Wong, and Jin-Quan Yu of TSRI, and Dr. Phillip Frost, former Chairman of Teva Pharmaceutical Industries Ltd. The first Lerner Prize laureate will visit Israel during the annual meeting of the Organic Chemistry Section in May 2025.

I am delighted to introduce the newly elected members of the ICS Executive Board, a group of esteemed professionals who will undoubtedly contribute significantly to the ICS: Roey J. Amir of Tel Aviv University, Itsik Bar-Nahum of Adama, Orna Breuer of Rafael, Ori Gidron of the Hebrew University, Sharon Gazal of Teva, Soliman Khatib of the Tel-Hai College, Dorit Taitelbaum of the Ministry of Education, Michael Meijler (Secretary-General) of Ben Gurion University, David Margulies of the Weizmann Institute, Tomer Zidki (Treasurer) of Ariel University, Igor Rahinov of the Open University, Hagai Shpaisman of Bar-Ilan University, and Ehud Keinan (President) of the Technion. The newly elected Inspection Committee includes Yitzhak Mastai of Bar-Ilan University and Amnon Bar Shir of the Weizmann Institute.

Finally, please help develop the ICE magazine under the leadership of Prof. Arlene Wilson-Gordon, and contribute an article to the ICE on any topic that resonates with you, including popular science, history of science, report on an event, opinions, etc. Your unique perspective is valuable to us. Please, don't hesitate to contact Arlene or me on these matters.

Enjoy your reading,

**Ehud Keinan**

President, the Israel Chemical Society

# Magnetic Resonance – from spectroscopic tools to practical technological devices

**Aharon Blank**

Schulich Faculty of Chemistry, Technion- Israel Institute of Technology, 3200003, Haifa, Israel

Email: [ab359@technion.ac.il](mailto:ab359@technion.ac.il)

## Abstract:

Magnetic resonance, a well-established field, has historically been utilized primarily in spectroscopy and medical imaging. From its inception, it has also underpinned practical technological devices, including microwave sources and amplifiers. This trend persists today, with ongoing technological advancements in magnetic resonance enhancing its applications in both spectroscopy and medicine. Furthermore, these advancements facilitate the development of innovative devices and instruments, such as sensitive sensors, advanced amplifiers, and tools for quantum computing. In this brief review, I will focus on the recent developments emerging from the magnetic resonance laboratory at the Technion. These advancements are not only enhancing the spectroscopic applications of magnetic resonance but are also leading to the creation of novel microwave devices.

## 1. Introduction

Magnetic resonance is a pivotal technique in both spectroscopy and medical imaging, offering profound insights into molecular structures and human anatomy. In spectroscopy, magnetic resonance manifests primarily as nuclear magnetic resonance (NMR) spectroscopy and electron spin resonance (ESR) spectroscopy. NMR spectroscopy exploits the magnetic properties of certain atomic nuclei, which absorb and re-emit electromagnetic radiation at characteristic frequencies when subjected to a strong magnetic field. This process provides detailed information about molecular structure, dynamics, reaction states, and chemical environments. NMR is invaluable in various fields such as organic chemistry, biochemistry, and material science. In addition to NMR, ESR spectroscopy (also known as electron paramagnetic resonance, EPR) is another vital application of magnetic resonance. ESR is used to study materials and molecules that

contain unpaired electrons, which occur in various systems, including transition metal complexes, free radicals, and defects in solid materials. By analyzing the interaction of these unpaired electrons with a magnetic field, ESR provides insights into the electronic structure, local environment, and dynamics of these species. This makes ESR an essential tool for investigating reaction mechanisms in chemistry, studying the properties of conductive and magnetic materials in physics, and deciphering molecular structure and understanding the behavior of free radicals in biological systems.

Magnetic resonance is also a valuable tool in the context of medical diagnostics, primarily known for magnetic resonance imaging (MRI). MRI focuses on the hydrogen nuclei in water and fat molecules within the body to produce detailed images without ionizing radiation. This non-invasive technique

**Aharon Blank** is a full professor at the Schulich Faculty of Chemistry, Technion – Israel Institute of Technology. He was born in 1972, and graduated from the Hebrew University of Jerusalem in 1992 with degrees in mathematics, physics and chemistry (cum laude). He completed his master's degree at Tel Aviv University in 1997 in electrical engineering – physical electronics under the supervision of Prof. Raphael Kastner and finished his PhD in 2002 at the Hebrew University of Jerusalem in physical chemistry – electron spin resonance (ESR), under the supervision of the late Prof. Haim Levanon. During the years 1992–1998, he served at the Israeli Air Force (IAF) as a scientific officer. Following that he was the CTO in a medical device company (TopSpin Medical), developing miniature intravascular MRI. After his PhD, he spent 3 years at Cornell University (2002–2005) as a postdoc in the group of Prof. Jack Freed (on a Rothschild post-doctoral fellowship), developing the subject of electron spin resonance microscopy, and since 2005 he is a faculty member at the Technion. He is the recipient of the 2022 ICS–Adama Prize for Technological Innovation.



is particularly effective for soft tissue imaging, aiding in diagnosing various conditions, planning treatments, and tracking disease progression.

NMR spectroscopy, ESR spectroscopy, and MRI are all applications of magnetic resonance, each serving distinct purposes: NMR and ESR in molecular-level analysis in various scientific fields, and MRI in detailed, non-invasive medical imaging and diagnostics.

Magnetic resonance has also found practical applications in a variety of technological devices, extending its influence beyond the realms of spectroscopy and medical imaging. Two notable examples of such applications are masers and yttrium iron garnet (YIG) microwave sources. Masers, which stand for “Microwave Amplification by Stimulated Emission of Radiation,” are devices that amplify microwave radiation through the principle of stimulated emission. Many of the first masers, built in 1950’s, used the electron spins in paramagnetic species. When these spins are aligned in a magnetic field, their energy levels are typically separated by microwave frequency (~1-10 GHz), and can be made to have population inversion (more spins in the upper energy than in the lower one). Under these conditions, small incoming microwave radiation will be amplified by the stimulated emission of the spins. This principle has since been applied in various contexts, such as ultra-precise atomic clocks and deep-space communication systems. Masers serve as the predecessors to lasers and operate on similar principles but at microwave frequencies. Yttrium iron garnet (YIG) microwave sources are another application of magnetic resonance. YIG is a ferrimagnetic material and exhibits a strong magnetic resonance effect. When a YIG sphere is placed in a magnetic field, it can resonate with microwave radiation at a frequency dependent on the strength of the magnetic field. This property makes YIG an excellent frequency-tuning element for microwave oscillators and filters. YIG-tuned oscillators are used in radar systems, electronic warfare, and signal processing, where precise control of microwave frequencies is essential. The ability to adjust the magnetic field allows for a wide range of frequency tuning, making YIG devices incredibly versatile.

Both masers and YIG microwave sources demonstrate the adaptability of magnetic resonance principles in creating practical, high-performance technological devices. Masers leverage magnetic resonance for signal amplification, while YIG devices utilize it for frequency tuning in microwave technology. These applications showcase the broad potential of magnetic resonance beyond its traditional scientific uses, contributing significantly to advancements in communication, navigation, and electronic systems.

## 2. Scope of activity

The magnetic resonance (MR) laboratory at the Technion operates over the broad range of scientific and technical fields described above. These activities include:

- Improving the spectroscopic capabilities of MR by primarily providing more sensitive detection, which enables the measurements of smaller samples.
- Providing better spectral resolution for unique type of MR techniques, thus providing better molecular structure information.
- Enabling new capabilities for MRI by enhancing the NMR signal of some specific metabolites of interest.
- Developing and testing new microwave devices for sensitive detection of microwave signals.

In this short review we will describe some of our activities in relation to the abovementioned items, thereby providing an overview of how advanced MR spectroscopic capabilities can evolve to realize practical unique microwave devices.

## 3. Results

### 3.1 Improving the sensitivity and spectroscopic capabilities of MR

One line of action we recently took with respect to improving the spectroscopic capabilities of MR is to enable the detection of liquid samples in microfluidics systems with ESR. Microfluidics is a well-established technique to synthesize, process, and analyze small amounts of materials for chemical, biological, medical, and environmental applications. Typically, it involves the use of reagents with a volume smaller than ~1 microliter—ideally even nano- or picoliters. When the sample of interest contains paramagnetic species, it can in principle be quantified and analyzed by ESR spectroscopy. However, conventional ESR is typically carried out with a sample volume of ~1 ml, thereby making it incompatible with most microfluidics applications. In a recent work, we showed that by using a new class of miniature surface resonators combined with photolithography to prepare microfluidic patterns, ESR can be applied to measure small liquid samples, down to picoliter volumes, without considerable sacrifice of concentration sensitivity [1]. Our experiments, carried out with resonators whose mode volumes range from ~1 to 3.6 nL, showed that with a sample volume of ~0.25 nL good signals could be obtained from solutions with spin concentrations of less than 0.1  $\mu\text{M}$ . All our experiments are performed at room temperature, making our technique compatible with future microfluidics applications that might employ a complete system of compact resonators, microfluidic chips, miniature magnets, and a compact ESR-on-a-chip spectrometer. This could result in a completely new approach to processing and measuring paramagnetic liquid samples for use in a

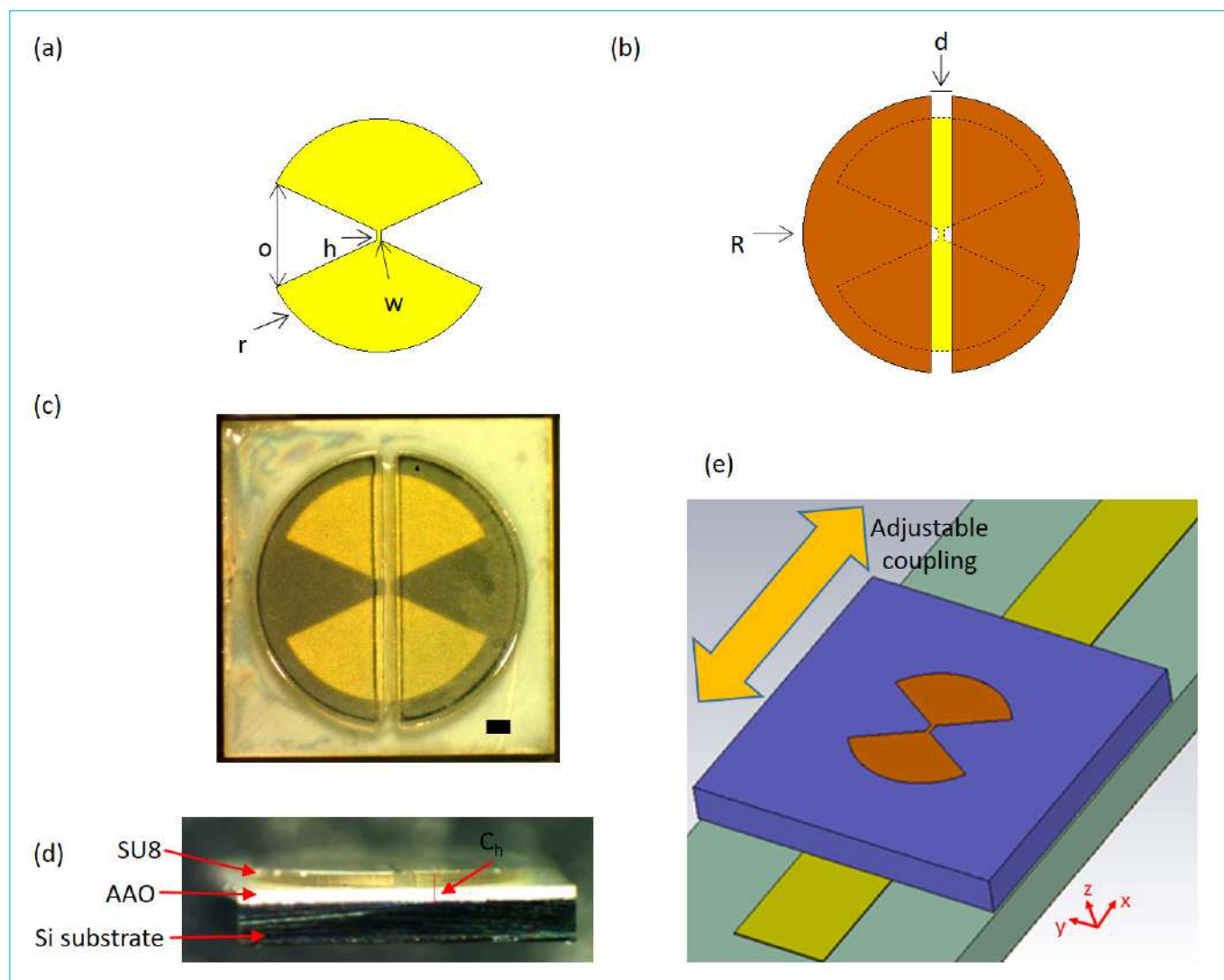


**Figure 1. Microfluidics system with ESR detection.** (a) Schemes of a miniature ESR resonator (yellow) and (b) the microfluidic channel placed on it (brown). The resonator is realized with a Ti(10 nm)/Cu(500 nm)/Au(10 nm) metallic layer on a single crystal of intrinsic silicon measuring  $1.6 \times 1.6 \times 0.2$  mm. (c) and (d) show images of the fabricated resonator with an anodic aluminum oxide (AAO) wafer and a microfluidic channel implemented on its surface. The AAO wafer minimizes sample dehydration. (c) Top view (scale bar is 100  $\mu\text{m}$ ). (d) Side view. (e) Coupling of the resonator to microwave is achieved via a thin microstrip line mechanically placed exactly below the resonator's central bridge (the narrow part of the resonator). Coupling is adjusted by moving the resonator along the x-axis of the microstrip (orange arrow in the figure). In this position, magnetic inductive coupling is maximal between the microstrip and the bridge.

variety of chemical, biological, medical, and environmental applications.

Figure 1 shows the microfluidics ESR system we developed. It includes a miniature resonator for concentrating the microwave magnetic field used to excite the electron spins and detect the ESR signal of the small liquid sample placed on it. The liquid sample is confined to flow in a narrow ( $\sim 50$   $\mu\text{m}$ ) channel at the center of the resonator. This system was tested with a test sample of liquid free radical solution (trityl

radical, 0.83 mM concentration) and demonstrated absolute spin sensitivity of up to  $\sim 5.2 \times 10^6$  spins/ $\sqrt{\text{Hz}}$  and concentration sensitivity as good as  $0.03$   $\mu\text{M}/\sqrt{\text{Hz}}$ .

### 3.2 Improving the spectral resolution of MR

As noted above, nuclear magnetic resonance (NMR) spectroscopy provides atomic-level molecular structural information. However, in molecules containing unpaired electron spins, some NMR signals, for nuclei close to the electron spins, are difficult to measure directly. In such

cases, data is obtained using the electron-nuclear double resonance (ENDOR) method, where nuclei are detected through their interaction with the nearby unpaired electron spins. Unfortunately, electron spins spread the ENDOR signals, which challenges current acquisition techniques, often resulting in low spectral resolution that provides limited structural details. In a recent work, we showed that by using miniature microwave resonators to detect a small number of electron spins, integrated with miniature NMR coils, one can excite and detect a wide bandwidth of ENDOR data using a single radiofrequency pulse (called “time-domain ENDOR” [2]. This facilitates the measurement of ENDOR spectra with

narrow lines spread over a large frequency range at much better spectral resolution than conventional approaches, which helps reveal details of the paramagnetic molecules’ chemical structure that were not accessible before.

Figure 2 shows the unique setup we developed with the micro-ESR resonator and the corresponding micro-NMR coil. Figure 3 compares the NMR spectral data for a test sample of  $\gamma$ -irradiated single crystal of malonic acid, showing the enhanced resolution obtained with our new setup and methodology.

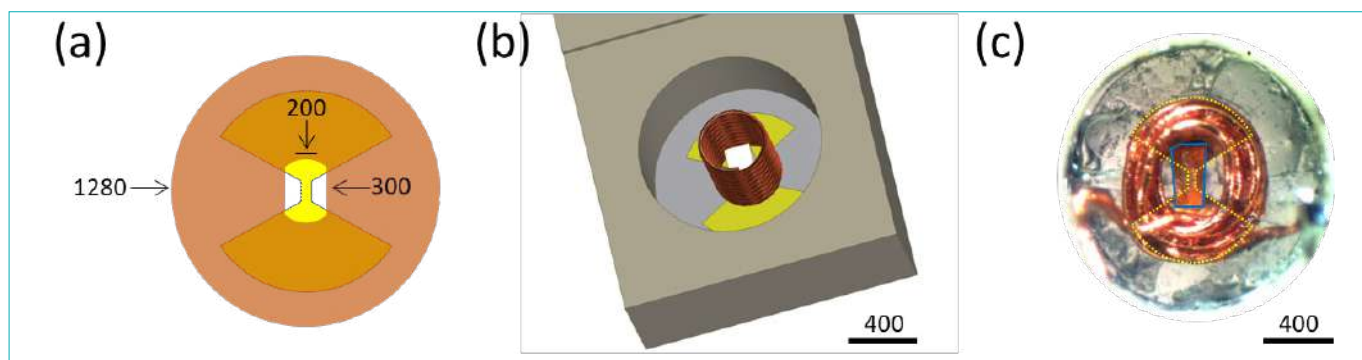


**Figure 2. A miniature ESR resonator with an ENDOR coil placed on it. (a)** Drawing of the resonator with a 25- $\mu\text{m}$ -thick sample-positioning well placed on top. **(b)** Illustration of the resonator (with a sample and RF coil) attached to a sample holding stick (gray). **(c)** A micrograph of the resonator with a photolithographic well, an RF coil, and a test sample mounted inside the well (emphasized by the blue line). The yellow dotted line shows the metallic resonator layout positioned under the RF coil. All dimensions are in microns.

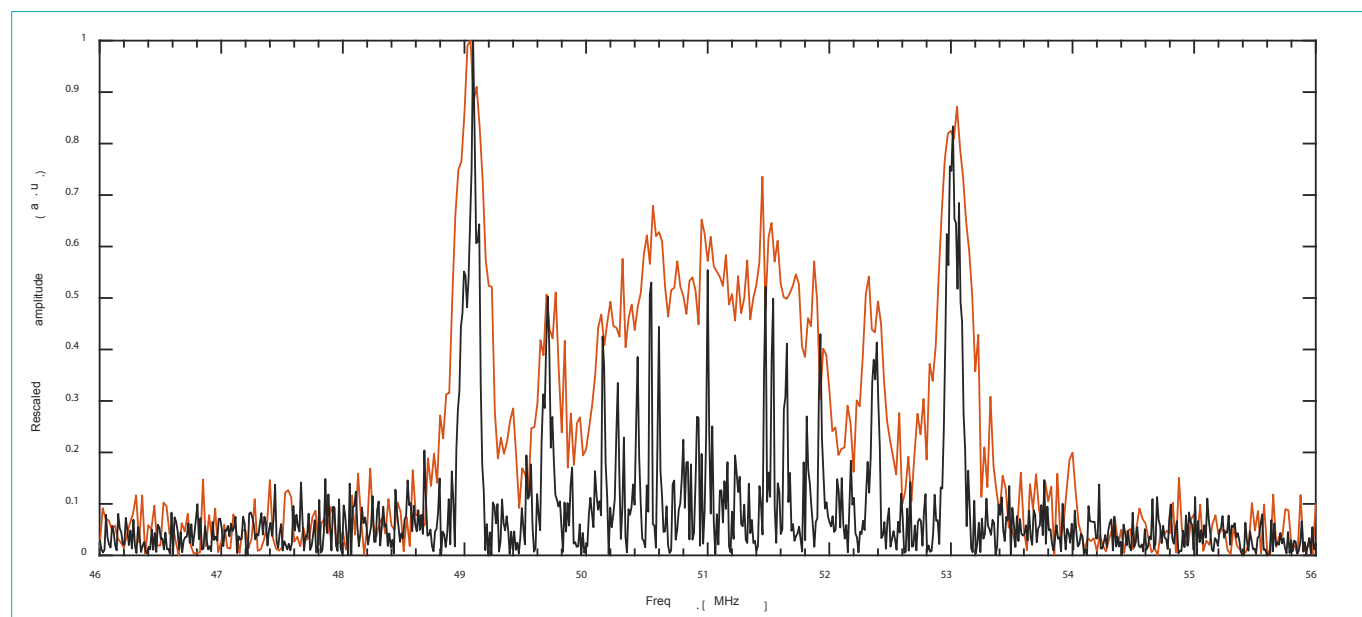


**Figure 3. Comparison of Davies and time-domain ENDOR measurements for an irradiated malonic acid single crystal.** Fourier transform of the time-domain ENDOR signal collected around 51 MHz (solid black line), and Davies ENDOR frequency sweep, acquired with a 40- $\mu\text{s}$  RF pulse and 25-kHz frequency steps (solid orange line).

### 3.3 Enhancing the NMR signal of metabolites of interest and maintaining it for a long period of time

Non-invasive tracking of biochemical processes in the body is paramount for diagnostic medicine. Among the leading techniques is spectroscopic magnetic resonance imaging (MRI) that tracks metabolites with amplified (hyperpolarized) magnetization signal. Clinical imaging with such hyperpolarized metabolites can detect chemically specific tissue signatures through nuclear magnetic resonance (NMR) spectroscopy. It merges MRI's superior soft tissue contrast and spatial resolution with improvement in specificity by amplifying the magnetization of targeted metabolites introduced to the subject just before scanning.

Until now, the short-lived magnetization window of these magnetization-enhanced agents has generally been too brief for clinical imaging. In our recent work, we offer a possible solution to this problem [paper in preparation]. By amalgamating two materials – one possessing diagnostic/metabolic activity and the other characterized by robust magnetization retention, we can significantly slow the magnetization decay of the diagnostic metabolic probe. The probe continuously receives fresh magnetization from its companion material, effectively creating a magnetization vehicle for clinical practice. The resulting magnetization lifetime is found to be in some cases more than 10 minutes long, with magnetization enhancement factors of more than four orders of magnitude. These diagnostic probes could retain

their magnetized state from the time of injection until they reach the organ of interest. Once validated, this innovative metabolic MRI approach could have numerous impactful applications for human clinical imaging. Its potential spans the fields of diagnostic imaging, therapeutic monitoring, and surveillance after treatment.

Figure 4 shows an example from our recent results. In this experiment we prepared a sample of glycine co-crystallized with  $\text{CaCO}_3$ . This sample was then subjected to  $\gamma$ -irradiation which generated stable paramagnetic defects in the crystal. These defects have unpaired electrons, which can be used to transfer their high magnetization to nearby nuclei under specific conditions of low temperature ( $\sim 1.5$  K), static magnetic field of  $\sim 6$  T and microwave irradiation. Once this magnetization transfer was complete, we took out the sample from the device and measured its signal relaxation time, which proved to be more than 4 minutes (Figure 4 – left). This is much longer than the few tens of seconds at most found for solid glycine at normal conditions. The reason for this extra-long magnetization lifetime is the fact that the accompanying crystal,  $\text{CaCO}_3$ , has a long intrinsic magnetization lifetime and it can keep replenishing the lost magnetization of the glycine. After the measurement of the lifetime of the magnetization in the solid state, we dissolved the glycine- $\text{CaCO}_3$  crystallites in acidic water and measured their NMR signal, which showed enhancement of a few tens of thousands compared to the regular thermal signal of dissolved glycine (Figure 4 – right).

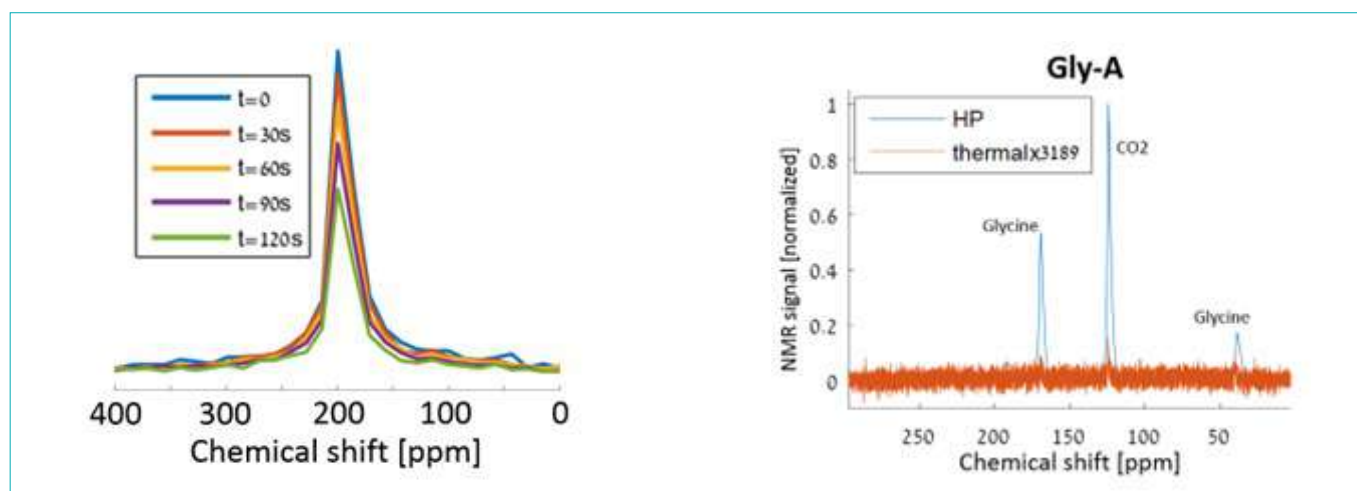


**Figure 4. Hyperpolarization experiments for glycine in  $\text{CaCO}_3$ .** (left)  $^{13}\text{C}$  NMR signals acquired for the solid-state sample in the spectrometer immediately after shuttling of the sample from the polarizer to the spectrometer. The acquisitions take place 30 s apart and employ a  $\sim 10$  degree tip angle. (right) Hyperpolarized spectra shortly after dissolution vs. thermal spectra. The data demonstrates the preservation of hyperpolarization in ambient conditions and the enhancement factors that remain available in the liquid state after a considerable time interval. Thermal signal was averaged over 3189 scans representing an enhancement of up to  $\sim 10,000$  (depending on the spectral peak chosen).

### 3.4 New microwave devices for sensitive detection of microwave signals

Up to this point in our story, magnetic resonance was used only as an observation tool – mainly seeking spectroscopic information that is vital for chemical and biological analysis, as well as improving medical diagnostics. In this part, however, we see that magnetic resonance can be used to construct actual practical technological devices – namely, ultra-low noise microwave amplifiers.

The technology for amplification and detection of microwave (MW) signals with minimal addition of noise is critical to a variety of applications, such as deep-space communications, radio astronomy, radar, microwave spectroscopy, and quantum technology (e.g., quantum computing, quantum sensing, and quantum communication). In these applications, the signal of relevance is very weak, sometimes at the level of tens to hundreds of MW photons per second. Therefore, any noise added to the signal during the amplification process might overwhelm it and eliminate the possibility of detecting it within a reasonable averaging time. Currently, three main types of amplifiers are used to amplify and subsequently possibly detect MW signals with very low addition of noise. (a) Conventional electronic amplifiers, predominantly based on high-electron-mobility transistor (HEMT) semiconductor technology. They optimally operate at  $\sim 5$  K or below and add  $\sim 10$  noise photons to the signal in 1 second for 1 Hz bandwidth [3]. (The number of noise photons per second is linear with the acquisition bandwidth.) (b) Amplifiers based on superconducting circuits. These include the families of SQUIDs (superconducting quantum interference devices) based amplifiers, radio frequency (RF) single electron transistors, and quantum Josephson parametric amplifiers [4], as well as the more recent Josephson traveling-wave parametric amplifier [5] and kinetic inductance parametric amplifiers [6]. Such amplifiers typically operate at  $\sim 10$ – $25$  mK and make use of a variety of nonlinear phenomena occurring in superconductors to amplify microwave signals with quantum-limited noise performance (e.g., adding 0.5 photons of noise per second for 1 Hz of bandwidth). (c) Solid-state maser (microwave amplification by stimulated emission of radiation) devices. These amplifiers rely on paramagnetic species, mainly ions embedded in a crystal such as ruby ( $\text{Cr}^{3+}$  in a crystal of  $\text{Al}_2\text{O}_3$ ). Under an external static magnetic field, the paramagnetic species in the solid-state maser have at least three energy levels for their unpaired electrons (Figures 5a, b). One can use microwave pumping to reach a state of population inversion in which there are more electrons in a higher energy level than in a lower one. Under such conditions, incoming microwave radiation causes the stimulated emission of additional microwave radiation – namely, the amplification of the incoming signals. Solid-state

masers operate efficiently only at low temperatures ( $\sim 1$  K) and typically add a few photons of noise to the signal per second for 1 Hz bandwidth [7].

Until now, maser technology, developed in the 1950s and 1960s, was used mainly in niche yet important applications in space communication and radio astronomy. (For example, detection of the black body radiation of the universe, remnant of the “Big bang”.) At present, it has been mostly abandoned in favor of the conventional electronic amplifiers mentioned above due to its complicated implementation, requirement for low operation temperature, and limited bandwidth/gain performance.

With the rising age of quantum technology, new scientific and technological endeavors are coming into play, requiring amplification of very weak MW signals with quantum-noise limited performance for applications ranging from the read-out of quantum bits [8] to dark matter detection [9]. These needs can currently be met only by the superconducting-based amplifier technology mentioned above, which necessitates the use of ultra-low cryogenic temperatures that make its operation very complicated and limited in scope. Clearly, it would be very beneficial to have a complementary technology for quantum-noise-limited microwave amplifiers that could be operated at much higher temperatures, even at room temperature.

In a recent work, we demonstrated the operation of such an amplifier, based on maser technology that, when optimized, could be used to amplify weak microwave signals at moderate cryogenic temperatures ( $\sim 10$  K) with quantum limited noise performance [10]. Our device is based on a new type of active maser material – namely, single crystal diamond with high concentration of color defects in it. These defects, called NV (nitrogen-vacancy) centers, are made of nitrogen that substitutes one of the carbons in the diamond lattice with a missing carbon (vacancy) near it (Figure 5c). The negatively-charged defect is paramagnetic, with 2 unpaired electron spins. Under the influence of a static magnetic field, its ground state splits into three energy levels and at this point light illumination can be added to pump the spin states to the central level (Figure 5d). The resulting population inversion state can be used for low noise microwave amplification.

Figure 6a shows a photo of the maser device, when one of its bounding walls is removed. A green LED light illuminates the diamonds that are situated inside a specially-designed microwave cavity. As noted above, the light pumps the energy levels of the NVs in the diamond to their inverted spin state (Figure 5d) so that incoming irradiation can be amplified. Figure 6b presents the gain of the maser device vs. input frequency, for various input power levels, at a temperature

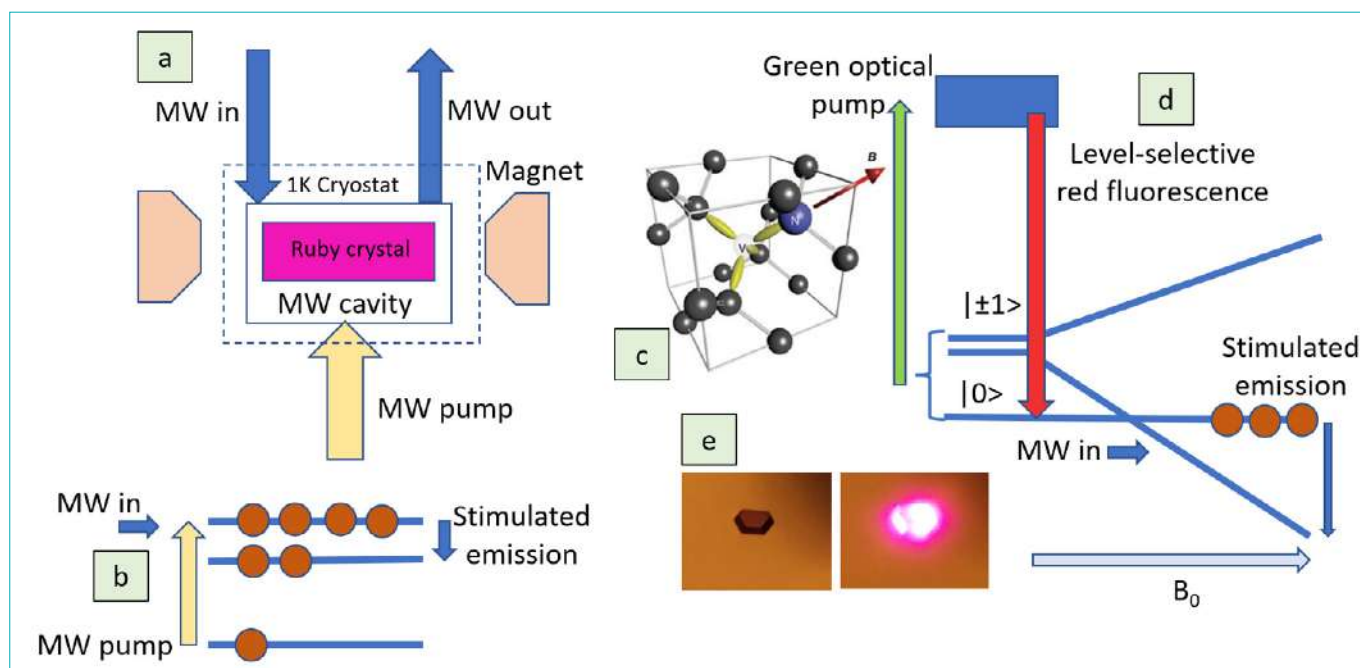


**Figure 5. Conventional solid-state maser as compared to diamond-based maser.** (a) Schematic overview of a conventional solid-state maser employing a ruby single crystal embedded in a microwave ( $\mu\text{w}$ ) cavity and subjected to a static magnetic field. (b) The relevant three energy levels of a typical solid-state maser. The separation between levels is dictated by the strength of the static magnetic field. Microwave radiation is used to create population inversion, enabling stimulated emission also in the  $\mu\text{w}$  regime (albeit for lower energy than the pumped one). This type of maser can operate only at a temperature of  $\sim 1$  K or below; at higher temperatures, all the levels are almost equally populated, and the spin-lattice relaxation time,  $T_1$ , becomes too short. (c) The structure of a nitrogen-vacancy (NV) color defect in a diamond crystal, with spin  $S = 1$ . (d) The three Zeeman levels of NV<sup>-</sup> ground state. At zero magnetic field, the  $m_s = 0$  level ( $|0\rangle$ ) is situated below the two degenerate  $m_s = \pm 1$  levels. When subjected to green light, it undergoes red fluorescence with other non-radiative transitions leading to enhanced population of the  $|0\rangle$  state. By applying a static magnetic field, one obtains population inversion between the  $|0\rangle$  and  $|-1\rangle$  states. In contrast to conventional solid-state masers, the selective population mechanism performs well also at room temperature. The spin temperature is given by:  $T_s \approx (\hbar\omega_0/2k_B)(N/\Delta n)$ , where  $\omega_0$  is the transition frequency,  $N$  is the number of spins and  $\Delta n$  is the level population difference. For  $\Delta n \rightarrow N$  the spin temperature approaches  $\sim 0$  K. (e) Photo of a synthetic diamond crystal processed in by our lab with many NVs.

of 30 K. The maser's small signal ( $< -90$ -dBm input) gain reaches more than 20 dB at 30 K. The bandwidth is  $\sim 0.5$  MHz for the high gain at 30 K and increases up to  $\sim 5$  MHz for the small gain at high input power. Overall, the voltage gain  $\times$  bandwidth is found to be  $\sim 5.8 \pm 0.5$  MHz for all power levels at 30 K.

#### 4. Summary and conclusions

Magnetic resonance stands as one of the most adaptable fields in science, with its applications spanning from the determination of chemical structures to medical imaging and quantum information processing. This technique's multidisciplinary nature draws researchers from diverse domains, including natural and life sciences, as well as engineering. From a scientific perspective, magnetic resonance has been a focal point for at least seven Nobel Prizes across physics, chemistry, and medicine to date. Industrially,

it represents a multibillion-dollar sector targeting a broad spectrum of medical and chemical applications.

In this concise review, we have observed that despite magnetic resonance being discovered nearly 70 years ago, and magnetic resonance imaging (MRI) being over 40 years old, the field still harbors significant potential for innovation in methodologies, approaches, and applications. These innovations include novel methods to enhance the sensitivity and spectral resolution of magnetic resonance, advancements in MRI's ability to provide chemical insights from within the body, and the development of new technical devices based on magnetic resonance principles. These ongoing developments ensure that the field remains dynamic. We believe it will continue to evolve, rejuvenating itself and offering surprising resolutions and solutions to contemporary challenges in science, technology, and medicine.

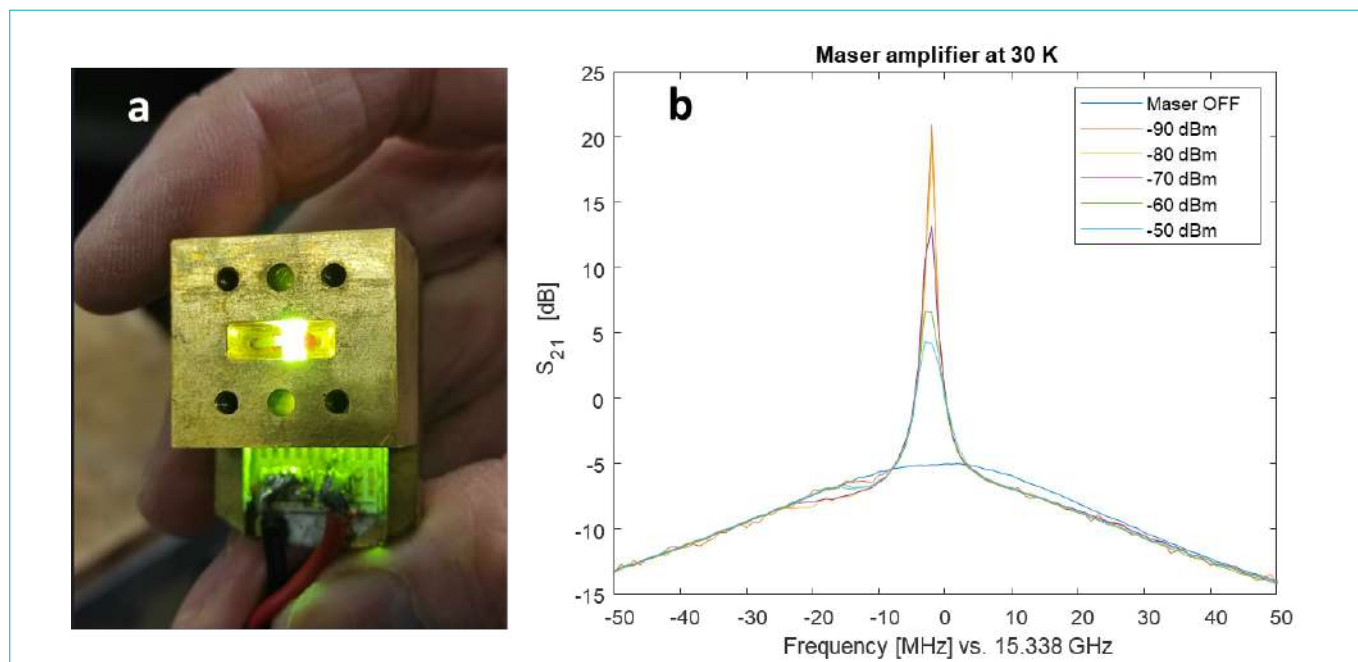


**Figure 6.** Diamond-based maser device in action. **(a)** Photograph of the maser device with optical pumping turned on. **(b)** Gain of the maser amplifier when operated at 30 K, with varying levels of input power.

## References

1. N. Dayan, Y. Ishay, Y. Artzi, D. Cristea, B. Driesschaert, A. Blank, Electron spin resonance microfluidics with subnanoliter liquid samples, *Journal of Magnetic Resonance Open*, 2020, **2–3**, 100005.
2. N. Dayan, Y. Artzi, M. Jbara, D. Cristea, A. Blank, Pulsed Electron-Nuclear Double Resonance in the Fourier Regime, *ChemPhysChem*, 2023, **24**, e202200624.
3. M.W. Pospieszalski, Extremely low-noise cryogenic amplifiers for radio astronomy: past, present and future, in *22nd International Microwave and Radar Conference (MIKON)*, 2018, 1–6.
4. X. Gu, A.F. Kockum, A. Miranowicz, Y.-x. Liu, F. Nori, Microwave photonics with superconducting quantum circuits, *Phys. Rep.*, 2017, **718–719**, 1–102.
5. C. Macklin, K. O'Brien, D. Hover, M.E. Schwartz, V. Bolkhovskiy, X. Zhang, W.D. Oliver, I. Siddiqi, A near-quantum-limited Josephson traveling-wave parametric amplifier, *Science*, 2015, **350**, 307–310.
6. D.J. Parker, M. Savytskyi, W. Vine, A. Laucht, T. Duty, A. Morello, A.L. Grimsom, J.J. Pla, Degenerate Parametric Amplification via Three-Wave Mixing Using Kinetic Inductance, *Physical Review Applied*, 2022, **17**, 034064.
7. M.S. Reid, *Low-noise systems in the Deep Space Network*, Wiley, Hoboken, N.J., 2008.
8. Z.R. Lin, K. Inomata, W.D. Oliver, K. Koshino, Y. Nakamura, J.S. Tsai, T. Yamamoto, Single-shot readout of a superconducting flux qubit with a flux-driven Josephson parametric amplifier, *Appl. Phys. Lett.*, 2013, **103**, 132602.
9. K.M. Backes, D.A. Palken, S.A. Kenany, B.M. Brubaker, S.B. Cahn, A. Droster, G.C. Hilton, S. Ghosh, H. Jackson, S.K. Lamoreaux, A.F. Leder, K.W. Lehnert, S.M. Lewis, M. Malnou, R.H. Maruyama, N.M. Rapidis, M. Simanovskaia, S. Singh, D.H. Speller, I. Urdinaran, L.R. Vale, E.C. van Assendelft, K. van Bibber, H. Wang, A quantum enhanced search for dark matter axions, *Nature*, 2021, **590**, 238–242.
10. A. Sherman, O. Zgzdzai, B. Koren, I. Peretz, E. Laster, A. Blank, Diamond-based microwave quantum amplifier, *Science Advances*, 2022, **8**, eade6527.

# Aromatic materials – a twisted tale

## Ori Gidron

Institute of Chemistry and the Center for Nanoscience and Nanotechnology, The Hebrew University of Jerusalem, Edmond J. Safra Campus, 9190401 Jerusalem, Israel

Email: [ori.gidron@mail.huji.ac.il](mailto:ori.gidron@mail.huji.ac.il)

### Abstract:

Twisting aromatic molecules out of planarity can produce new electronic, (chiro)optical and magnetic properties. One of the greatest challenges is to induce helicity to a  $\pi$ -conjugated backbone without disturbing the  $\pi$ -conjugation, with helicenes being the most well-known example of such systems. While helicenes became a common structural motif in polyaromatic systems, polymers, and even metallacycles, their para-fused analogs, twisted acenes (twistacenes), are significantly less explored. In this report, I will discuss the introduction of the first helically-locked twisted acenes, which are conformationally stable at different twisting angles depending on the tether length. This allowed us to systematically monitor the effect of twisting on electronic and chiroptical properties of acenes, and to include twistacenes as building units in helical macromolecules and polymers.

## 1. Introduction

Aromatic molecules, which constitute approximately two thirds of the 20 million known organic molecules [1], play fundamental roles in biology (for example, aromatic base pair interactions contribute to the stability of DNA double helices) [2], in medicine (many small-molecule drugs are aromatic) [3] and in materials chemistry. The field of organic electronics relies on the ability of aromatic molecules to absorb or emit light and to transfer electrons or holes [4]. The advantage offered by using aromatic molecules, as opposed to inorganic molecules, as active electronic materials arises from the ability to tune their properties, such as their color (emission/absorption wavelength), charge mobility, flexibility, and reactivity, by functionalizing their backbones. An

alternative approach to tuning the abovementioned factors involves modifying their topology, for example, by inducing distortion from an ideal planar geometry [5].

Although planarity is one of the prerequisites of aromaticity according to Hückel's rule, chemists have synthesized a range of non-planar, curved molecules that exhibit aromaticity, from fullerenes up to carbon nanotubes. In natural systems, helicity is a widespread non-planar motif that is found from the galactical scale (e.g., the Milky Way) to the molecular scale (e.g., the DNA double helix). Helical molecules contain a stereogenic center that induces chirality without the need for a stereogenic atom. Such chirality is termed helical chirality and is known to play important functions in living systems. For synthetic systems, the realization of such helically chiral structures poses a great challenge, in particular in  $\pi$ -conjugated backbones.

**Ori Gidron** received his MSc in chemistry from the Weizmann Institute of Science (2007) under the supervision of Professor M. van der Boom. He then joined the group of Professor M. Bendikov at the Weizmann Institute of Science and received his PhD in 2012, for which he was awarded the Dov-Elad Prize for Excellence in Chemical Research. In June 2013, he accepted a Marie Curie (IEF) Postdoctoral Fellowship to work in the group of Professor F. Diederich at ETH Zurich on supramolecular assemblies of carbon-rich materials. Prof. Gidron became a senior lecturer at the Hebrew University of Jerusalem in 2015 and was promoted to associate professor in 2020. In 2022, he received the Israel Chemical Society (ICS) Excellent Young Scientist Prize. His main interests are chiral organic semiconductors, curved aromatic systems, and furan-containing materials.



Perhaps the best-known family of helically-chiral aromatic molecules is helicenes (Figure 1, left), which are polycyclic aromatics in which the backbone is composed of *ortho*-fused benzenes, such that it adopts a screw shape. Although they were first synthesized over 100 years ago, they continue to fascinate chemists [6]. Helicenes, as any helical structure, possess intrinsically chiral backbones characterized by either left- or right-handed helicity (*M* and *P*, respectively, in Figure 1, right). However, for several reasons, helicene-based materials have been found not to be ideal for application in electronic devices. The energy difference between the highest occupied and lowest unoccupied molecular orbitals (the HOMO–LUMO gap or HLG) of helicenes is relatively high with only a slight reduction observed upon elongation [7]. Moreover, elongation of helicenes beyond [6]helicene does not significantly improve their chiroptical properties [8]. In addition, poor solid-state packing results in very low charge mobility in organic field-effect transistors (OFETs), which further limits their applicability [9].

Acenes, which are the *para*-fused analogs of helicenes, can be viewed as one-dimensional graphene nanoribbons. Uniquely among polyaromatic hydrocarbons, acenes have only one Clar sextet irrespective of how many annulated rings they contain (rings designated in blue in Figure 1, right) [10], and therefore chain elongation (i.e., increased annulation) leads to rapidly decreasing HOMO–LUMO gaps and to profound effects on their electronic, optical, and magnetic properties [11]. This is in contrast to helicenes which have a larger number of Clar sextets – for example [6]helicene consists of 3 Clar sextets (rings designated in blue in Figure 1, left). While increasing chain length also increases their reactivity, acenes are considered indispensable to organic electronics, and are embedded in active materials for OFETs, light emitting diodes, and singlet fission in organic solar cells [12]. Moreover, as higher acenes display a triplet ground state, they are potential candidates for spintronic devices [13]. Nevertheless, the low stability and solubility of acenes imposes difficulties on their synthesis and limits their application [14].

The seminal work of Pascal [15], followed by others [16], demonstrated that acenes can be readily twisted by the inclusion of bulky groups, whose steric bulk also increases acene stability and solubility [17]. These twisted acenes, known as twistacenes, are also chiral with either *M* or *P* helicity (Figure 1, right). However, with few exceptions, the low racemization barriers of twistacenes prohibited further application of these materials in their enantiopure form [18]. In addition, inducing twisting by means of backbone substitution (also known as side-group engineering) confounds efforts to investigate the effects of degree of

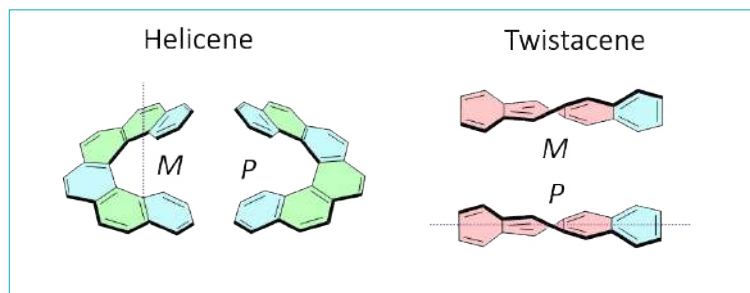


**Figure 1.** Structures of helicenes (left) and twistacenes (right) of *P* and *M* helicity. Clar sextets are indicated by blue-colored rings.

twisting independently from effects arising from the number and nature of the substituents utilized to induce that twisting [19]. Therefore, it is clear that to obtain a controllable degree of twisting to acenes while minimizing substituent effect and locking the helicity to a specific handedness, a different approach must be applied.

## 2. The "cyclophane approach" for twisting aromatic compounds

The enforcement of conformational non-planarity on aromatic rings imposes considerable strain on them and thus significantly complicates their synthesis. Access to highly strained systems has been achieved through several synthetic routes, including via cyclophanes, cycloparaphenylenes, and acenes [20].

Cyclophanes are composed of one or more aromatic rings connected by a bridge, which can induce distortion of the aromatic ring from planarity [21]. For example, [2,2]paracyclophane deviates from planarity by  $14^\circ$  and its strain energy is 31 kcal/mol [22, 23]. Extremely bent polyaromatic cyclophanes were synthesized by Bodwell's group, which leveraged pyrene's large aromatization energy to increase twisting by shortening the alkyl tether [24].

Acenes are easily twisted: calculations performed on anthracene show that less than 10 kcal/mol (ca. 3.3 kcal/mol per ring) is required to achieve an end-to-end twist of  $40^\circ$  (ca.  $13^\circ$  per ring) [25]. A common method of twisting acenes is via backbone substitution. Attaching phenyl ring substituents at the *peri* positions can significantly increase acene twist, with Pascal finding that polysubstituted anthracene and tetracene exhibit core twisting of  $63^\circ$  and  $97^\circ$ , respectively [26]. Alternatively, but less commonly, acene twisting can be achieved by diagonally tethering the two ends of the acene to each other to create a cyclophane bridge. 2,6-tethered naphthalenes were synthesized in this manner and found to have a dihedral twist of up to  $32^\circ$  [27].

In this report, we discuss findings from our efforts over the past five years, which were inspired by this work. Specifically, our aim was to identify and synthesize inherently helically chiral, stable,  $\pi$ -conjugated backbones that can be 'locked' into different desired torsion angles without modifying backbone substitution. To this end, we developed methods to helically lock anthracene into a twisted configuration by using an intramolecular diagonally-attached tether. By applying tethers of different lengths, we synthesized twistacenes possessing various end-to-end backbone twists and utilized them to investigate how degree of backbone twist affects optical, electronic, and magnetic properties and, thus, the application of twistacenes in electronic devices.

Among the series of tethered twistacenes synthesized by our group, the **Ant-C $n$**  series is particularly interesting. Member of this series have an anthracene (**Ant**) backbone twisted by the diagonal attachment of an ether-capped methylene chain (**C $n$** ) as a tether possessing variable length ( $n=3-6$  carbon atoms) [28]. To avoid competing intermolecular reactions during ether bridge formation, we utilized a preorganization step (Figure 2a) involving a precursor that was pre-twisted by 22° (calculated at the DFT/B3LYP/6-31G(d) level of density-functional theory (DFT)) by the substitution of two phenyl groups at the *peri* positions, one on each side of the anthracene. In this manner, we synthesized a series of twisted anthracenes

in which backbone torsion increases as tether length decreases from hexyl to propyl (Figure 2b). Experimental and computational measurements produced similar values for the degree of twisting this imposes on the anthracene backbone, which was found to be 22–38° according to X-ray structural crystallography; Figure 2c) or 22–43° according to calculations. The calculated torsional energy barrier to conversion between **Ant-C $n$**  enantiomers possessing *M* and *P* helicities is very high (B3LYP/6-31G(d)) (Figure 2d) and consequently enantiomeric conversion does not occur easily. For example, twisting non-tethered acenes from +43° to -43° requires overcoming a maximum energy barrier of only 1.5 kcal/mol compared with a barrier of nearly 50 kcal/mol to achieve the same twist in **Ant-C3**. Consequently, whereas non-tethered acenes readily form racemic mixtures (Figure 2d, purple trace), **Ant-C3** does not (Figure 2d, red trace).

### 3. How twisting affects the electronic and optical properties of twisted aromatics

HOMO and LUMO energy levels and the corresponding HLG determine the color and reactivity of polyaromatic materials, and are also major factors (together with morphology) in determining the performance of polyaromatic materials in electronic devices [30]. The HLG commonly decreases with increasing  $\pi$ -orbital overlap and increases when  $\pi$ -orbital overlap is disrupted, as this shortens the conjugation length

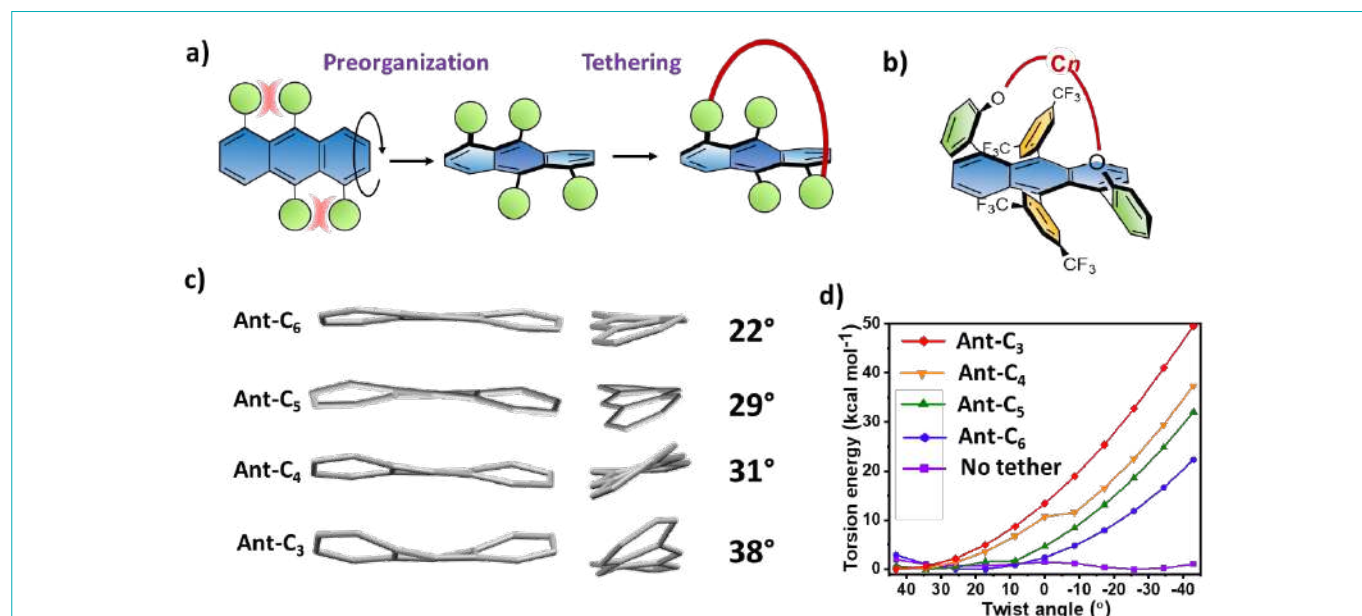


**Figure 2.** (a) Schematic representation of the synthetic concept for tethered twistacenes. The preorganization induced by the substituents is followed by intramolecular tethering. (b) The structure of **Ant-C $n$** . C3–6 = *n*-propyl to *n*-hexyl, respectively. (c) X-ray structures of the anthracene core for **Ant-C3** and the corresponding end-to-end dihedral angles. The substituents are removed for clarity. (d) Calculated (B3LYP/6-31G(d)) relative energies required to twist the acene cores of **Ant-C3** (red trace), **Ant-C4** (orange trace), **Ant-C5** (green trace), **Ant-C6** (blue trace), and untethered anthracene (purple trace). Adapted with permission from ref 29. Copyright 2019 American Chemical Society.

[28]. Twisting aromatics out of planarity is expected to impair  $\pi$ -conjugation whereas increasing planarity is expected to improve it and find expression in a bathochromic shift in the absorption spectrum. However, when measuring the absorbance of **Ant-C $n$** , which is inherently twisted, we were initially surprised to observe a bathochromic shift that increases with increasing twist (Figure 3a) [29]. DFT calculations support the observed bathochromic shift, and also provide evidence of a fundamental difference between twisting and bending acenes: whereas twisting increases the energy of the HOMO and decreases the energy of the LUMO, bending produces a similar increase in the energies of both the HOMO and LUMO (Figure 3b) [31]. Therefore, twisting acenes results in a bathochromic shift, while bending is not expected to result in a significant change in the absorption of the lowest energy transition.

We found that the fluorescence of acenes decays rapidly with twisting, with the fluorescence quantum efficiency decreasing from 30% to 5% upon twisting the anthracene core from 22° to 43° (Figure 3c) [28]. After a photon is excited to the

first excited state, it can potentially undergo decay back to the ground state via a radiative or non-radiative pathway. Alternatively, it can potentially undergo intersystem-crossing to an excited triplet state.

To investigate the reason for the observed twist-induced fluorescence quenching, we performed an ultrafast transient absorption study combined with time-resolved fluorescence measurements. We found that, as twisting increases, the rate of intersystem-crossing also increases [32]. Quantum chemical calculations indicate that this increase in intersystem crossing results from an increase in the spin-orbit coupling, rather than from changes in the relative energies of the singlet and triplet excited state. This provides a means of controlling the ISC rate, which is important because many processes such as thermally delayed activated fluorescence (TDAF) and triplet-triplet-annihilation (TTA), which can result in highly efficient organic light-emitting diodes (OLEDs), depend on harvesting emissions from triplet states [33, 34]. The degree of twisting also affects the reactivity: we found that twistacenes undergo Diels-Alder cycloaddition and cycloreversion with

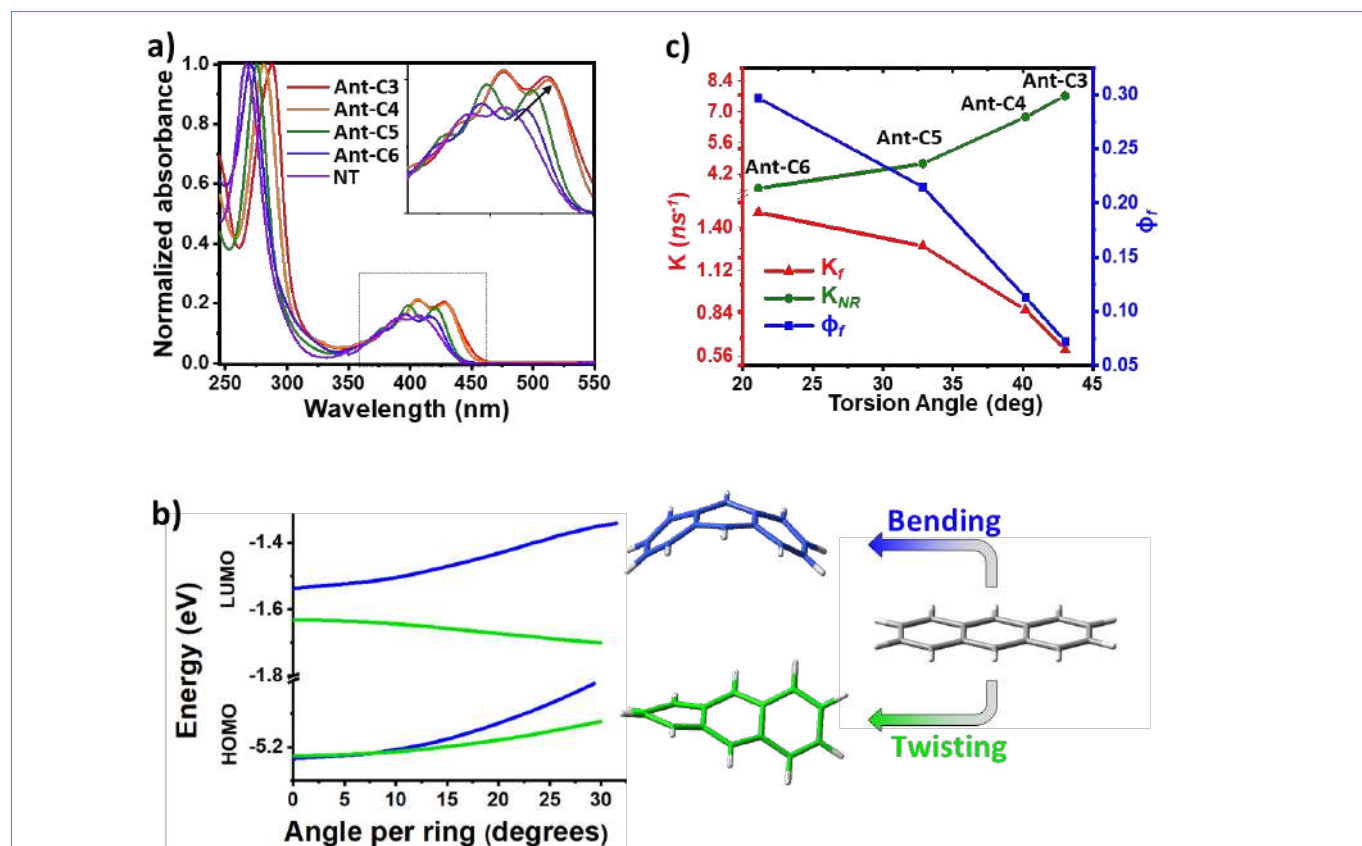


**Figure 3.** a) Experimental UV-vis spectra of **Ant-C $n$**  and of the untethered precursor anthracene (NT). (b) Calculated (B3LYP/6-31G(d)) HOMO and LUMO energies for twist vs. bent anthracene. (c)  $\phi_f$ ,  $k_f$ , and  $k_{NR}$  (fluorescence quantum efficiency, fluorescence lifetime and non-radiative lifetime, respectively) measured for **Ant-C $n$**  in chloroform vs the calculated (B3LYP/6-31G(d)) torsion angles. Reprinted with permission from refs. 28 and 31.

oxygen, and that the rate of Diels-Alder cycloaddition and cycloreversion increases with increasing twist, as observed both experimentally and computationally. This is explained by strain release which is more significant for highly-twisted systems [35].

#### 4. The effect of twisting on the absorption and emission of circularly polarized light

Chiral molecules have the propensity to absorb and emit circularly polarized (CP) light. In CP light, the electric and magnetic field vectors rotate perpendicularly to the direction of light propagation, either clockwise or counter-clockwise. CP light is applied in many technological fields, including in 3D displays, bio-responsive images, and quantum computing [36]. One important area is the development of OLEDs. In OLEDs that emit unpolarized light, antiglare filters are commonly added to eliminate glare from external light sources, but this approach filters out 50% of the emitted light and thereby greatly reduces device efficiency. In contrast, OLEDs possessing an enantiopure active layer are expected to emit CP light having only the desired handedness, thus CP-OLEDs are expected to exhibit greatly improved energy

efficiency over traditional OLEDs [37] and consequently constitute a very active area of research.

Our family of twistacenes, in which members possess different degrees of twist, allowed us to study how twisting affects the absorption and emission of CP light [38, 39]. We found that both the absorption and emission of CP light increase linearly with degree of twist (Figure 4). By contrast, the elongation of helicenes does not generate stronger chiroptical activity [8]. DFT-calculations indicate that, although the orientation of the electric and magnetic dipole moments ( $\mu_e$  and  $\mu_m$ , respectively) is never parallel in helicenes, in twistacenes these dipole moments are always parallel or antiparallel, regardless of their degree of twist, and thus they generate the maximal value for the rotational strength ( $R$ ) according to the equation  $R = \mu_e \mu_m \cos\Theta$ , where  $\Theta$  is the angle between  $\mu_e$  and  $\mu_m$  [40]. This renders twistacenes an ideal structural element for application as active materials in chiroptical devices. We also found that the combination of helical and axial chirality (as opposed to only helical chirality) greatly enhances the anisotropy of CP light [39].

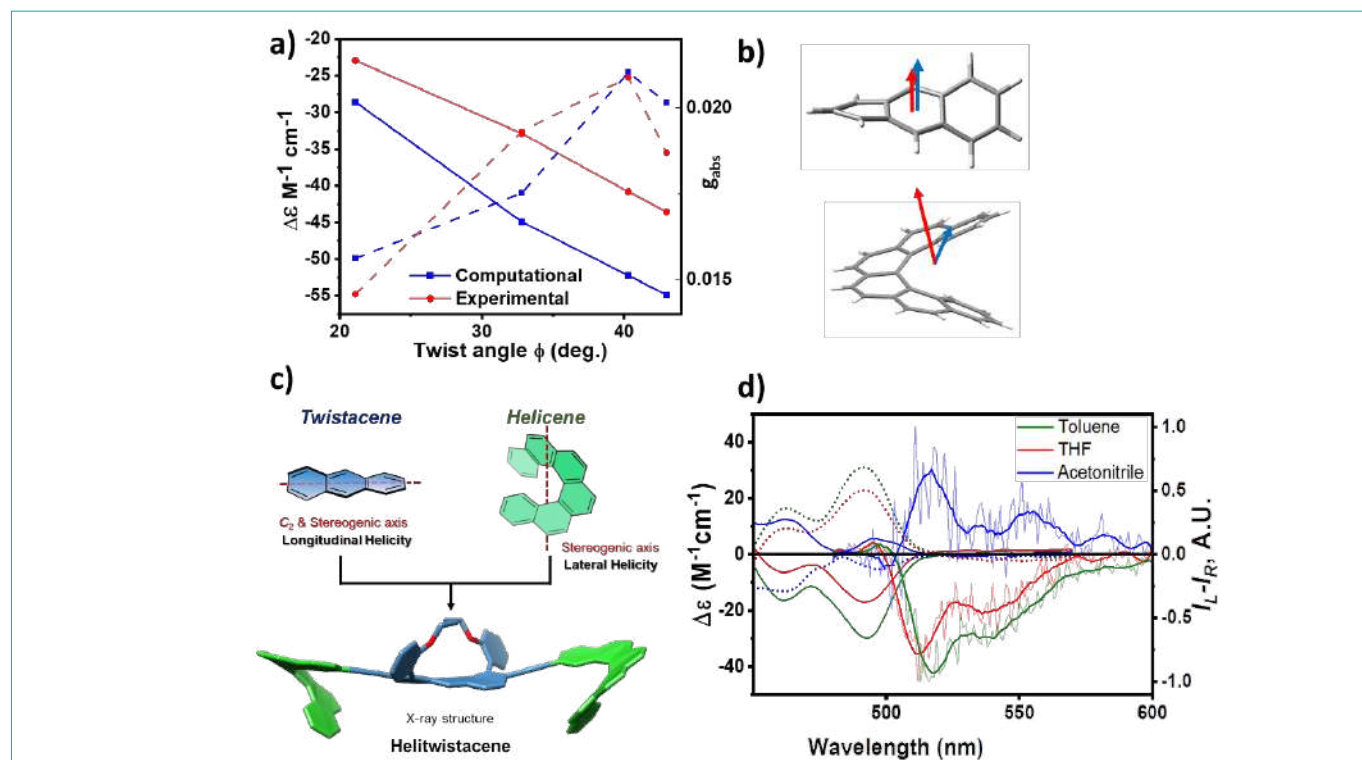


**Figure 4.** Computational (blue) and experimental (red) Cotton effects (solid lines) and anisotropy factors (dashed lines) for **Ant-Cn**. (b) Schematic representations of electric ( $\mu_e$ , blue) and magnetic ( $\mu_m$ , red) transition dipole moments of the lowest-energy transitions for anthracene at a 30° twist per benzene ring (top) and [6]helicene (bottom). Adapted from ref. 38. (c) Structure of helitwistacenes, combining [6]helicene and tethered twistacenes. (d) ECD and CPL of helitwistacenes with solvents of different polarity, showing sign inversion for the most polar solvent (acetonitrile). Reprinted from ref. 41.

Twistacenes and helicenes express chirality in different manners: in helicenes, the stereogenic axis crosses the interior void within the molecule and bisects the  $C_2$  axis, whereas the stereogenic axis of twistacenes is the  $C_2$  axis that runs the length of the aromatic backbone. Helical chirality is therefore expressed in lateral helicity in helicenes and in longitudinal helicity in twistacenes. By combining these two elements, tethered twistacenes and helicenes, we introduced a new family of compounds, which we termed helitwistacenes [41]. We found that, for both electronic circular dichroism (ECD) and circularly polarized light spectroscopy, signal sign is dependent on the extent of twisting, or on external factors such as solvent polarity, and we were able to show inversion of these signals upon modifying these factors (Figure 4c).

## 5. Conformational engineering of aromatic materials

The active layer in organic electronic devices comprises organic semiconductors, particularly  $\pi$ -conjugated oligomers and polymers, in place of the inorganic semiconductors traditionally used. In principle, the synthesis of electronic materials from organic compounds is expected to offer greater versatility than is obtainable from inorganic compounds. In particular, organic aromatics offer the possibility of using chemical means to tailor active materials to exhibit the small bandgaps required for efficient organic solar cells, the different colors in demand for use in organic light-emitting diodes and smart windows, and the high solubilities desired for increased processability.

Efforts to actualize the theoretical potential of organic electronics by developing synthetic approaches to obtaining

materials possessing a wide range of desired properties in a readily controllable manner have engaged my own and other research groups for many years. One widely researched approach is that of side-group engineering, in which the  $\pi$ -conjugated organic backbone is substituted with electron-accepting or -donating groups, solubilizing groups, or chiral units (Figure 5a). Alternatively, the main-chain engineering approach tunes material properties by incorporating different units into the  $\pi$ -conjugated backbone itself. Instead of changing the composition of the backbone, the third approach involves engineering its molecular conformation to obtain desired properties. Conformational engineering seeks to lock the conformation of the backbone and thereby control the degree of rotation around the backbone's inter-unit single bond (Figure 5b). Such locking is typically achieved via non-covalent interactions or functionalization of the backbone with sterically bulky side-groups. Interesting material properties, including thermally-activated delayed fluorescence (TADF, which is important for light-emitting devices) as a result of increased intersystem crossing to the triplet excited state, have been obtained by locking the degree of backbone rotation in this manner. Conformational locking can produce intrinsically helical  $\pi$ -conjugated backbones, and thus opens the way to chiral conducting polymers potentially possessing electron spin filtering and magneto-optic properties. However, conformational engineering is generally unpopular because it disrupts  $\pi$ -conjugation, thereby significantly impairing the semiconducting and aromatic properties of the backbone. Consequently, although helicity is crucial to fundamental biomolecules, such as DNA and proteins, it remains less common in synthetic  $\pi$ -conjugated

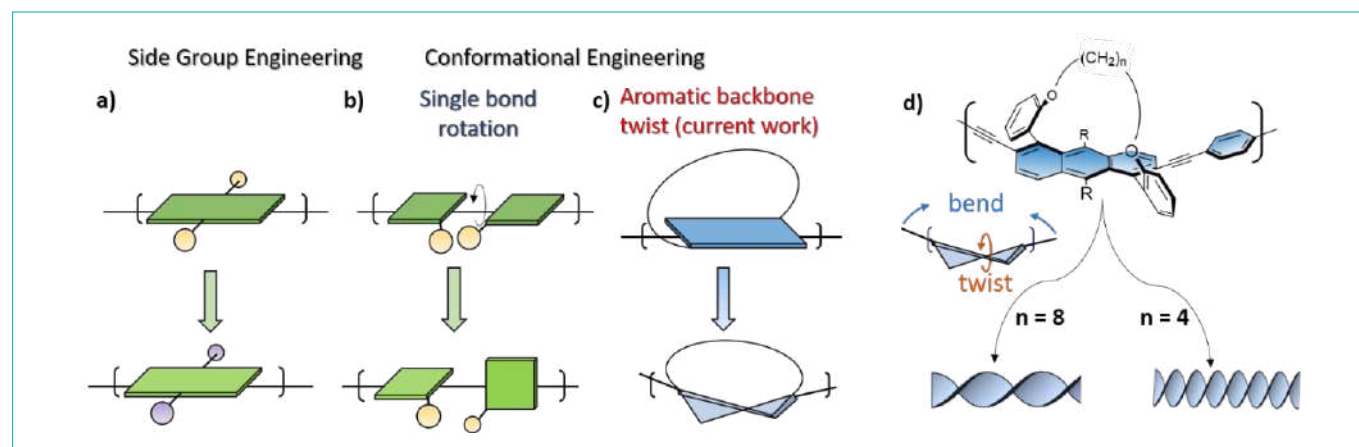


**Figure 5.** Methods for modulating the properties of organic  $\pi$ -conjugated backbones. (a) Side-group engineering. (b-c) Conformational engineering of the backbone by (b) rotation around inter-ring single bonds and (c) using an end-to-end tether of various lengths to twist a fused aromatic backbone in a tunable manner, as introduced by our group. (d) Molecular representation of **Ant-C $n$**  as the most promising of the tethered twistacene  $\pi$ -conjugated oligomers conceptualized in (c). The primary and secondary structures exhibited upon twisting and bending, respectively, the backbones of these twistacene oligomers (and, ultimately, the backbones of their polymers) exhibit varying degrees of helicity depending on the length of the tether ( $(CH_2)_n$ , where  $n = 4, 6$  or  $8$  methylene groups).  $R = CC(CH_3)_3$ . Adapted from ref. 43.

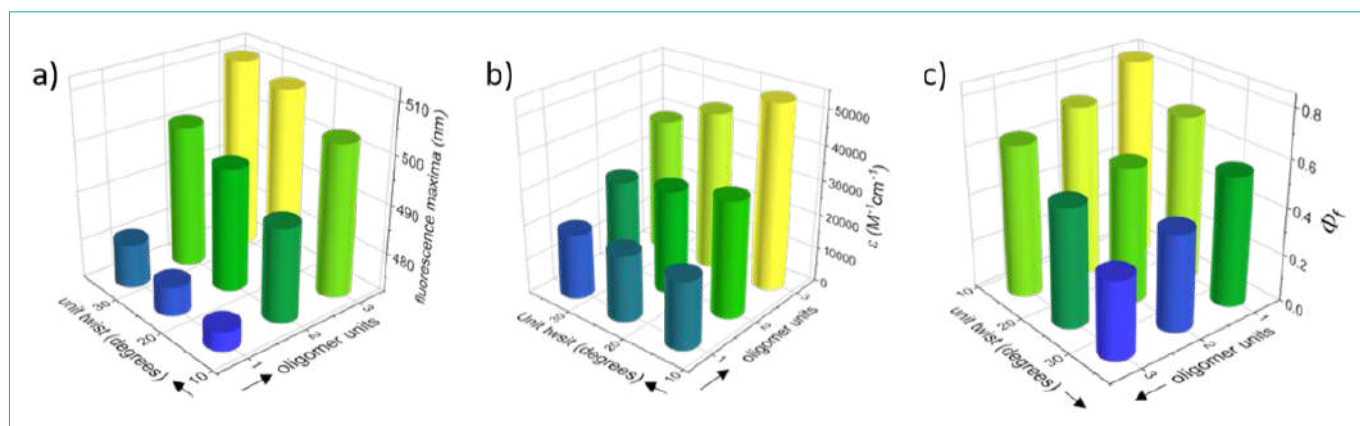


**Figure 6.** 3D graphs displaying the effect of backbone unit twist (Y axis) and backbone length (X axis) on (a) extinction coefficients at maximal absorption; (b) fluorescence maxima; and (c) fluorescence quantum yields ( $\Phi_f$ ). Adapted from ref. 43.

polymers. Prior to our recent work, the synthesis of a material characterized by both good  $\pi$ -conjugation (which typically requires molecular planarity to ensure good p orbital overlap) and helical chirality (which involves deviation from planarity by definition) was considered a contradiction in terms.

To achieve the goal of locking a controllable degree of twist into a  $\pi$ -conjugated backbone without impairing backbone conjugation required abandoning the notion of twisting around a single bond in favor of synthesizing an intrinsically twisted aromatic unit for subsequent polymerization (Figure 5c). Exploring this approach required that we first identify suitable monomeric units and then develop methods to synthesize them and to oligomerize and polymerize them.

The search for likely candidate molecules focused on acenes, as the most fundamental polyaromatic hydrocarbon, since they can be considered one dimensional nanographenes. We investigated several candidates computationally to identify the most promising twistacene unit, namely, **Ant-C $n$** , for which we then developed synthetic methods. As mentioned in section 2, backbone twisting is induced by an alkyl-ether tether covalently attached on the diagonal between the ends of the anthracene molecule, with twist angle controlled by the length of the tether. The optical and electronic properties of the resulting **Ant-C $n$**  building block are directly affected by the degree of twist. However twisting barely affects  $\pi$ -electron delocalization or conjugation, as shown by electron paramagnetic resonance (EPR) studies [42].

Having achieved synthesis of the basic building **Ant-C $n$**  building block, we then sought means to extend it. The controlled oligomerization and polymerization of a helical acene unit that is intrinsically twisted to varying degrees presents considerable synthetic challenges. We ultimately

overcame these challenges by using acetylene end-units as linkers to couple the building blocks to extend the monomer (**Ant-C $n$** ) to its dimer (**2-Ant-C $n$** ) and trimer (**3-Ant-C $n$** ), where the **C $n$**  tether contained 4, 6, or 8 methylene groups. Using this approach produces monomers, dimers, and trimers whose helicity remains controlled by the degree of twist imposed on the monomer by the tunable tether length (Figure 5d) [43].

Having introduced  $\pi$ -conjugated backbones with different conjugation lengths and twist angles, we explored the effect of both factors on the electronic, optical and chiroptical properties of the novel materials. We found that both backbone length and twist affect electronic and optical properties. Synergistic effects of increasing backbone length and twist affect properties such as the optical bandgap and the fluorescence maxima (Figure 6a), whereas antagonistic effects are observed for other properties, such as the extinction coefficient (Figure 6b). For fluorescence quantum efficiency, backbone twist has a greater effect than backbone length (Figure 6c).

As tethering induces not only backbone twist but also bends the backbone to various degrees, the polymer adopts a helical secondary structure. The secondary helical structure is expressed in chiroptical properties: backbones formed of units with a shorter tether (greater twist) show a non-linear increase in their maximum ellipticity. The non-linear nature of the increase suggests the occurrence of chiral amplification of the effects of the primary and secondary helical structures on incident circularly polarized light, with both helicities (and, consequently, their amplification) controlled by tether length. Indeed, calculated structures show that the tether controls not only the primary structure, but also the degree

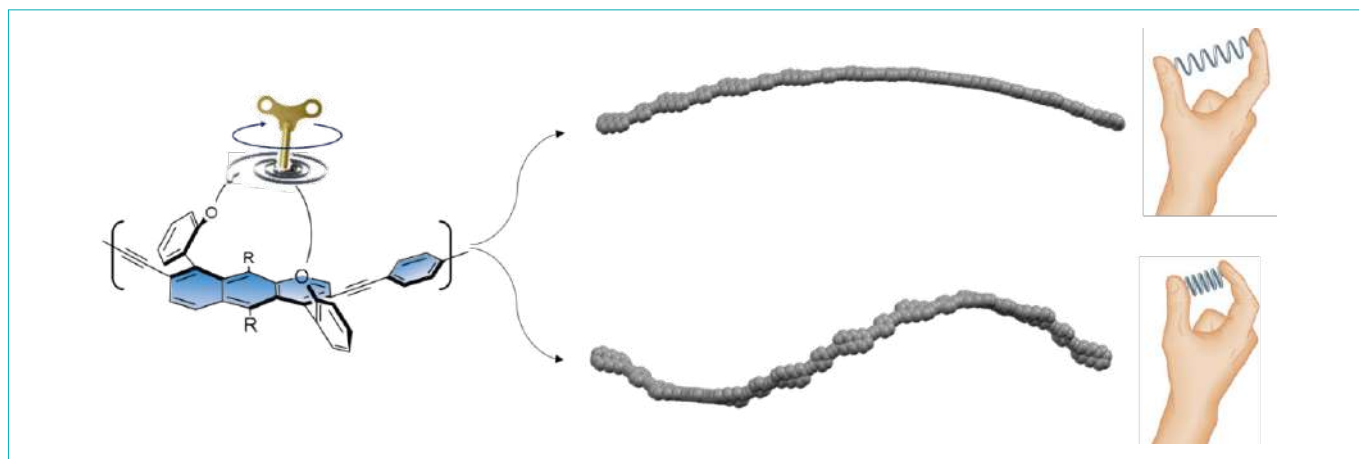


**Figure 7.** Conceptual representation of how tuning the tether length of the repeat aromatic unit results in oligomer or polymer backbones with different helicities. The two middle structures are calculated nonamer skeletons with end-to-end anthracene twists of either  $10^\circ$  or  $40^\circ$ . The pitch of the secondary helical structure is controlled by the tether length. Adapted from ref. 43.

of helicity of the secondary structure, allowing us to tune helicity while maintaining  $\pi$ -conjugation (Figure 7).

## 6. Summary and outlook

By twisting aromatic molecules out of planarity, we can control their electronic, (chiro)optical, and magnetic properties. This conformational engineering tool can either replace or be applied in addition to the more commonly used functionalization tool. The introduction of a family of helically-locked tethered twistacenes with different degrees of twisting allowed us to study the effect of twisting on the abovementioned properties, and also to include these building units in oligomers and polymers, thereby obtaining materials with new properties. One example of such materials are helitwistacenes, which display sign inversion in both the absorption and emission of CP light under different conditions. Nearly a 100 years after the Hückel approximation [44], it is clear that adding a ‘twist’ to aromatic compounds alters their properties, which can lead to new design principles for organic electronic and spintronic materials [45].

## References

1. A. T. Balaban, D. C. Oniciu and A. R. Katritzky, *Chem. Rev.*, 2004, **104**, 2777–2812.
2. V. G. S. Box and F. Jean-Mary, *J Mol Model*, 2001, **7**, 334–342.
3. E. Persch, O. Dumele and F. Diederich, *Angew. Chem. Int. Ed.*, 2015, **54**, 3290–3327.
4. S. R. Forrest and M. E. Thompson, *Chem. Rev.*, 2007, **107**, 923–925.
5. H. Huang, L. Yang, A. Facchetti and T. J. Marks, *Chem. Rev.*, 2017, **117**, 10291–10318.
6. M. Gingras, *Chem. Soc. Rev.*, 2013, **42**, 1051–1095.
7. K. Mori, T. Murase and M. Fujita, *Angew. Chem. Int. Ed.*, 2015, **54**, 6847–6851.
8. Y. Nakai, T. Mori and Y. Inoue, *J. Phys. Chem. A*, 2012, **116**, 7372–7385.
9. Y. Yang, R. C. da Costa, M. J. Fuchter and A. J. Campbell, *Nat. Photon.*, 2013, **7**, 634–638.
10. J. E. Anthony, *Angew. Chem. Int. Ed.*, 2008, **47**, 452–483.
11. M. Bendikov, F. Wudl and D. F. Perepichka, *Chem. Rev.*, 2004, **104**, 4891–4946.
12. M. Einzinger, T. Wu, J. F. Kompalla, H. L. Smith, C. F. Perkinson, L. Nienhaus, S. Wieghold, D. N. Congreve, A. Kahn, M. G. Bawendi and M. A. Baldo, *Nature*, 2019, **571**, 90–94.
13. T. Wang, P. Angulo-Portugal, A. Berdonces-Layunta, A. Jancarik, A. Gourdon, J. Holec, M. Kumar, D. Soler, P. Jelinek, D. Casanova, M. Corso, D. G. de Oteyza and J. P. Calupitan, *J. Am. Chem. Soc.*, 2023, **145**, 10333–10341.
14. K. J. Thorley and J. E. Anthony, *Isr. J. Chem.*, 2014, **54**, 642–649.
15. R. A. Pascal, *Chem. Rev.*, 2006, **106**, 4809–4819.
16. J. Xiao, H. M. Duong, Y. Liu, W. Shi, L. Ji, G. Li, S. Li, X.-W. Liu, J. Ma, F. Wudl and Q. Zhang, *Angew. Chem. Int. Ed.*, 2012, **51**, 6094–6098.
17. W. Fan, T. Winands, N. L. Doltsinis, Y. Li and Z. Wang, *Angew. Chem. Int. Ed.*, 2017, **56**, 15373–15377.
18. J. Lu, D. M. Ho, N. J. Vogelaar, C. M. Kraml, S. Bernhard, N. Byrne, L. R. Kim and R. A. Pascal, *J. Am. Chem. Soc.*, 2006, **128**, 17043–17050.
19. N. I. Nijegorodov and W. S. Downey, *J. Phys. Chem.*, 1994, **98**, 5639–5643.
20. M. Rickhaus, M. Mayor and M. Juriček, *Chem. Soc. Rev.*, 2016, **45**, 1542–1556.
21. P. G. Ghasemabadi, T. Yao and G. J. Bodwell, *Chem. Soc. Rev.*, 2015, **44**, 6494–6518.
22. C. J. Brown and A. C. Farthing, *Nature*, 1949, **164**, 915–916.
23. D. J. Cram and H. Steinberg, *J. Am. Chem. Soc.*, 1951, **73**, 5691–5704.
24. G. J. Bodwell, J. J. Fleming, M. R. Mannion and D. O. Miller, *J. Org. Chem.*, 2000, **65**, 5360–5370.

25. J. E. Norton and K. N. Houk, *J. Am. Chem. Soc.*, 2005, **127**, 4162–4163.
26. Y. Xiao, J. T. Mague, R. H. Schmehl, F. M. Haque and R. A. Pascal Jr., *Angew. Chem. Int. Ed.*, 2019, **58**, 2831–2833.
27. T. Otsubo, Y. Aso, F. Ogura, S. Misumi, A. Kawamoto and J. Tanaka, *Bull. Chem. Soc. Jpn.*, 1989, **62**, 164–170.
28. A. Bedi, L. J. W. Shimon and O. Gidron, *J. Am. Chem. Soc.*, 2018, **140**, 8086–8090.
29. A. Bedi and O. Gidron, *Acc. Chem. Res.*, 2019, **52**, 2482–2490.
30. M. Rusishvili, L. Grisanti, S. Laporte, M. Micciarelli, M. Rosa, R. J. Robbins, T. Collins, A. Magistrato and S. Baroni, *Phys. Chem. Chem. Phys.*, 2019, **21**, 8757–8766.
31. A. M. Armon, A. Bedi, V. Borin, I. Schapiro and O. Gidron, *Eur. J. Org. Chem.*, 2021, **2021**, 5424–5429.
32. P. Malakar, V. Borin, A. Bedi, I. Schapiro, O. Gidron and S. Ruhman, *Phys. Chem. Chem. Phys.*, 2022, **24**, 2357–2362.
33. R. J. Vázquez, J. H. Yun, A. K. Muthike, M. Howell, H. Kim, I. K. Madu, T. Kim, P. Zimmerman, J. Y. Lee and T. G. III, *J. Am. Chem. Soc.*, 2020, **142**, 8074–8079.
34. M. B. Smith and J. Michl, *Chem. Rev.*, 2010, **110**, 6891–6936.
35. A. Bedi, A. Manor Armon and O. Gidron, *Org. Lett.*, 2020, **22**, 7809–7813.
36. J. Crassous, M. J. Fuchter, D. E. Freedman, N. A. Kotov, J. Moon, M. C. Beard and S. Feldmann, *Nat Rev Mater*, 2023, **8**, 365–371.
37. L. Wan, Y. Liu, M. J. Fuchter and B. Yan, *Nat. Photon.*, 2023, **17**, 193–199.
38. A. Bedi and O. Gidron, *Chem. Eur. J.*, 2019, **25**, 3279–3285.
39. A. Bedi, G. Schwartz, U. Hananel, A. M. Armon, I. Shioukhi, G. Markovich and O. Gidron, *Chemical Communications*, 2023, **59**, 2011–2014.
40. N. Berova, L. D. Bari and G. Pescitelli, *Chem. Soc. Rev.*, 2007, **36**, 914–931.
41. I. Shioukhi, H. Batchu, G. Schwartz, L. Minion, Y. Deree, B. Bogoslavsky, L. J. W. Shimon, J. Wade, R. Hoffman, M. J. Fuchter, G. Markovich and O. Gidron, *Angew. Chem. Int. Ed.*, 2024, e202319318.
42. A. Bedi, R. Carmieli and O. Gidron, *Chem. Commun.*, 2019, **55**, 6022–6025.
43. A. Bedi, A. Manor Armon, Y. Diskin-Posner, B. Bogosalvsky and O. Gidron, *Nat. Commun.*, 2022, **13**, 451.
44. E. Hückel, *Z. Physik*, 1931, **70**, 204–286.
45. T. S. Metzger, H. Batchu, A. Kumar, D. A. Fedotov, N. Goren, D. K. Bhowmick, I. Shioukhi, S. Yochelis, I. Schapiro, R. Naaman, O. Gidron and Y. Paltiel, *J. Am. Chem. Soc.*, 2023, **145**, 3972–3977.

# Slippery science

## Oded Hod

School of Chemistry and The Raymond and Beverly Sackler Center for Computational Molecular and Materials Science

Email: [odedhod@tauex.tau.ac.il](mailto:odedhod@tauex.tau.ac.il)

### Abstract:

This is the story of a young man who, while standing at the office doorstep of one of the founding fathers of Israel's chemical physics community, overheard a sentence that shaped his entire career.

Many years ago, at the beginning of this millennium, I was walking around the green paths of the Givat Ram Campus of the Hebrew University of Jerusalem, breathing deeply the clean air, while “shopping” for a PhD position, as coined by my admirable teacher Prof. Ronnie Kosloff. At some point I found myself standing at the doorstep of the great Prof. Raphael Levine. Since my first eye opening quantum mechanics lesson with the late Prof. Victoria Buch, taken at the very same building, I knew that quantum dynamics is what I want to do for a living and that it will never fail to amaze me. This feeling strengthened profoundly when I studied the advanced counterparts of this course, taught skillfully by Prof. Kosloff during a semester-long strike on a sofa in his Jerusalem apartment with his children using him as their living playground, and by Prof. Levine himself. Raphy, if I may use his nickname, was standing in his office, his iconic pipe in his mouth, listening to a student, who seemed to be very convinced by what he had to say. A few minutes later, Raphy interrupted the poor student and said in his calm voice: “When I look in your eyes, I fail to identify the spark and urge to send experimentalists to their

laboratories.” Now, those who know me can testify that I am a Markovian person, namely, memory is not one of my strong skills. But this specific moment, I will remember till the end of my life. While I knew for a long time that I wanted to be a theoretician, this was the first time when I realized what theory was all about. This very moment shaped my entire independent career, as will soon become clear.

It was Prof. Michael Urbakh, who first introduced me to the field of nanotribology – the science of friction, wear, and lubrication at nanoscale interfaces. I was most amazed when he described the intriguing phenomenon of structural superlubricity, where the atomic lattices of two contacting rigid and flat surfaces form an incommensurate interface that slides with ultralow friction and exhibits friction coefficients lower than  $10^{-3}$ . When he described to me the pioneering 2004 experiment by Dienwiebel *et al.* [1], demonstrating that a twisted nanoscale interface between two graphitic surfaces slides with essentially zero friction (to within experimental error bars), I was truly stunned. What appealed to me the most was the intuitive explanation that he offered, demonstrated

**Oded Hod** received his BSc from the Hebrew University, Israel, in 1994 and his PhD from Tel-Aviv University, Israel, in 2005. After a postdoctoral fellowship at Rice University, USA, he joined Tel Aviv University in 2008. His research involves computational nanomaterials science including electronic structure, mechanical, electromechanical, and tribological properties, density functional theory, molecular electronics, and electron dynamics and thermodynamics in open quantum systems. Prof. Hod holds the Heinemann Chair of Physical Chemistry, and is an alumnus of the Global Young Academy and the Israel Young Academy. He received Tel-Aviv University's Rector's Award for Excellence in Teaching four times, the 2017 Kadar Family Award for Outstanding Research, the 2022 Tenne Family Prize for Nanoscale Sciences of the Israel Chemical Society, and the 2024 Tel Aviv University Rector's Prize for Teaching Innovation and Creativity.



simply by two egg-box foams that he keeps in his office, each representing the electron density profile associated with the atoms of a given surface (see Figure 1). When stacked in a commensurate configuration, the two foams strongly resist shear stress. This results from the fact that sliding in this case involves the simultaneous crossing of multiple potential energy barriers, all of which are relatively high. However, when twisted into an incommensurate configuration, effective cancellation of lateral forces occurs resulting in a dramatic reduction in the resistance of the foams to slide. In the case of two graphene surfaces sliding across each other a similar picture arises, where the egg box foam peaks are replaced by the electron clouds associated with each atomic site and resistance to sliding occurs due to Pauli repulsions between these electrons as they cross each other.

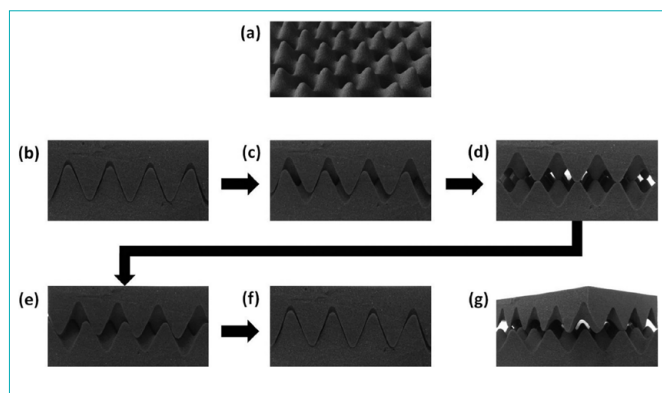


**Figure 1.** Egg-box foam model for commensurate and incommensurate sliding conditions. (a) Tilted view of a single egg-box lattice. (b)–(f) Relative sliding of two commensurate egg-box foams, where all unit cells cross high sliding barriers simultaneously. (g) A twisted incommensurate interface configuration, where some apexes slide uphill and other slide downhill, resulting in effective cancellation of lateral forces. Adapted with permission from *Phys. Rev. B* **86**, 075444 (2012).

This simple and intuitive explanation made me realize that in such interfaces there is an intimate relation between lattice geometry, interfacial commensurability, and friction. Inspired by this understanding we developed the registry index (RI) – a simple and intuitive geometric measure, based on projected overlaps of circles associated with atomic positions in adjacent surfaces, which quantifies the degree of commensurability of interfacing lattices [2-4]. Using this simple geometric tool, we were able to fully reproduce, down to fine details, not only the sliding potential energy surface, but also the measured twist angle dependence of the friction force at homogeneous nanoscale graphitic interfaces in both the high and ultralow friction regimes (see Figure. 2) [5].

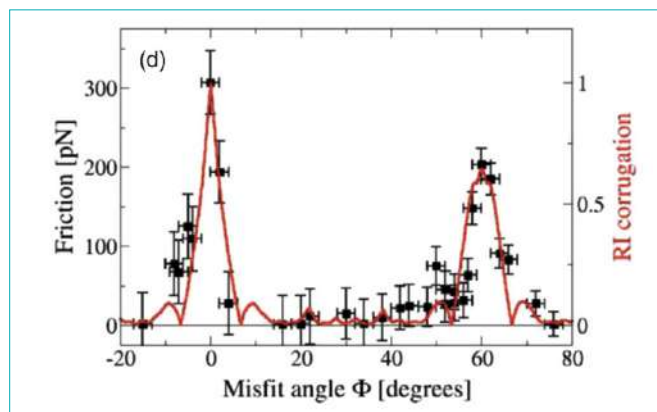


**Figure 2.** Measured friction (black circles; left axis) and corrugation of the registry index landscape (red line; right axis) as a function of the twist (misfit) angle for a hexagonal multilayer graphene flake sliding along the armchair direction of a graphite surface. Adapted with permission from *Phys. Rev. B* **86**, 075444 (2012).

The 2004 experiment by Dienwiebel *et al.* [1] generated great enthusiasm for the utilization of graphitic flakes to achieve large-scale superlubricity. Naively, one could suggest covering any two surfaces with a sufficiently thick graphite layer that will buffer the contact from the microscopic corrugation of the underlying substrates. Introducing graphitic flakes of random orientations into the flat interface would then result in multiple nanoscale junctions, most of which forming incommensurate contacts. This multi-nanocontact setup could then lead to macroscopic superlubricity, while avoiding the undesirable effects of large-scale surface elasticity. Unfortunately, this beautiful and simple idea was refuted by Filippov *et al.* in 2008, who showed that dynamical reorientation of the flakes aligns them at the lowest energy stacking which unfortunately is commensurate, such that the interface slides along the most highly corrugated potential energy path [6].

A few years later, the understanding that commensurability and friction are intimately related in layered material contacts led us to suggest a simple remedy to this problem [7]. Given that at the aligned configuration the homogeneous graphitic contact is commensurate, all that had to be done is to replace one of the contacting graphene surfaces by a similar surface of a different lattice parameter, thus forming a heterogeneous contact. The natural choice was hexagonal boron nitride (*h*-BN), which has the same hexagonal structure as graphene, but with boron and nitrogen atoms replacing each pair of adjacent carbon atoms. Since the two materials have a lattice mismatch of 1.8%, even at the aligned configuration, where the lattice vectors of the two surfaces are parallel to each other, an incommensurate flat contact is formed. In terms of the macroscopic analogy, one can imagine two egg-box foams

of different periodicity such that, even when aligned, they cannot be appropriately interlocked. In such a case, therefore, friction is expected to be small. To prove that this idea is feasible, we used the RI approach and showed that, indeed, as the area of the heterogeneous contact grows beyond the moiré supercell dimensions the corrugation of the sliding energy profile remains low regardless of the twist angle (see Figure 3). This suggested that heterogeneous contacts of layered materials should demonstrate superlubric behavior that is robust against dynamical twisting.

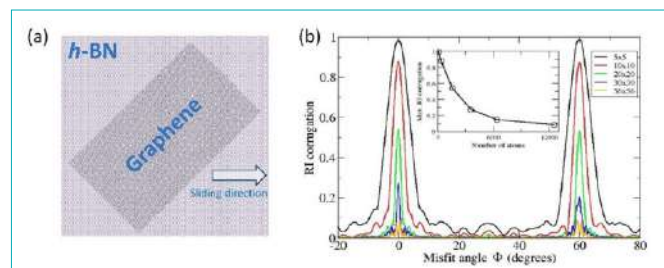


**Figure 3.** Effect of flake size and twist (misfit) angle on the corrugation of the sliding RI surface of the heterogeneous graphene/*h*-BN interface. (a) Schematic representation of a square graphene flake on top of an *h*-BN layer with a misfit angle of 45°. The sliding direction is marked by the white arrow. (b) Maximal variations of the RI calculated along linear paths in the sliding direction as a function of interlayer misfit angle. (Inset) Maximal RI corrugation as a function of flake size (number of atoms in the flake). The different diagrams presented in panel (b) are normalized to the size of the relevant graphene flake, such that a maximal RI corrugation of 1 is obtained for a strained graphene flake consisting of the same number of atoms and geometry having no lattice mismatch with the underlying *h*-BN layer. Adapted from *J. Phys. Chem. Lett.* **4**, 115–120 (2013) (published under CC-BY 4.0).

After giving a talk on this topic at a conference held in Beijing, China, Prof. Urbakh asked me to deliver a colloquium for the group of Prof. Quanshui Zheng of Tsinghua University. About two thirds into the colloquium, when I presented the idea of robust superlubricity, Prof. Zheng stopped me and started interrogating me regarding this specific prediction. About five minutes later, he halted and said: “I am going to measure this!” Well, this indeed is a decisive moment in the life of every theoretician. Someone is actually going to measure my prediction, I thought. What if it won’t work? Nonetheless, I finally had the opportunity to drive experimentalists to perform experiments, as Prof. Levine taught me, unwittingly, many years before.

A couple of years later and many sleepless nights of Prof. Zheng’s students, our prediction was finally verified [8–12]. Bravely, they considered layered material junctions of contact area, which is  $\sim 9,000,000$  times larger than the contact area studied in the canonical 2004 experiment. Yet, while the homogeneous graphitic contact presented very large frictional anisotropy, the heterogeneous system exhibited ultralow friction and superlubric behavior even for the aligned configuration (see Figure 4). Notably, these experiments were performed at room temperature and under ambient conditions, namely in the presence of surface contaminants. A simple run-in process was further shown to remove intercalated species from the sliding interface, pushing the system even further into the superlubric regime. Following that, several other experimental demonstrations of robust structural superlubricity in microscale heterogeneous interfaces have been presented in the literature, further demonstrating the generality of the effect [13].

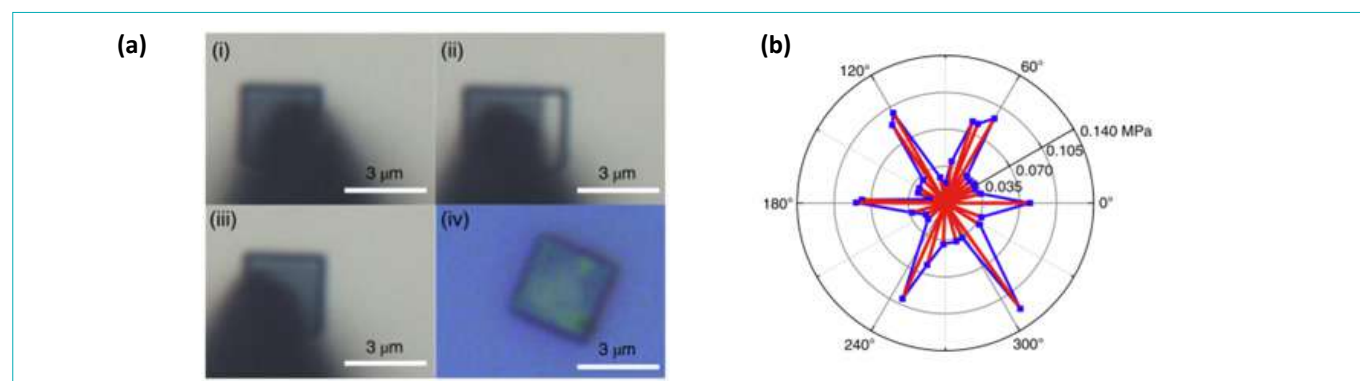


**Figure 4.** Experimental demonstration of robust superlubricity in a graphene/*h*-BN interface. (a) Optical images of a graphite/*h*-BN heterostructure fabrication. (i) Attachment of a tungsten probe to the SiO<sub>2</sub> cap of an HOPG mesa. (ii) Tungsten probe shearing of a graphitic mesa results in the drag of the mesa’s top section. (iii) Self-retraction motion exhibited by the dragged graphitic flake atop the lower graphite mesa section on release from the tungsten probe. (iv) Transfer of the graphitic flake onto the *h*-BN surface. (b) Dependence of the frictional stress on the twist angle between the monocrystalline graphitic flake and the *h*-BN substrate measured under ambient conditions (temperature of 22 ± 1 °C and relative humidity of 29 ± 3%). The sliding velocity was set to 200 nm/s and the normal load was kept at 19.7 μN. Adapted with permission from *Nat. Mater.* **17**, 894–899 (2018).

By harnessing some scientific intuition, a simple idea, basic geometric considerations, and a lot of luck we were therefore able to encourage experimentalists to perform groundbreaking studies that pushed the limits of structural superlubricity orders of magnitude forward. Following that, the powerful RI tool that we developed was extended to describe other homogeneous and heterogeneous layered material interfaces [7,14], curved contacts [3,15], as well as electric polarization profiles in non-centrosymmetrically stacked layered material interfaces [16]. Nonetheless, the RI approach assumes rigid interfaces, thus neglecting edge pinning effects and elastic considerations that may become vital to understand the mechanisms underlying friction in large-scale interfaces, especially when moiré superstructures emerge. To address these important issues, we had to resort to another computational resource, namely molecular dynamic simulations based on classical force-fields. Here, the story begins again with a twist, but this time of nanotubes. As kids in the small city of Rehovot, we used to play a little game called "קוצים" ("thorns"), where we twisted the skin on our friends' arms, giving them a prickly feeling. Many years later, Prof. Ernesto Joselevich of the Weizmann Institute of Science, who was my teaching assistant back in the previous millennium, had a habit of playing "thorns" with nanotubes. Using an ingenious experimental setup, he was able to twist the outer shell of multi-walled nanotubes and measure their mechanical and electronic response [17-18]. Being a young faculty member at the School of Chemistry of Tel Aviv University, I was quite surprised when Ernesto approached me asking whether I can perform simulations that will help provide an atomistic rationalization of the intriguing experimental results that he has obtained for twisted boron nitride nanotubes (BNNTs). With enthusiasm I approached my then graduate student, Dr. Itai Leven, and asked him to find an appropriate force-field for BNNTs. After a couple of days of literature search Itai came back with good news and bad news. The good news was that there exists a dedicated force-field, developed by Kolmogorov and Crespi, that appropriately accounts for the anisotropic nature of layered materials and can treat both the sliding and binding physics in layered interfaces [19-20]. The bad news was that this force-field was never parameterized for any interface, apart from bilayer graphene. This, in fact, turned out to be even better news, as it provided us with a whole new playground of opportunities for the development and parameterization of force-fields, dedicated to layered material interfaces, in the context of nano-tribology. After nearly ten years of work in collaboration with Michael, Prof. Leeor Kronik of the Weizmann Institute of Science, and several very talented students and post-doctoral fellows, our anisotropic interlayer potentials are currently publicly available for a variety of homogeneous and heterogeneous layered material interfaces composed of graphene, *h*-BN,

and several prominent members of the vast transition-metal dichalcogenides family [21-26].

These powerful simulation tools that provide a desirable compromise between physical accuracy and computational burden, allowed us to study a variety of interesting problems, and rationalize intriguing experimental findings. These include the faceting of multiwalled nanotubes [27-28]; frictional mechanisms of grain boundaries in polycrystalline surfaces [29-32]; bulk penetration of surface perturbations [33]; serpent-like motion, peeling, and direct growth of GNRs on semi-conducting surfaces [34-36]; surface reconstruction in marginally twisted layered interfaces leading to the emergence of ferroelectricity [37], and multi-contact superlubric interfaces of graphullerene and graphene [P. Ying, O. Hod, and M. Urbakh, *Superlubric Graphullerene Nano Lett.* **24**, 10599–10604 (2024)].

Beyond unveiling the mechanisms that underly existing experimental results, the developed force fields also have predictive power. This was demonstrated for the case of twist angle dependent interlayer heat transport through layered interfaces, which was predicted and explained computationally [38] prior to its experimental exploration [39]. It was also shown for the prediction of negative differential friction coefficients over moiré superstructures and grain boundaries in polycrystalline layered material surfaces [29-30, 40]. Here, a unique mechanism of energy dissipation at corrugated grain boundaries was identified, where a vertical snap-through motion of grain boundary protrusions results in enhanced energy dissipation into lattice phonon modes. The application of external normal load suppresses this out-of-plane motion and reduces the energy barrier associated with the snap-through process, resulting in a smoother transition and lower frictional energy loss. This prediction was recently verified experimentally for the friction over grain boundaries of polycrystalline graphene grown atop a Pt(111) surface [41].

Apart from grain boundaries, an additional source of friction that emerges with increasing contact area are surface defects, e.g. lattice vacancies, that may induce interlayer covalent bonding. This scenario eliminates the main computational advantage of treating anisotropic layered interfaces, namely the ability to distinctly distinguish between the description of intralayer and interlayer interactions. This, in turn, makes the development of traditional reactive anisotropic potentials a highly challenging task. A viable alternative that became available only in recent years can be found in machine learning potentials (MLPs). The main conceptual disadvantage of this methodology is that it lacks an explicit mathematical expression to describe the various interactions based on physical considerations. This blurs the

fundamental understanding of how individual interatomic interactions influence the overall properties and dynamical behavior of the system. Furthermore, since they do not utilize simple dedicated interaction expressions based on physical intuition, MLPs require extensive parameter sets and parameterization procedures, making them typically much more computationally demanding. Nonetheless, these apparent disadvantages mark also the main strengths of this approach as, given a sufficient large training set, often based on first-principles calculations and a large enough parameter set, the same machinery can, in principle, handle any scenario on the same footing, regardless of its complexity. Therefore, in the case of reactive sliding, where the distinction between intra- and inter-layer interactions becomes ill defined, we have recently adopted MLPs as a useful alternative to traditional physically motivated anisotropic force fields. This allows us to characterize the effects of structural defects and interlayer covalent bonding on the frictional properties of graphitic interfaces (see Figure 5 and P. Ying, X. Gao, A. Natan, M. Urbakh, and O. Hod, "Chemifrication and Superlubricity: Friends or Foes?", submitted (2024), and P. Ying, A. Natan, O. Hod, and M. Urbakh, "Effect of Interlayer Bonding on Superlubric Sliding of Graphene Contacts: A Machine-Learning Potential Study", *ACS Nano* **18**, 10133-10141 (2024)).

As discussed above, the scaling-up of robust structural superlubricity opens the door for novel friction-free and

wear-less technologies. Nonetheless, friction is often unjustly associated only with negative implications. In a recent study, we have been able to demonstrate how friction at the molecular level [42] can be harnessed to achieve enantio-separation [43-44]. Chiral molecules are molecules whose mirror image cannot be superimposed on their original structure, just like the palm of a human hand ( $\chi\epsilon\rho$  (kheir) in Greek). The two mirror image structures are called enantiomers. Notably, numerous bioactive molecules in living organisms are characterized by homo-chirality, e.g. chiral receptor molecules of a well-defined handedness. As a result, different enantiomers of chiral medical consumables may have different medicinal activity, to the point where one enantiomer may be of therapeutic benefit, whereas its mirror image can be toxic or harmful at the same dosage. Hence, the separation of enantiomers from of a racemic mixture is an important chemical process with vast pharmaceutical and economic implications. Traditional enantio-separation approaches are based on column chromatography technologies, where a dedicated chiral substrate selectively absorbs a given enantiomer over its counterpart. While this technology is very effective, it requires the development of specific chiral substrates for any given target molecule and is not environmentally friendly, considering the waste that obsolete substrates produce. Hence, the development of more generic, economically efficient, and green approaches is desirable. Here, friction may come into play.

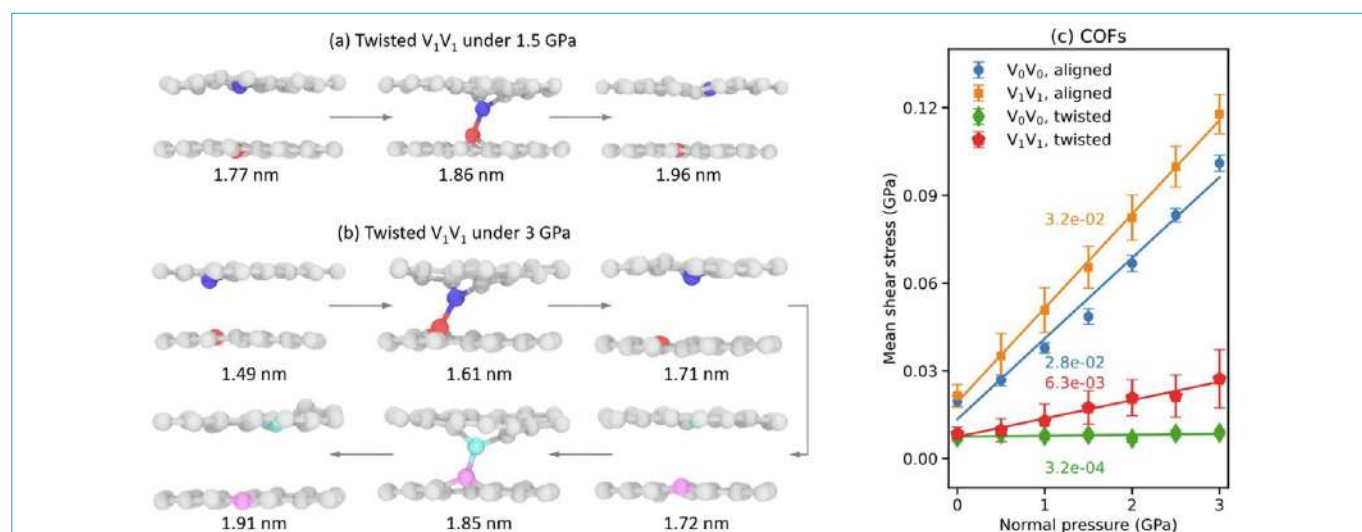


**Figure 5.** Results of MLP dynamical friction simulations of a double-vacancy defected graphene interface. (a) Snapshots from a twisted interface simulation trajectory, performed at room temperature and under an external pressure of 1.5 GPa, demonstrating a single bond formation and rupture event during sliding. (b) Same as panel (a) but under an external pressure of 3 GPa, where the system exhibits two consecutive events of bond formation and rupture. Only atoms in the vicinity of the defects are presented and atoms involved in interlayer bonding are highlighted. Lateral displacements are annotated below each snapshot. (c) Mean shear stress (averaged over a displacement of 5.2 nm of the ensemble-averaged trace) as a function of normal pressure for the aligned (orange) and twisted (red) double-defect interfaces. The defect density for the aligned and twisted interfaces are 0.24% and 0.34%, respectively. Results of the corresponding pristine interfaces are presented in blue and green, respectively. Adapted from *ACS Nano* **18**, 10133–10141 (2024) under CC-BY 4.0 license.

Imagine a soccer ball dropped on the surface of an ice-skating rink. The ball will bounce straight up regardless of if it was spinning about its center-of-mass or not. Should the ball be dropped over an asphalt surface, though, its spinning sense would dictate whether it would bounce forwards or backwards, due to the friction force acting at the contact region. By replacing the ball with a chiral molecule, whose rotational sense can be separately controlled for each of its enantiomers using an appropriate sequence of external electromagnetic pulses, frictional spatial enantio-separation may be achieved [43-44]. Since friction is a generic phenomenon, no specific substrate is required, and the only molecule-specific element in the separation procedure might be the design of the electromagnetic pulse train. Furthermore, since no adsorption is involved in the process, waste production and ecological signature are expected to considerably reduced.

At this point, you may have noticed that despite mentioning that I realized early on that quantum dynamics is what I want to do for a living, until now all I told you about revolves around classical mechanics. What I failed to disclose thus far is that many of the ideas that I mentioned actually emerged from my interest in, and work on, electron dynamics in open quantum systems. Being a PhD student at Tel Aviv University I had the privilege to be mentored by Prof. Eran Rabani and Prof. Roi Baer, and to take advanced courses in “Chemical Dynamics in Condensed Phases” by Prof. Abraham Nitzan, “Quantum Scattering Theory” by the late Prof. Abraham Ben-Reuven, and “Chemical Applications of Path Integrals” by Prof. Mordechai Bixon. Being in the department founded by the great Prof. Joshua Jortner and influenced by the spirit of these quantum dynamics founders and giants ignited my passion for the field of molecular electronics. I truly fell in love with the concept of being able to control electronic flow through molecular constrictions, design the junction properties via the chemical structure of the scattering center, and suggest new molecular scale electronic devices with novel functionalities.

My initial steps in this field were taken already during my PhD studies, where we predicted that one can use the Aharonov-Bohm effect to switch the conductance through a molecular ring by applying an external traversal magnetic field [45-51]. While this was well known for mesoscopic rings, because the response of the system is proportional to the magnetic flux it was widely accepted that molecular rings cannot exhibit such an effect with feasible magnetic fields, due to their small enclosed area. We have been able to show that while the full Aharonov-Bohm period in molecular rings remains way out of reach of present experimentally accessible magnetic fields, its sinusoidal shape can be altered by controlling the coupling between the circular molecule and the contacting metallic leads. Taking advantage of coherent interference

effects then allowed us to achieve sharp current response at low magnetic fields. This work served as a basis for later collaborative studies with Prof. Nitzan on the emergence of circular currents in molecular rings of various topologies [52-54].

I did not neglect my passion for quantum mechanics and dynamics during my post-doctoral term with Prof. Gustavo E. Scuseria at Rice University, Houston, Texas. There, I developed, in collaboration with Prof. Juan E. Peralta, a first-principles divide and conquer approach to study steady-state current characteristics of elongated molecular junctions [55]. We further developed a time-domain time-dependent density functional theory (TDDFT) code, within the Gaussian suite of programs, which allowed us to study spin dynamics in molecular magnets [56].

After establishing my own group, I set out on a quest to develop a theory and a computational scheme for the simulation of electron dynamics in open quantum systems, with emphasis on molecular electronics scenarios. The goal was to formulate a methodology that is theoretically simple, physically intuitive, and easy to implement, especially within the realm of TDDFT. I identified all three criteria in a method proposed separately by Sánchez et al. [57] and Subotnik et al. [58] that couples a finite model system, consisting of two explicit lead models and an extended molecule section (composed of the molecule and its adjacent lead sections) to external Fermionic leads of different thermal equilibria states, using the following augmented single-particle density-matrix-based Liouville–von Neumann (LvN) equation of motion (EOM):

$$\frac{d\rho(t)}{dt} = -\frac{i}{\hbar} [\mathbf{H}(t), \rho(t)] - \Gamma \begin{pmatrix} \rho_L - \rho_L^0 & \mathbf{0} & \rho_{L,R} \\ \mathbf{0} & \mathbf{0} & \mathbf{0} \\ \rho_{R,L} & \mathbf{0} & \rho_R - \rho_R^0 \end{pmatrix}, \quad (1)$$

where  $\hbar$  is the reduced Plank constant and  $i \equiv \sqrt{-1}$ . Here, the first term on the right-hand side is the standard propagator of the LvN EOM for a closed system, where  $\rho(t)$  is the single-particle density matrix, which in the block matrix representation has the following form:

$$\rho(t) = \begin{pmatrix} \rho_L & \rho_{L,EM} & \rho_{L,R} \\ \rho_{EM,L} & \rho_{EM} & \rho_{EM,R} \\ \rho_{R,L} & \rho_{R,EM} & \rho_R \end{pmatrix}, \quad (2)$$

and

$$\mathbf{H}(t) = \begin{pmatrix} \mathbf{H}_L & \mathbf{V}_{L,EM} & \mathbf{0} \\ \mathbf{V}_{EM,L} & \mathbf{H}_{EM} & \mathbf{V}_{EM,R} \\ \mathbf{0} & \mathbf{V}_{R,EM} & \mathbf{H}_R \end{pmatrix} \quad (3)$$

is the single particle Hamiltonian in the same block matrix representation. Here,  $\rho_i$  and  $H_i$  are the density and Hamiltonian matrix representation blocks of the left ( $i=L$ ) and right ( $i=R$ ) lead models, and the extended molecule ( $i=EM$ ) section, respectively, and  $\rho_{i,j}$  and  $V_{i,j}$  are the corresponding coherences and coupling blocks. For simplicity, direct lead-lead couplings are neglected. The second term on the right-hand side of Eq. (1) drives the lead state occupations towards Fermi-Dirac equilibrium distributions at a rate  $\Gamma$ , which can be determined from first principles [59], via diagonal block matrices  $(\rho_{i=L,R}^0)_{k,k'} = \delta_{k,k'} [1 + e^{(\epsilon_k^i - \mu_i)/(k_B T_i)}]^{-1}$ , where  $\{\epsilon_k^i\}$  are the sets of eigenenergies of the left and right lead sections  $\mu_i$  and  $T_i$  are the target chemical potentials and electronic temperatures of the leads, respectively, and  $k_B$  is the Boltzmann constant. This term effectively couples the left and right leads of the finite system, which are explicitly modeled, to two implicit reservoirs at different equilibria states, thus inducing dynamical current flow through the system.

I found the method to be so elegant and simple that immediately after reading the papers I implemented it for a tight-binding model. I was very happy to find out that it works extremely well in the case where the leads and the molecule are strongly coupled. However, in the weak-coupling limit, which is very common in the field of molecular electronics, it failed badly. Determined to remedy this, I joined forces with Leor, and together with our joint student, Dr. Tamar Zelovich, we set out to solve the problem. Over a period of a few months, we explored many ideas without success, and frustration led us to search for alternatives.

It may seem unrelated at first, but in my mail browser I have way too many folders, one of them though is a little treasure chest, which I call “ideas”. This is a folder where I file emails that I send to myself with ideas that come up every now and

then and I have no time to explore. While we were racking our brains trying to find out why the density-matrix approach fails to work at the most interesting and relevant limit, I sent myself several notes on ideas that I thought we should try. Unfortunately (or maybe fortunately), I did not have time to explore these ideas until one day, I and my daughter were ill and stayed at home. Suddenly, I found myself free of duties and my ideas mail folder was calling for me. I coded the first idea, namely the periodic resetting of the finite reservoir occupations and coherences every few time steps, and it failed. I then implemented the second idea, which involved an additional periodic resetting of the reservoir-system coherence blocks, and finally – it worked! After the initial thrill, I was still unsatisfied with this solution, which was based on an unphysical numerical trick. However, it provided very important insights regarding the missing ingredient in the original approach. By adding damping also to the reservoir-system coherence blocks, in the following manner:

$$\frac{d\rho(t)}{dt} = -\frac{i}{\hbar}[\mathbf{H}(t), \rho(t)] - \Gamma \begin{pmatrix} \rho_L - \rho_L^0 & \rho_{L,EM} & \rho_{L,R} \\ \rho_{EM,L} & \mathbf{0} & \rho_{EM,R} \\ \rho_{R,L} & \rho_{R,EM} & \rho_R - \rho_R^0 \end{pmatrix}, \quad (4)$$

everything finally worked like a charm. I was so excited that once I recovered from my illness, I rushed into Abraham Nitzan’s office and showed him the result. After a few seconds he answered: “Of course you have to damp the coherence matrix blocks, and by the way – you are missing a factor of 2.” He pointed me to his “Chemical Dynamics in Condensed Phases” book, which is based on his courses that I took ages before, and showed me the proof for the missing factor of 2. Luckily, I failed to understand the proof, so I came up with an alternative heuristic derivation (based on the substitution of a non-Hermitian Hamiltonian within the LvN EOM) of what

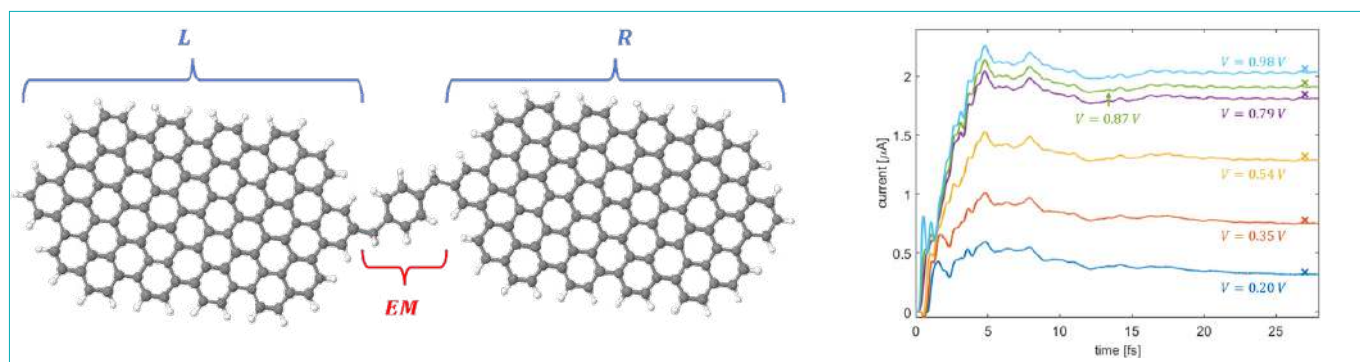


**Figure 6.** Demonstration of a TDDFT transport simulation using the DLvN approach. (a) Real-space formal partitioning of a molecular junction model composed of two finite graphene nanoribbons bridged by a benzene molecule, into left (L) and right (R) lead sections and an extended molecule (EM) region. (b) Time-dependent current calculated for the GNR junction shown in panel (a). Different bias voltages are considered (all values are marked in the figure) with reservoir electronic temperatures of  $T_L = T_R = 315.7$  K and a driving rate of  $\hbar\Gamma = 1.09$  eV. The colored  $\times$  marks designate the corresponding steady-state currents. Adapted with permission from *J. Chem. Theory Comput.* **19**, 7496–7504 (2023).

is now termed the driven Liouville von Neumann (DLvN) EOM [60-61]:

$$\frac{d\rho(t)}{dt} = -\frac{i}{\hbar} [\mathbf{H}(t), \rho(t)] - \Gamma \begin{pmatrix} \rho_L - \rho_L^0 & \frac{1}{2}\rho_{L,EM} & \rho_{L,R} \\ \frac{1}{2}\rho_{EM,L} & 0 & \frac{1}{2}\rho_{EM,R} \\ \rho_{R,L} & \frac{1}{2}\rho_{R,EM} & \rho_R - \rho_R^0 \end{pmatrix}. \quad (5)$$

It was only after deriving this EOM, when I realized that at the doorstep of my office there is an engraved tile designed by the late Prof. Ben-Reuven, who was the former resident of this office, with an equation that is reminiscent of the DLvN EOM. At this point I was also able to identify a misprint in the engraved equation, which you are more than welcome to explore next time you visit me.

The application of a simple unitary transformation to the EOM, termed the site-to-state transformation, allowed us to extend the applicability of the approach beyond phenomenological models to atomistic descriptions of realistic molecular junctions [59, 62-65]. This, in turn, paved the way for the application of the approach within the realm of TDDFT (see Figure. 6) [66]. Furthermore, the approach was shown to constitute an efficient numerical scheme to study the thermodynamic properties of open quantum systems [67-68]. I note in passing that the driving term appearing in Eq. (5) and the site-to-state transformation served as inspiration for the application of remote thermal baths and for the analyses of results obtained in some of our classical molecular dynamics simulations, such as the study of heat transport through twisted layered material interfaces [38].

Very recently, another related circle was closed, when I was approached by Prof. Harry Anderson of the University of Oxford, a world expert in the synthesis of macrocyclic molecules, regarding the possibility of measuring Aharonov-Bohm current switching in molecular rings. It is hard to describe the thrill that I experienced while realizing that my old studies with Profs. Rabani, Baer, and Nitzan triggered the interest of a leading chemist, such as Prof. Anderson. These days, we are finalizing our first manuscript on the subject, demonstrating that the experimental realization of our predictions of molecular Aharonov-Bohm interferometry is on the verge of being within our reach with present technologies.

Developing theoretical tools and computational methodologies that enable the prediction of novel physical phenomena, which eventually leads to experimental efforts towards their verification and utilization, is for me a great privilege. It fully complies with the important philosophical lesson that I unintentionally learned from Prof. Levine regarding the scientific role of theory and computation. I apologize in advance to many other people, teachers, colleagues, students,

friends, and supporters, who have deeply influenced my career and life, but unfortunately could not be mentioned as I ran out of space. You all know who you are, many of you appear in the citation list below, and I am grateful for everything you did for and with me. Having said that, none of the above could have happened without the support of my wonderful parents, Dr. Emila Freibrun and Prof. Israel (Izzy) Hod, who implanted in me curiosity and the love for science and supported me in any possible way; my amazing wife, Adi, who sacrificed so much so I could proceed with my career and supported me (and continues to do so) unconditionally throughout this long and fascinating journey; my perfect daughters Ophir, Ariel, and Elah for shining their light and teaching us the meaning of life; and my brothers and sister, Nir, Shahar, and Sivan, for serving as role models, each in their own field. Finally, it is far from being time for summaries. There are still many more little treasures to explore in my "ideas" email folder. The eternal dance between theory, computation, and experiment, in which I am honored to play even the tiniest role, continues.

## Acknowledgment

O.H. is grateful for the generous financial support of the Heinemann Chair of Physical Chemistry.

## References

1. M. Dienwiebel *et al.*, Superlubricity of Graphite. *Phys. Rev. Lett.* **92**, 126101 (2004).
2. N. Marom *et al.*, Stacking and Registry Effects in Layered Materials: The Case of Hexagonal Boron Nitride. *Phys. Rev. Lett.* **105**, 046801 (2010).
3. O. Hod, Quantifying the Stacking Registry Matching in Layered Materials. *Isr. J. Chem.* **50**, 506-514 (2010).
4. O. Hod, The Registry Index: A Quantitative Measure of Materials' Interfacial Commensurability. *ChemPhysChem* **14**, 2376-2391 (2013).
5. O. Hod, Interlayer Commensurability and Superlubricity in Rigid Layered Materials. *Phys. Rev. B* **86**, 075444 (2012).
6. A. E. Filippov, M. Dienwiebel, J. W. M. Frenken, J. Klafter, M. Urbakh, Torque and Twist Against Superlubricity. *Phys. Rev. Lett.* **100**, 046102 (2008).
7. I. Leven, D. Krepel, O. Shemesh, O. Hod, Robust Superlubricity in Graphene/h-BN Heterojunctions. *J. Phys. Chem. Lett.* **4**, 115-120 (2013).
8. D. Wang *et al.*, Thermally Induced Graphene Rotation on Hexagonal Boron Nitride. *Phys. Rev. Lett.* **116**, 126101 (2016).
9. D. Mandelli, I. Leven, O. Hod, M. Urbakh, Sliding Friction of Graphene/Hexagonal-Boron Nitride Heterojunctions: a Route to Robust Superlubricity. *Sci. Rep.* **7**, 10851 (2017).
10. Y. Song *et al.*, Robust Microscale Superlubricity in Graphite/Hexagonal Boron Nitride Layered Heterojunctions. *Nat. Mater.* **17**, 894-899 (2018).

11. O. Hod, E. Meyer, Q. Zheng, M. Urbakh, Structural Superlubricity and Ultralow Friction Across the Length Scales. *Nature* **563**, 485-492 (2018).
12. R. Ribeiro-Palau *et al.*, Twistable Electronics with Dynamically Rotatable Heterostructures. *Science* **361**, 690-693 (2018).
13. M. Liao *et al.*, Ultra-Low Friction and Edge-Pinning Effect in Large-Lattice-Mismatch van der Waals Heterostructures. *Nat. Mater.* **21**, 47-53 (2022).
14. A. Blumberg, U. Keshet, I. Zaltsman, O. Hod, Interlayer Registry to Determine the Sliding Potential of Layered Metal Dichalcogenides: The Case of 2H-MoS<sub>2</sub>. *J. Phys. Chem. Lett.* **3**, 1936-1940 (2012).
15. I. Oz *et al.*, Nanotube Motion on Layered Materials: A Registry Perspective. *J. Phys. Chem. C* **120**, 4466-4470 (2016).
16. W. Cao, O. Hod, M. Urbakh, Interlayer Registry Dictates Interfacial 2D Material Ferroelectricity. *ACS Appl. Mater. Interfaces* **14**, 57492-57499 (2022).
17. E. Joselevich, Twisting Nanotubes: From Torsion to Chirality. *ChemPhysChem* **7**, 1405-1407 (2006).
18. J. Garel *et al.*, Ultrahigh Torsional Stiffness and Strength of Boron Nitride Nanotubes. *Nano Letters* **12**, 6347-6352 (2012).
19. A. N. Kolmogorov, V. H. Crespi, Registry-Dependent Interlayer Potential for Graphitic Systems. *Phys. Rev. B* **71**, 235415 (2005).
20. M. Reguzzoni, A. Fasolino, E. Molinari, M. C. Righi, Potential Energy Surface for Graphene on Graphene: Ab Initio Derivation, Analytical Description, and Microscopic Interpretation. *Phys. Rev. B* **86**, 245434 (2012).
21. I. Leven, I. Azuri, L. Kronik, O. Hod, Inter-Layer Potential for Hexagonal Boron Nitride. *J. Chem. Phys.* **140**, 104106 (2014).
22. I. Leven, T. Maaravi, I. Azuri, L. Kronik, O. Hod, Interlayer Potential for Graphene/h-BN Heterostructures. *J. Chem. Theory Comput.* **12**, 2896-2905 (2016).
23. T. Maaravi, I. Leven, I. Azuri, L. Kronik, O. Hod, Interlayer Potential for Homogeneous Graphene and Hexagonal Boron Nitride Systems: Reparametrization for Many-Body Dispersion Effects. *J. Phys. Chem. C* **121**, 22826-22835 (2017).
24. W. Ouyang, O. Hod, R. Guerra, Registry-Dependent Potential for Interfaces of Gold with Graphitic Systems. *J. Chem. Theory Comput.* **17**, 7215-7223 (2021).
25. W. Ouyang *et al.*, Anisotropic Interlayer Force Field for Transition Metal Dichalcogenides: The Case of Molybdenum Disulfide. *J. Chem. Theory Comput.* **17**, 7237-7245 (2021).
26. W. Jiang *et al.*, Anisotropic Interlayer Force Field for Group-VI Transition Metal Dichalcogenides. *J. Phys. Chem. A* **127**, 9820-9830 (2023).
27. I. Leven, R. Guerra, A. Vanossi, E. Tosatti, O. Hod, Multiwalled Nanotube Faceting Unravelling. *Nat. Nanotechnol.* **11**, 1082-1086 (2016).
28. R. Guerra, I. Leven, A. Vanossi, O. Hod, E. Tosatti, Smallest Archimedean Screw: Facet Dynamics and Friction in Multiwalled Nanotubes. *Nano Lett.* **17**, 5321-5328 (2017).
29. X. Gao, W. Ouyang, O. Hod, M. Urbakh, Mechanisms of Frictional Energy Dissipation at Graphene Grain Boundaries. *Phys. Rev. B* **103**, 045418 (2021).
30. X. Gao, W. Ouyang, M. Urbakh, O. Hod, Superlubric Polycrystalline Graphene Interfaces. *Nat. Commun.* **12**, 5694 (2021).
31. X. Gao, M. Urbakh, O. Hod, Stick-Slip Dynamics of Moiré Superstructures in Polycrystalline 2D Material Interfaces. *Phys. Rev. Lett.* **129**, 276101 (2022).
32. Y. Song *et al.*, Velocity Dependence of Moiré Friction. *Nano Lett.* **22**, 9529-9536 (2022).
33. D. Mandelli, W. Ouyang, M. Urbakh, O. Hod, The Princess and the Nanoscale Pea: Long-Range Penetration of Surface Distortions into Layered Materials Stacks. *ACS Nano* **13**, 7603-7609 (2019).
34. W. Ouyang, D. Mandelli, M. Urbakh, O. Hod, Nanoserpents: Graphene Nanoribbon Motion on Two-Dimensional Hexagonal Materials. *Nano Lett.* **18**, 6009-6016 (2018).
35. W. Ouyang, O. Hod, M. Urbakh, Registry-Dependent Peeling of Layered Material Interfaces: The Case of Graphene Nanoribbons on Hexagonal Boron Nitride. *ACS Appl. Mater. Interfaces* **13**, 43533-43539 (2021).
36. B. Lyu *et al.*, Catalytic Growth of Ultralong Graphene Nanoribbons on Insulating Substrates. *Adv. Mater.* **34**, 2200956 (2022).
37. M. Vizner Stern *et al.*, Interfacial Ferroelectricity by van der Waals Sliding. *Science* **372**, 1462-1466 (2021).
38. W. Ouyang, H. Qin, M. Urbakh, O. Hod, Controllable Thermal Conductivity in Twisted Homogeneous Interfaces of Graphene and Hexagonal Boron Nitride. *Nano Lett.* **20**, 7513-7518 (2020).
39. S. E. Kim *et al.*, Extremely Anisotropic van der Waals Thermal Conductors. *Nature* **597**, 660-665 (2021).
40. D. Mandelli, W. Ouyang, O. Hod, M. Urbakh, Negative Friction Coefficients in Superlubric Graphite--Hexagonal Boron Nitride Heterojunctions. *Phys. Rev. Lett.* **122**, 076102 (2019).
41. Y. Song *et al.*, Non-Amontons Frictional Behaviors of Grain Boundaries at Layered Material Interfaces. *Submitted*, (2023).
42. R. Pawlak *et al.*, Single-Molecule Tribology: Force Microscopy Manipulation of a Porphyrin Derivative on a Copper Surface. *ACS Nano* **10**, 713-722 (2016).
43. Y. Chen, L. Xu, M. Urbakh, O. Hod, Spatial Separation of Enantiomers by Field-Modulated Surface Scattering. *J. Phys. Chem. C* **127**, 10997-11004 (2023).
44. Y. Chen, O. Hod, Chirality Induced Spin Selectivity: A Classical Spin-Off. *J. Chem. Phys.* **158**, 244102 (2023).
45. O. Hod, R. Baer, E. Rabani, Feasible Nanometric Magnetoresistance Devices. *J. Phys. Chem. B* **108**, 14807-14810 (2004).
46. O. Hod, E. Rabani, R. Baer, Magnetoresistance Devices Based on Single-Walled Carbon Nanotubes. *J. Chem. Phys.* **123**, 051103-051104 (2005).
47. O. Hod, R. Baer, E. Rabani, A Parallel Electromagnetic Molecular Logic Gate. *J. Am. Chem. Soc.* **127**, 1648-1649 (2005).
48. O. Hod, E. Rabani, R. Baer, Magnetoresistance of Nanoscale Molecular Devices. *Acc. Chem. Res.* **39**, 109-117 (2005).

49. O. Hod, R. Baer, E. Rabani, Inelastic Effects in Aharonov-Bohm Molecular Interferometers. *Phys. Rev. Lett.* **97**, 266803 (2006).
50. G. Cohen, O. Hod, E. Rabani, Constructing Spin Interference Devices from Nanometric Rings. *Phys. Rev. B* **76**, 235120 (2007).
51. O. Hod, R. Baer, E. Rabani, Magnetoresistance of Nanoscale Molecular Devices Based on Aharonov–Bohm Interferometry. *J. Phys: Condens. Matter* **20**, 383201 (2008).
52. D. Rai, O. Hod, A. Nitzan, Circular Currents in Molecular Wires. *J. Phys. Chem. C* **114**, 20583-20594 (2010).
53. D. Rai, O. Hod, A. Nitzan, Magnetic Field Control of the Current through Molecular Ring Junctions. *J. Phys. Chem. Lett.* **2**, 2118-2124 (2011).
54. D. Rai, O. Hod, A. Nitzan, Magnetic Fields Effects on the Electronic Conduction Properties of Molecular Ring Structures. *Phys. Rev. B* **85**, 155440 (2012).
55. O. Hod, J. E. Peralta, G. E. Scuseria, First-Principles Electronic Transport Calculations in Finite Elongated Systems: A Divide and Conquer Approach. *J. Chem. Phys.* **125**, 114704 (2006).
56. J. E. Peralta, O. Hod, G. E. Scuseria, Magnetization Dynamics from Time-Dependent Noncollinear Spin Density Functional Theory Calculations. *J. Chem. Theory Comput.* **11**, 3661-3668 (2015).
57. C. G. Sánchez *et al.*, Molecular Conduction: Do Time-Dependent Simulations Tell You More Than the Landauer Approach? *J. Chem. Phys.* **124**, 214708 (2006).
58. J. E. Subotnik, T. Hansen, M. A. Ratner, A. Nitzan, Nonequilibrium Steady State Transport via the Reduced Density Matrix Operator. *J. Chem. Phys.* **130**, 144105 (2009).
59. T. Zelovich *et al.*, Parameter-Free Driven Liouville-von Neumann Approach for Time-Dependent Electronic Transport Simulations in Open Quantum Systems. *J. Chem. Phys.* **146**, 092331 (2017).
60. T. Zelovich, L. Kronik, O. Hod, State Representation Approach for Atomistic Time-Dependent Transport Calculations in Molecular Junctions. *J. Chem. Theor. Comput.* **10**, 2927-2941 (2014).
61. O. Hod, L. Kronik, The Driven Liouville von Neumann Approach to Electron Dynamics in Open Quantum Systems. *Isr. J. Chem.* **63**, e202300058 (2023).
62. T. Zelovich, L. Kronik, O. Hod, Molecule–Lead Coupling at Molecular Junctions: Relation between the Real- and State-Space Perspectives. *J. Chem. Theory and Comput.* **11**, 4861-4869 (2015).
63. O. Hod, C. A. Rodríguez-Rosario, T. Zelovich, T. Frauenheim, Driven Liouville von Neumann Equation in Lindblad Form. *J. Phys. Chem. A* **120**, 3278-3285 (2016).
64. T. Zelovich, L. Kronik, O. Hod, Driven Liouville von Neumann Approach for Time-Dependent Electronic Transport Calculations in a Nonorthogonal Basis-Set Representation. *J. Phys. Chem. C* **120**, 15052-15062 (2016).
65. T. Maaravi, O. Hod, Simulating Electron Dynamics in Open Quantum Systems under Magnetic Fields. *J. Phys. Chem. C* **124**, 8652-8662 (2020).
66. A. Oz, A. Nitzan, O. Hod, J. E. Peralta, Electron Dynamics in Open Quantum Systems: The Driven Liouville-von Neumann Methodology within Time-Dependent Density Functional Theory. *J. Chem. Theory Comput.* **19**, 7496-7504 (2023).
67. I. Oz, O. Hod, A. Nitzan, Evaluation of Dynamical Properties of Open Quantum Systems Using the Driven Liouville-von Neumann Approach: Methodological Considerations. *Mol. Phys.* **117**, 2083-2096 (2019).
68. A. Oz, O. Hod, A. Nitzan, Numerical Approach to Nonequilibrium Quantum Thermodynamics: Nonperturbative Treatment of the Driven Resonant Level Model Based on the Driven Liouville von-Neumann Formalism. *J. Chem. Theory Comput.* **16**, 1232-1248 (2020).

# Additive manufacturing: from 2D to 4D printing

**Doron Kam, May Yam Moshkovitz, Ouriel Blich, Alexander Kamyshny, and Shlomo Magdassi\***

Institute of Chemistry, The Hebrew University of Jerusalem, Jerusalem, 9190401 Israel

\*Email: [magdassi@mail.huji.ac.il](mailto:magdassi@mail.huji.ac.il)

## Abstract:

Additive manufacturing (AM), revolutionizing traditional fabrication processes, is based on precise material deposition with various printing technologies. Our research group focuses on investigating and developing new printing materials, mainly based on colloid chemistry, ink formulation, material property control, and suitability for the various printing processes. Our journey begins with 2D printing, particularly in printed electronics, where nanotechnology and innovative inks play a crucial role. The evolution to 3D printing introduces a paradigm shift, enabling the creation of intricate structures with unprecedented precision, utilizing materials ranging from wood to hydrogels and inorganics. Next, we move into the emerging field of 4D printing, which is 3D structures that can change their structure as a response to external stimuli. 4D printing enables the creation of drug-loaded systems, shape-memory polymers, and sophisticated soft robotics devices. Throughout this journey, the interplay between material science, engineering, and applications across various industries propels the discoveries in additive manufacturing. In this manuscript, we will present some of the major activities performed by our research group in the field of materials for functional printing.

## Introduction

Additive manufacturing (AM) has revolutionized traditional manufacturing paradigms by directly enabling layer-by-layer construction of intricate structures from digital designs. This article embarks on a journey through printing in 2D, 3D, and 4D while focusing on investigating and developing new printing materials.

AM relies on the precise deposition and layering of materials to create objects. Colloid chemistry is at the forefront of AM because it provides the fundamental principles for formulating inks, controlling material properties, and ensuring the suitability of layer-by-layer processes for the construction of objects. Since many printing compositions contain micro and nanoparticles (NPs), colloid chemistry

plays a major role in the progress of the field of additive manufacturing. Inks, serving as the basic medium for transferring digital images and structures onto various substrates, must maintain stability at the colloidal level to ensure consistent and precise printing outcomes. In 2D printing, such as traditional paper printing, stable colloids prevent ink agglomeration, ensuring the surface's uniform coverage and color distribution. In the context of 3D printing, where intricate three-dimensional objects are built layer-by-layer, colloid stability becomes imperative to maintain the printing material's viscosity and flow properties, influencing the printed object's final structural integrity. As we advance into 4D printing, where materials can dynamically transform over time, the importance of colloid stability becomes even more pronounced. Controlling the stability of colloids in

**Shlomo Magdassi** is a professor at The Hebrew University of Jerusalem's Institute of Chemistry and serves as the academic director for the university's Center for Functional and 3D Printing. His research centers on micro and nanomaterials, with a focus on their applications in 2D 3D and 4D printing. Over the course of his career, he has published more than 350 papers, edited four books, and holds approximately 300 patents and applications. His industrial research outcome includes creating numerous commercial activities, including start-up companies, licensing agreements, and worldwide sales. In recognition of his contributions, he was awarded the 2022 Johann Gutenberg Prize by the Society for Imaging Science and Technology and the 2022 ICS Excellent Scientist Prize. He is also a Fellow of the National Academy of Inventors.



inks allows for precise deposition and spatial arrangement of materials during the printing process, creating dynamic structures that can respond to external stimuli. In essence, colloid stability is a linchpin for the reliability, quality, and transformative potential of inks in the diverse landscape of 2D, 3D, and 4D printing technologies. In this article, we present some of the activities performed in the research group over the years in the field of printing, starting from technologies and materials for 2D printing, continuing to the field of 3D printing, and finally, presenting the field of 4D printing.

## 2D printing

Twenty years ago, our lab started developing printing approaches based on nanoinks to fabricate various functional devices. The main focus was on printed electronics, i.e., the application of printing technologies to fabricate electronic devices [1, 2]. A large variety of direct writing and additive deposition techniques are available for the fabrication of conductive elements of 2D electronic devices, such as spin, spray, dip, and bar coating, as well as various printing methods like flexo and gravure. Among the printing technologies, Drop-On-Demand (DOD) inkjet printing is a powerful technology that has gained a lot of interest since it is a non-contact, fast, low-cost, and eco-friendly method, which can be easily scaled up and results in minimal wastage of materials. This method was successfully applied in our lab for the fabrication of electronic devices with printing materials such as silver NPs, copper complexes and particles, and carbon nanotubes (CNTs).

The main functional material in inks for fabricating electrical circuits of flexible electronic devices is the conductive material. The most widely used conductive materials are metal NPs, which are dispersed in a proper liquid vehicle containing various components (stabilizer, viscosity, surface tension modifiers, binding agent, etc.) of printable functional ink.

As to substrates that are used in printed electronics, almost any material is suitable, but the main focus nowadays is on flexible substrates, such as various polymeric films, paper, textiles, etc. (flexible, plastics electronics). Considering the current requirements for high-quality electronic devices, our lab focused mainly on the 2D printing of metal NPs and CNTs to fabricate electronic and optoelectronic devices.

To provide good electrical conductivity of metallic printed structures, highly conductive metals that are stable to oxidation, such as silver and gold, are the best for utilization in conductive inks and, currently, silver is the most widely used material. Our main research in this field focused on silver NPs, starting from synthesizing the particles at very high concentrations, developing new ink formulations, and sintering these particles even at room temperature. However, due to its high cost, a major challenge in this field is to replace silver and other noble metals with cheaper ones, such as copper. This would depend on the success in avoiding their oxidation at ambient conditions since, otherwise, an inert atmosphere would be required during the fabrication process. We developed a method for the synthesis of copper NPs with long-term stability by coating the individual particles with a dense layer of air-stable noble metal to minimize or prevent oxygen penetration to the surface of the NPs. Such hybrid core-shell NPs were obtained by transmetalation, wherein the surface of a preformed copper particle functions (and is sacrificed) as a reducing agent for the second metal with higher reduction potential, which results in the formation of a metal shell on the surface of the core metal. This approach enabled us to obtain copper NPs with an average size of 40 nm coated by a silver shell with an average thickness of 2 nm (Cu@Ag NPs). Such NPs were shown to be stable to oxidation for at least six months at ambient conditions both in aqueous dispersion and in powder form [3].

Since, after printing, the conductivity of the formed 2D objects is usually low due to the presence of remaining

All the authors are members of Prof. Shlomo Magdassi's group. Left to right: **May Yam Moshkovitz** and **Ouriel Bliah** are PhD students, **Dr. Doron Kam** is a postdoctoral fellow, and **Dr. Alexander Kamyshny** is a senior researcher at the Institute of Chemistry.



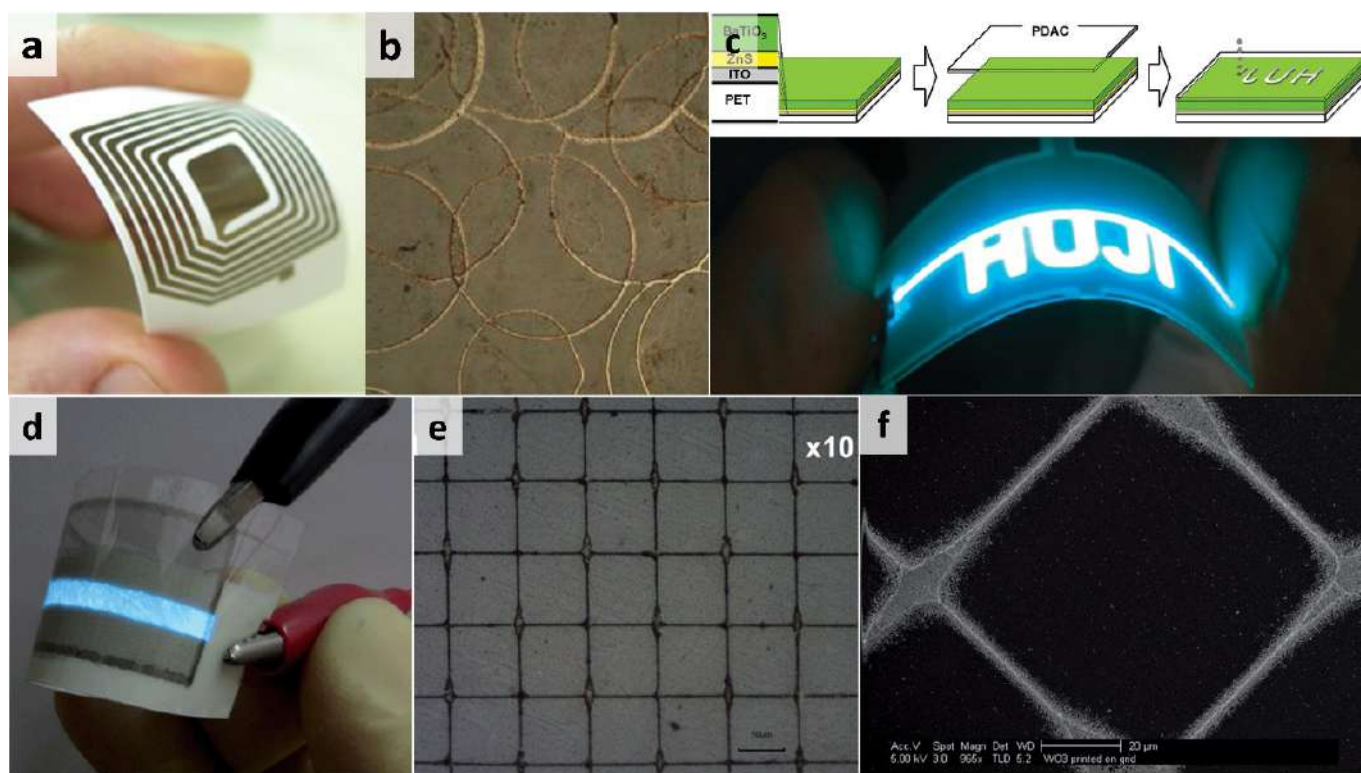


**Figure 1.** 2D printed electronics. (a) flexible RFID antenna inkjet printed on photo paper with Cu@Ag core-shell nanoink. Reproduced from ref. [5] (CC BY). (b) Microscopic images of a 2D array of transparent electrodes of interconnected rings formed by Ag NPs on PET. Reproduced from ref. [6] © 2009, American Chemical Society. (c) A four-layer flexible ELD (PET:ITO:ZnS:BaTiO<sub>3</sub>) with an inkjet-printed top Ag electrode. Reproduced from ref. [7] © 2010, American Chemical Society. (d) Working ELD with electrodes made of inkjet-printed CNTs. Reproduced from ref. [8] with permission from the Royal Society of Chemistry. (e) Microscopic image and (f) SEM image of rectangular Ag grid on PET were used as transparent electrodes for working flexible electrochromic device (scale bars are 200 and 20  $\mu\text{m}$ , respectively). Reproduced from ref. [8] with permission from the Royal Society of Chemistry.

stabilizing agents (for example, adsorbed polymer or surfactant molecules) and other non-volatile electrically insulating ink additives that prevent the formation of continuous conductive structures, a post-printing process is required. This process enables the removal of the insulating materials, thus enabling close contact of the particles until fully merged. Such removal can be achieved by organic material decomposition, desorption, or evaporation. In the case of metallic NPs, they should be sintered (welded without melting) in order to form a continuous metallic network with conductivity approaching that of bulk metal. Traditionally, sintering is performed by heating the printed patterns to elevated temperatures or, less often, by high-energy light pulses, plasma, and microwave irradiation. A much simpler approach (chemical or physicochemical), which does not require high energy consumption or sophisticated equipment, was developed in our lab. This method is based on removing the protective layer from the surface of NPs by chemical agents at room temperature, by ligand exchange of

the stabilizing agent by simple ions (desorption) resulting in coalescence of metal NPs at room temperature. Sintering at room temperature was demonstrated for silver NPs, and even for two different materials, silver and gold [4].

The methods for ink formulations and printing techniques that were developed in our lab for the fabrication of conductive 2D patterns were shown to be well suited for manufacturing various electronic devices such as transparent conductive films, flexible touch panels, electroluminescent devices (ELDs), RFIDs, solar cells, etc. Examples of some of these devices are demonstrated in Figure 1.

### 3D printing

Moving from 2D to 3D printing marks a paradigm shift in manufacturing capabilities, enabling the fabrication of complex, customized structures with unprecedented precision. A three-dimensional object is obtained by

repeatedly creating two-dimensional layers one on top of the other. The general basic principles behind 3D printing technologies are follows. First, a 3D model is created using a computer and sliced into 2D layers for a printable command sequence. Then, the file is sent to a printer, which forms a pattern of the material in predesigned locations at the XY plane. This process is repeated on the Z-axis, according to the sliced printing file.

Executing these principles relies on converting a liquid ink into a solid layer by a suitable trigger. Different 3D printing technologies were established based on different triggers. For example, the well-known extrusion-based 3D printing technology fused deposition modeling (FDM) relies on a thermoplastic filament that, upon temperature triggers, constructs an object. The filament 'ink' liquifies in an extruder by heating and rapidly cools upon contact with the substrate to preserve the desired printed shape.

If we replace the material in the extruder with a non-thermoplastic ink, we enter the general field of direct ink writing (DIW) technique, where the main trigger is rheology. The ink should have sufficient viscosity to stay in the extruder without dripping and should flow when applying pressure during extrusion. Moreover, as the ink is extruded, it must preserve the predesigned locations by rapidly retaining high viscosity upon contact with the printer platform, a property known as shape fidelity.

Another common technology, known as digital light processing (DLP), uses monomers and oligomers to selectively photocure the ink upon exposure to light. The interaction between light and photoinitiator (PI) triggers a photopolymerization process that cures the resin at the predesigned locations and converts the liquid ink into a solid object. For most processes, ink is poured into a vat, and a print head moves to a defined layer thickness where predesigned pixels are exposed to light.

Many techniques have been developed based on photopolymerization to activate and confine objects upon exposure to radiation at different wavelengths. These technologies typically enable the fabrication of large objects up to tens of centimeters. In most cases, polymerization occurs throughout the optical path, but two-photon polymerization (TPP) is a unique case where polymerization occurs only in a voxel at the focal point. TPP ink is transparent at the light-source wavelength but absorbs multiphotons at shorter wavelengths. Therefore, it is not limited to print head movement and enables spatial polymerization. This freedom comes at the expense of the maximum achievable object, which is limited to mm-scale size but enables a sub-micron resolution, the highest today. In the following sections, we

will describe some of the research performed in the field of 3D printing of organic and inorganic materials.

### Organic materials

A major bottleneck in the 3D printing of organic polymers is the lack of materials that can compete with the ones used for manufacturing by conventional processes, for example, materials with superior mechanical properties such as high-performance polymers with high-temperature resistance and excellent mechanical properties, or stable stretchable materials. We present here two examples addressing these needs: (a) new photopolymerizable compositions were developed, based on a dual-curing mechanism, that are stable even at a temperature above 250°C, without deterioration of their mechanical properties [9], and (b) stretchable materials that are based mainly on photopolymerizable urethane acrylate, which have a stretching ability of about 1000%, without mechanical failure [10].

We also combine the field of AM with sustainability. Throughout history, wood has remained a crucial raw material, and the techniques employed for its processing are consistently evolving to enhance forest-based economies. Traditional carpentry and conventional wood processing industries rely on top-down subtractive methods, which involve cutting a tree and carving or cutting it into smaller components to produce various objects. In contrast, 3D printing processes can enormously impact the material's life cycle, resulting in minimal waste material, and our research in 3D printing of 100% wood-based objects involves emulating the composition of plant cells. Thus, we have developed new compositions while utilizing finely pulverized or reclaimed wood, often considered a low-value byproduct of the wood industry [11]. A wood-based binder, derived from potential industrial side streams composed of cellulose nanocrystals (CNCs) and xyloglucan (XG), was developed, demonstrating a sustainable approach to 3D printing with wood materials (Figure 2a).

Printing wood embodies a significant advance in the processing and the realization of biomaterials. Biomaterials are mostly known to contribute to the biomedicine industry. Within this field, the 3D printing of hydrogels has emerged as a cutting-edge and transformative technology, mainly in medical-related fields. For example, 3D printing can be used to fabricate complex hydrogel structures, creating customized scaffolds, implants, and drug delivery systems with tailored shapes and functionalities. The convergence of 3D printing and hydrogel technology holds significant promise for advancing regenerative medicine, tissue engineering, and pharmaceutical development, ushering in a new era of personalized and intricately designed biomaterials. Most of the research in this field is based on extrusion-based

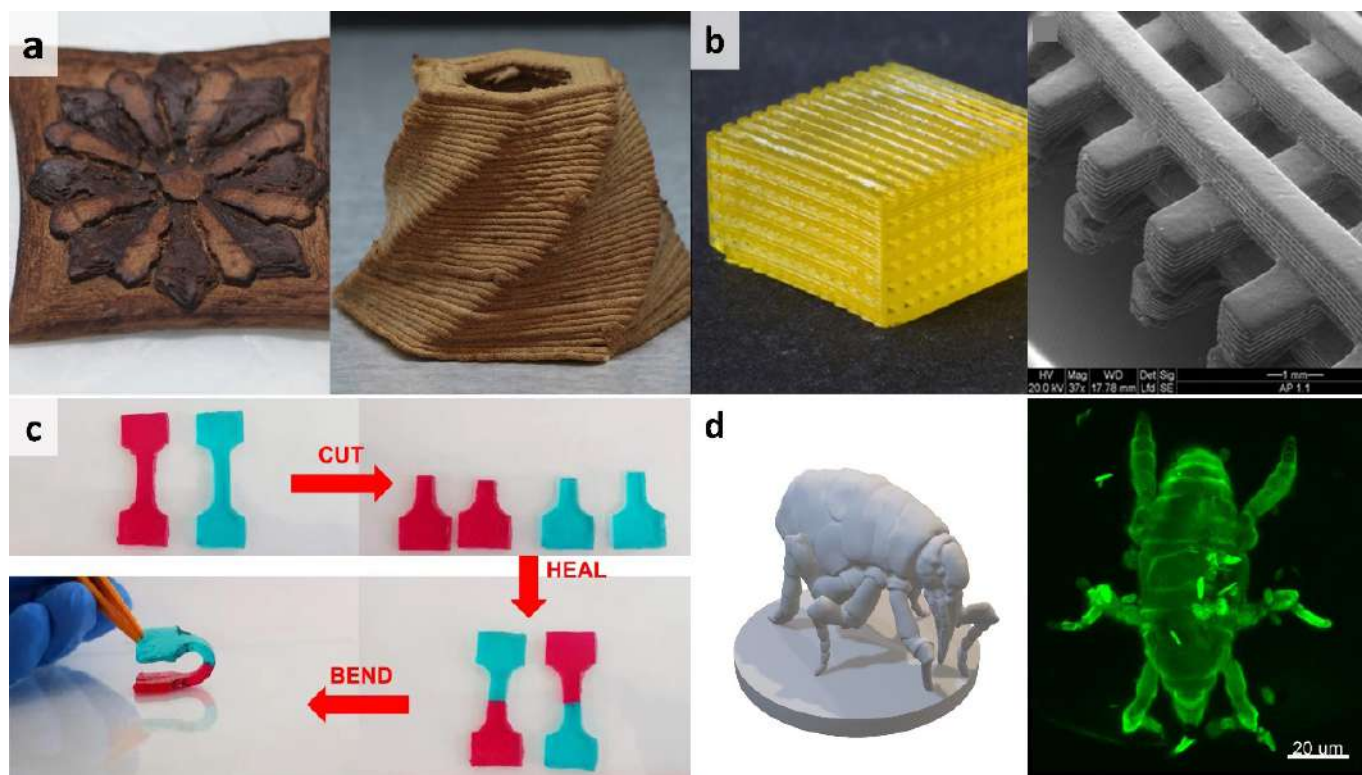


**Figure 2.** (a) 3D printing of objects composed of wood materials. Multimaterial DIW of two wood types and a wooden vase. Reproduced with permission from ref. [11] © 2019 WILEY-VCH Verlag GmbH & Co. KGaA, Weinheim. (b) Photo and SEM image of DLP printed woodpile-structured hydrogel scaffold using water-dispersible PI. Reproduced from ref. [12] (CC BY-NC 4.0). (c) Self-healing hydrogels printed using DLP. Reproduced from ref. [13] (CC BY-NC 4.0). (d) CAD model and confocal image of a complex overhang model of a monster flea printed with resilin protein using TPP. Reproduced from ref. [14] (CC BY-NC 4.0).

printing technologies with limited resolution. However, for technologies based on photopolymerization, the large amount of water in the hydrogel brings a significant challenge due to the lack of efficient water-soluble PIs. PIs play a crucial role in performing the radical polymerization process and, consequently, the obtained properties of the printed object. Moreover, the PI efficiency is also evaluated by the time required to expose each printed layer, a limiting parameter from which the total printing time can be determined. So far, there is a very small number of water-compatible PIs at a much higher cost than the commonly available organic-soluble ones.

To address this need, we have developed a new process that enables the formation of water-compatible PIs. A new water-dispersible 2,4,6-trimethylbenzoyl-diphenylphosphine oxide (TPO) was prepared by rapidly converting volatile microemulsions into water-dispersible powder [12]. TPO was dissolved in an organic (“oil”) phase containing surfactants and cosolvents mixed with water to obtain an oil-in-water microemulsion that was then spray-dried. This process can

be used for a variety of PIs, enabling easy and quick printing using DLP processes (Figure 2b).

Moreover, when the limitation of PI solubility in water is overcome, a hydrogel with self-healing ability could be rapidly printed via DLP using only commercially available materials [13]. Self-healing hydrogels are materials that can autonomously repair or regenerate their structure after being damaged, making them resilient to wear and tear. This property is enabled due to the formation of a semi-interpenetrated polymeric network while the autonomous restoration rapidly occurs at room temperature. Hydrogels based on poly(vinyl alcohol) (PVA) and photocurable monomers, like acrylic acid and polyethylene glycol diacrylate, were printed, cut, and rejoined. After rejoining, upon contact the objects healed, resulting in 72% deformation recovery after 12 hours (Figure 2c).

Self-healing hydrogels mimic the behavior of living tissues, which can autonomously repair minor damages, but their composition, although biocompatible, is synthetic. In order

to move to completely biological systems, it is necessary to abandon the synthetic monomers and focus on the building blocks of biology, the proteins. If, until now, we crosslinked monomers by functional groups in the photopolymerization process, the biological equivalent of functional groups are the amino acids. One polymerization possibility is to oxidize tyrosine residues by exciting ruthenium-based PI with visible light to form a dityrosine bond, as we demonstrated in printing proteins. Such a protein is resilin, which is an intrinsically disordered elastic rubber-like protein known for its resilience and fatigue lifetime. Resilin contains over 6% tyrosine residues that can be leveraged into the photopolymerization process. However, the production of proteins yields very small amounts of material that can be used as ink, so adopting a suitable AM technique like TPP is necessary [14].

TPP of resilin at a sub-micron resolution enabled us to obtain complex architecture objects composed of 100% resilin protein (Figure 2d). Such a process can facilitate cell-laden scaffolds. Furthermore, like many systems derived from photoinitiation, the light dose is related to the crosslinking of resilin protein, which is manifested by a change in mechanical properties. That is, by changing printing parameters, it is possible to control the mechanical properties of the objects, which enables the alignment of living cells.

### Inorganic materials

Ceramic and glass materials, classified as inorganic non-metallic substances, are widely known for their excellent mechanical strength, hardness, and good thermal and chemical stability. These materials are found in various industries, including chemical, electronics, aerospace engineering, and biomedical applications. Traditionally, ceramic and glass materials have been manufactured through casting of a mixture of powders.

Traditional industry produces glass objects by heating silica in a mold after reaching its melting point. Alternatively, sol-based aqueous ink enables the 3D printing of transparent silica glass objects at ambient temperature by photopolymerization. Sol-gel is a chemical process that transforms sol into a gel-like material through controlled polymerization within a particle-free solution. Using particle-free inks enables the avoidance of light scattering, sedimentation of particles, and too-high viscosities, which are common problems usually encountered while using ceramic-based inks. The printed structures undergo aging (condensation reaction continues within the gel network, and the structure stiffens) and then sintering (fusing the particles at high temperature). The sol-gel-based structures gradually transform from gel to fused silica without going through a melting process. This allows for maintaining the initial structure of the object at low

temperatures, having a variety of optical properties, refractive indices, and density control [15].

Combining organic and inorganic materials enables the making of materials with improved properties. However, due to their high organic content, these hybrids usually have low thermal stability and mechanical strength. Here, we developed a hybrid sol-gel-based ink with very high silica content by combining a small amount of modified metal-alkoxy precursors with conventional metal-alkoxy sol-gel precursors that enable the formation of oligomer sol with high silica content [16]. The printed silica is characterized by excellent mechanical strength compared to currently used high-performance polymers (139 MPa). They are also characterized by very high stability at elevated temperatures (HDT > 270 °C), high transparency (90 %), and lack of cracks, with glossiness similar to that of typical silica glass (Figure 3a).

Sol-gels can undergo drying through conventional methods or supercritical drying (SCD), resulting in the formation of aerogels. Aerogels, recognized as the lightest solid materials, have applications in thermal insulation, tissue engineering scaffolds, catalyst supports, and micrometeorite collection. Their unique drying process sets them apart from conventional methods involving room temperature or heating by undergoing supercritical drying. In this process, the liquid component is replaced by a gas under supercritical conditions, yielding a highly porous and lightweight solid structure characterized by low density and high surface area. We have used the SCD process to fabricate objects composed of porous silica. The resulting 3D structures are composed of 100% silica, have very low density ( $157 \pm 7 \text{ mg ml}^{-1}$ ), a high surface area ( $580 \pm 50 \text{ m}^2 \text{ g}^{-1}$ ), and low thermal conductivity, positioning them as potential lightweight components with applications in miniature devices (Figure 3b) [17].

One step forward is exploring unique silica-based materials with different properties, such as chirality or ordered mesopores, for example, chiral organosilica 3D structures fabricated with printed enantioselective separation columns. We have found that the macroscopic shape of these monoliths significantly enhances the adsorption performance and enantioselectivity due to the porosity by design and material property [18]. In addition, 3D-ordered mesoporous silica objects, known for their tunable nanometric pores, were printed by mixing silica-forming precursors with surfactants that self-assemble into elongated micelles [19]. The condensation polymerization of silica precursors resulted in a ceramic-like framework with ordered channels leading to a highly ordered porous material (Figure 3c). These 3D-printed silica monoliths exhibit an exceptionally high surface area

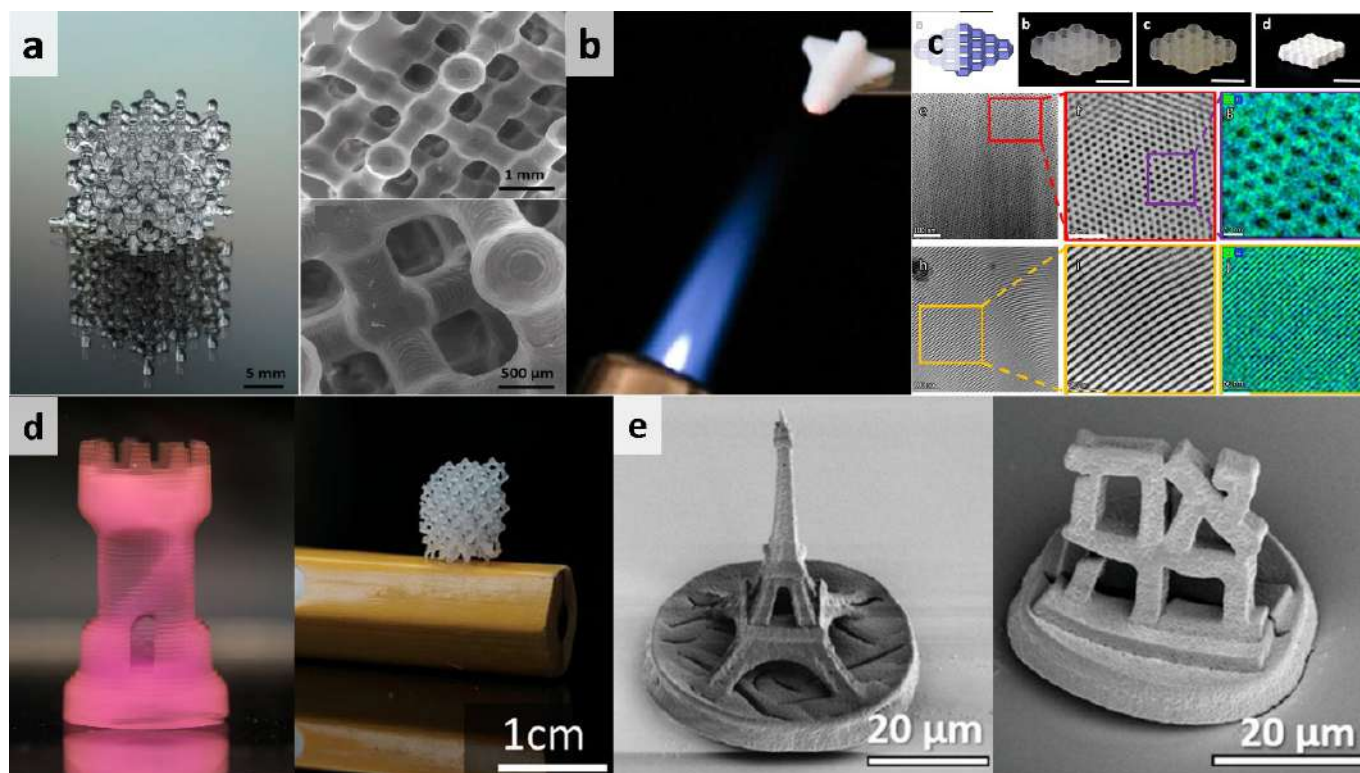


**Figure 3.** (a) Photo and SEM image of printed pure silica glass structure with 50  $\mu\text{m}$  resolution along the Z-axis. Reproduced from ref. [16] (CC BY). (b) Printed silica aerogel against a blowtorch. Reproduced with permission from ref. [17] © 2021 Elsevier Ltd. (c) (top) Hexagonal morphology of the ordered mesoporous silica structures (CAD model, a printed structure, after aging at 22  $^{\circ}\text{C}$  for one week, and calcined structure). (bottom) STEM micrographs showing the pores viewed along the (1, 0) direction, the arrangement of the rods viewed along the (1, 1) direction, and overlay mapping of Si (blue) and O (green) based on EDS scans. Reproduced from ref. [19] (CC BY). (d) 3D-printed  $\gamma$ -alumina structures: (left) after printing and (right) after sintering at 850  $^{\circ}\text{C}$ . Reproduced from ref. [20] (CC BY-NC-ND). (e) Printed submicron YAG structures after heating to 1500  $^{\circ}\text{C}$ . Reproduced with permission from ref. [21] © 2020 WILEY-VCH Verlag GmbH & Co. KGaA, Weinheim.

of 1900  $\text{m}^2 \text{g}^{-1}$ , low density, and high thermal and chemical stability.

Until now, we have discussed silica-based materials. However, synthesizing materials beyond silica, including oxides, nitrides, and hybrid organic-inorganic compounds, can be 3D printed with the same sol-gel processing. One benefit of sol-gel processes is the ability to control the particle size precisely, allowing for tailoring material properties and offering control over mechanical, thermal, and optical characteristics. Additionally, the process is performed at relatively lower temperatures (up to 100  $^{\circ}\text{C}$ ) than traditional techniques. The low processing temperature minimizes the risk of undesirable phase transformations and promotes energy efficiency in ceramic production.

One oxide sol-gel-based material is a high-resolution transparent porous crystalline  $\gamma$ -alumina 3D structure [20]. The material that we developed is both transparent and porous due to nanometric-sized crystals and pores. The resulting  $\gamma\text{-Al}_2\text{O}_3$  structures have surface areas exceeding 1800  $\text{m}^2 \text{g}^{-1}$  and optical transmission surpassing 80% at 600 nm. Supercritical drying enables precise control over pore dimensions and surface area (Figure 3d). Another material that we have developed based on non-silica precursors is yttrium aluminum garnet (YAG), doped with neodymium (Nd) (Figure 3e) [21]. These complex structures possess transparency within the visible spectrum and exhibit light emission at 1064 nm due to Nd doping. In addition, other ceramics were developed and 3D printed in the lab, for example, nanoelectromechanical systems resonators [22], and 3D-printed tungsten [23].

## 4D printing

The most recent addition to the field of additive manufacturing is 4D printing, a dynamic extension of 3D printing that introduces the dimension of time. 4D printing involves the use of materials that can change their shape or properties over time in response to external stimuli, such as heat, light, water, or other triggers. The fourth dimension in 4D printing refers to the transformation that occurs after the object has been 3D printed. In the following, we will present several examples in this field.

We have printed very complex hydrogels that are impossible to produce by conventional means to obtain drug-loaded structures, which change their structure and thus enable new drug-release characteristics [24]. These systems exhibited pH-responsive bi-functionalities of both swelling and drug release depending on the predesigned surface area (Figure 4a).

Moreover, the use of extrusion-based 3D printing technology, such as the DIW technique for printing wood, can mimic the plant cell architecture, resulting in the morphing of the objects [5]. The predesigned 3D printing pathway enables ink orientation and degree of alignment control apart from the stated purpose of form building (Figure 4b). This ability stems from using CNCs, which are highly crystalline, nano-sized, rod-shaped particles that affect the shear alignment induced by the extruding process.

The deformation can happen in reverse, and instead of printing and changing the shape, it is possible to print, then distort the shape, and return it to its original structure. Thermally-induced shape memory polymers represent a fascinating frontier in material science that can be utilized for this deformation. Unlike conventional materials, these polymers can memorize and recover their original shapes in response to thermal stimuli. Polycaprolactone (PCL) is a type of thermoplastic polyester that exhibits heat-activated shape memory properties. The shape memory effect in PCL arises from its ability to undergo a reversible phase transition between a temporary shape and a permanent shape in response to changes in temperature. Initially, the PCL ink is printed using a vat heated to a temperature above the PCL melting temperature, allowing it to become malleable through the DLP process, forming a specific temporary 3D shape. The object is then cooled below its melting temperature, locking it into a temporary shape. During this cooling process, the polymer transitions from a malleable state to a rigid state, effectively “memorizing” the temporary shape. When PCL is exposed to heat again, either through direct heating or exposure to ambient temperature, it reverts to its original, permanent shape (Figure 4d) [25].

4D printed objects are not limited to shape changes; other properties can evolve through time as a response of the 3D object to external stimuli. Mechanoluminescent materials, for example, emit light as a response to structure change upon application of mechanical stimuli. Using DIW to embed mechanoluminescent materials within elastomeric monomers enabled us to print multiple materials within one object [26]. Thus, it results in multiple color emissions that can be used to generate anisotropic light emission upon pressures from different directions, to be used as a pressure sensor (Figure 4c).

Finally, the growing field of soft robotics was integrated into the world of 4D printing thanks to their shared emphasis on materials with adaptive properties. Soft robotics uses soft materials to create a movement of objects made of deformable bodies, such as smart grippers and swimming robots, without using a conventional motor. In 4D printing, the printed structures can undergo predetermined shape changes to perform a required action, such as gripping. The morphing of the object can result from various stimuli, such as an electrical signal, application of pressure, heat, or light. To achieve a gripper capable of handling very soft and fragile materials, we have developed new materials and a process to print a soft gripper composed of stretchable foams.

For DLP printing, UV-curable water-in-oil emulsion inks were developed using stretchable polyurethane diacrylate (PUA) [8]. The cured PUA emulsion resulted in a foam structure with a microporosity at the dimensions of the water droplets. By DLP printing, the ink can be cured at predesigned locations, enabling the achievement of a macroporosity based on a cellular design. This enables dual porosity by material and by design, leading to unique mechanical properties. These emulsion-based printing compositions provide high elongation (up to 450%) and excellent compressibility (more than 80%) and were used to fabricate jointless soft pneumatic actuators for robotic grippers (Figure 4e–f).

## Conclusion

In conclusion, this paper presents an overview of the research activities performed in our lab in the fields of 2D, 3D, and 4D printing. It contributes to the collective knowledge that drives the continuous evolution of additive manufacturing in the scientific and industrial arenas. AM foundation lies in precise material deposition, and colloid chemistry emerges as a cornerstone in AM, particularly in the formulation of inks, determining material properties, and ensuring the stability crucial for precise layer-by-layer construction. The transition from 2D to 3D printing signifies a paradigm shift, enabling the creation of intricate structures with unprecedented precision and unlocking the ability to create complex structures with

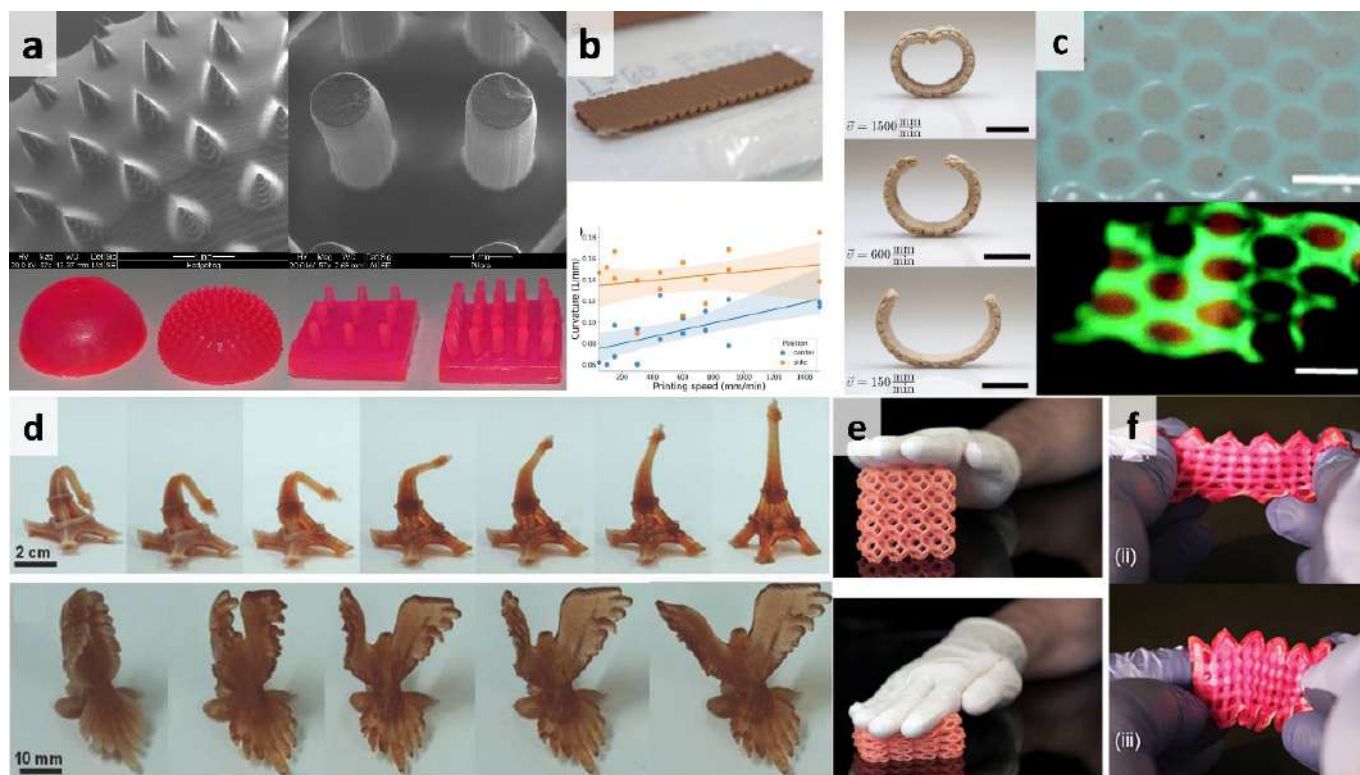


**Figure 4.** (a) Photos and SEM of 4D printed (DLP) responsive hydrogel for drug-delivery systems. (b) Photos of 4D printed (DIW) wood warping “as printed” rectangular, and the dried warped objects with the dependence of curvature as a function of printing speed. Reproduced from ref. [5] (CC BY). (c) Dual light-emitting hexagonal mesh patterned mechanoluminescent devices at rest (above) and under stretching (bottom). Reproduced from ref. [26] with permission from the Royal Society of Chemistry. (d) 4D printed (DLP) shape memory objects reverting to their original shape. Reproduced from ref. [25] © 2015 WILEY-VCH Verlag GmbH & Co. KGaA, Weinheim. (e) 3D-printed foam-like structures with dual porosity. Reproduced from ref. [8] with permission from the Royal Society of Chemistry. (f) Pneumatic elastic lattice actuator used for soft robotics. Reproduced from ref. [27] (CC BY).

a large variety of materials, including synthetic polymers, wood, hydrogels, glass, and ceramics. The shift into 4D printing introduces a dynamic dimension, enabling printed objects to undergo shape changes and exhibit responsive properties over time.

Each stage in our journey in the field of additive manufacturing reflects various technological advancements and the synergistic interplay between chemistry, material science, and engineering. Fortunately for chemists, the materials are a bottleneck in many printing technologies, and we expect that new innovative materials and printing technologies will bring significant scientific and industrial impact.

## References

1. S. Magdassi and A. Kamyshny, Eds., *Nanomaterials for 2D and 3D Printing*, John Wiley & Sons, 2017.
2. A. Kamyshny and S. Magdassi, *Chem. Soc. Rev.*, 2019, **48**, 1712–1740.
3. M. Grouchko, A. Kamyshny and S. Magdassi, *J. Mater. Chem.*, 2009, **19**, 3057–3062.
4. M. Grouchko, P. Roitman, X. Zhu, I. Popov, A. Kamyshny, H. Su and S. Magdassi, *Nat. Commun.*, 2014, **5**, 2994.
5. D. Kam, I. Levin, Y. Kutner, O. Lanciano, E. Sharon, O. Shoseyov and S. Magdassi, *Polymers*, 2022, **14**, 733.
6. M. Layani, M. Grouchko, O. Milo, I. Balberg, D. Azulay and S. Magdassi, *ACS Nano*, 2009, **3**, 3537–3542.
7. S. Magdassi, M. Grouchko, O. Berezin and A. Kamyshny, *ACS Nano*, 2010, **4**, 1943–1948.
8. O. Bliach, S. Joe, R. Reinberg, A. B. Nardin, L. Beccai and S. Magdassi, *Mater. Horiz.*, 2023, **10**, 4976–4985.
9. I. Binyamin, E. Grossman, M. Gorodnitsky, D. Kam and S. Magdassi, *Adv. Funct. Mater.*, 2023, **33**, 2214368.
10. D. K. Patel, A. H. Sakhaei, M. Layani, B. Zhang, Q. Ge and S. Magdassi, *Adv. Mater.*, 2017, **29**, 1606000.

11. D. Kam, M. Layani, S. Barkai, Minerbi, D. Orbaum, S. Abrahami BenHarush, O. Shoseyov and S. Magdassi, *Adv. Mater. Technol.*, 2019, **4**, 1900158.
12. A. A. Pawar, G. Saada, I. Cooperstein, L. Larush, J. A. Jackman, S. R. Tabaei, N.-J. Cho and S. Magdassi, *Sci. Adv.*, 2016, **2**, 1–8.
13. M. Caprioli, I. Roppolo, A. Chiappone, L. Larush, C. F. Pirri and S. Magdassi, *Nat. Commun.*, 2021, **12**, 2462.
14. D. Kam, A. Olender, A. Rudich, Y. Kan-Tor, A. Buxboim, O. Shoseyov and S. Magdassi, *Adv. Funct. Mater.*, 2023, **33**, 2210993.
15. I. Cooperstein, E. Shukrun, O. Press, A. Kamyshny and S. Magdassi, *ACS Appl. Mater. Interfaces*, 2018, **10**, 18879–18885.
16. E. Shukrun, I. Cooperstein, S. Magdassi, E. Shukrun, I. Cooperstein and S. Magdassi, *Adv. Sci.*, 2018, **5**, 1800061.
17. E. S. Farrell, N. Ganonyan, I. Cooperstein, M. Y. Moshkovitz, Y. Amouyal, D. Avnir and S. Magdassi, *Appl. Mater. Today*, 2021, **24**, 101083.
18. E. Shukrun Farrell, R. Siam, M. Y. Moshkovitz, D. Avnir, R. Abu-Reziq and S. Magdassi, *Addit. Manuf.*, 2022, **60**, 103265.
19. E. Shukrun Farrell, Y. Schilt, M. Y. Moshkovitz, Y. Levi-Kalisman, U. Raviv and S. Magdassi, *Nano Lett.*, 2020, **20**, 6598–6605.
20. M. Y. Moshkovitz, D. Paz and S. Magdassi, *Adv. Mater. Technol.*, 2023, **8**, 2300123.
21. I. Cooperstein, S. R. K Chaitanya Indukuri, A. Bouketov, U. Levy, S. Magdassi, I. Cooperstein, A. Bouketov, S. Magdassi, S. R. K C Indukuri and U. Levy, *Adv. Mater.*, 2020, **32**, 2001675.
22. S. Stassi, I. Cooperstein, M. Tortello, C. F. Pirri, S. Magdassi and C. Ricciardi, *Nat. Commun.*, 2021, **12**, 6080.
23. X. Zan, X. Wang, K. Shi, Y. Feng, J. Shu, J. Liao, R. Wang, C. Peng, S. Magdassi and X. Wang, *J. Phys. D Appl. Phys.*, 2022, **55**, 444004.
24. L. Larush, I. Kaner, A. Fluksman, A. Tamsut, A. A. Pawar, P. Lesnovski, O. Benny and S. Magdassi, *J. 3D Print. Med.*, 2017, **1**, 219–229.
25. M. Zarek, M. Layani, I. Cooperstein, E. Sachyani, D. Cohn and S. Magdassi, *Adv. Mater.*, 2016, **28**, 4449–4454.
26. D. K. Patel, B. El Cohen, L. Etgar and S. Magdassi, *Mater. Horiz.*, 2018, **5**, 708–714.
27. S. Joe, O. Bliah, S. Magdassi and L. Beccai, *Adv. Sci.*, 2023, **10**, 2302080.

# The chiral-induced spin selectivity effect

**Ron Naaman**

Department of Chemical and Biological Physics, Weizmann Institute, Rehovot, 7610001 Israel

Email: [ron.naaman@weizmann.ac.il](mailto:ron.naaman@weizmann.ac.il)

## Abstract:

The chiral induced spin selectivity (CISS) effect was discovered about 25 years ago at the Weizmann Institute. Since then, it became apparent that the effect has implications and applications in various fields, chemistry, physics, and biology. In addition, it enables efficient production of hydrogen from water and improves the operation of fuel cells. In this perspective, the effect is described and its impact in various cases is presented.

## Introduction

The chiral-induced spin selectivity (CISS) effect means that the motion of electrons through a chiral system depends on their spin [1]. Hence, the effect has two “players”: chiral systems and electron spins. Chiral molecules were discovered in the 19<sup>th</sup> century, when Pasteur, Lord Kelvin, and van’t Hoff confirmed that some molecules appear in two configurations that are mirror images of each other, like two hands (hand is *kheir* in Greek). The two configurations are called enantiomers. Since their discovery, scientists have utilized chiral molecules only because of their structure. No special electronic properties were associated with them, apart from their optical activity, which serves to characterize the enantiomers. The other component that governs this effect is the electron spin, namely, the electron’s angular momentum.

This property was discovered when spectroscopists observed extra peaks in the hydrogen spectrum [2]. These peaks were not predicted by the Bohr model of the atom and required the introduction of another source of angular momentum, namely, the electron spin. The concept that for two electrons to be in the same quantum state they must have opposite spins determines our understanding of the electronic structure of materials; for example, the spin is an essential property for understanding atomic electronic structure and chemical bonds. However, physicists and chemists typically refer to the spin only in systems where there is an unpaired electron.

The CISS effect shows that when chiral systems are considered, the spins play an important role in understanding various properties, even if the total spin of the system is zero, namely, there is an even number of electrons and all the electrons are supposed to be “paired” so that the sum of their spins is zero.

**Ron Naaman** earned his BSc in 1973 from Ben-Gurion University of the Negev, and his PhD in 1978 from the Weizmann Institute of Science, Israel. He worked as a postdoctoral researcher at Stanford University in California, and spent a year in the Department of Chemistry at Harvard University. In 1981, Ron joined the Weizmann Institute in the Department of Isotope Research (later renamed the Department of Chemical Physics). From 1989–1995, he chaired the Institute’s Chemical Services Unit and from 1995–2000, he headed the Department of Chemical Physics. From 2008-2010, Ron was the Chair of the Scientific Council at the Institute. He was awarded the Kolthof Prize from the Technion (2014), the excellent research prize from the Israel Vacuum Society (2013) and from the Israel Chemical Society (2018), the Humboldt-Meitner award (2019), the ICS Gold Medal (2022) and the Chiral Medal (2023). He serves as an associate editor for PCCP. Ron Naaman is a Fellow of the American Physical Society, Fellow of the Royal Society of Chemistry, and Member of Academia Europaea. He has published more than 350 scientific papers.



## How was this effect discovered?

In 1995, Mayer and Kessler published a study on spin-polarized electrons scattered from chiral molecules in the gas phase [3]. In this study they reported an asymmetry of about  $1.5 \times 10^{-4}$ , which was above their detection limit, but still very small. This asymmetry means that the deflection of electrons from chiral molecules depends on their spin. Concomitantly, we studied electron transmission through monolayers of biomolecules, like DNA. In these experiments (see Figure 1), photoelectrons are ejected from a gold substrate coated with a self-assembled monolayer (SAM) of biomolecules. The energy distribution of the electrons that pass through the monolayer is measured by an electron energy analyzer.

When we read the paper by Mayer et al., we thought that perhaps if the chiral molecules are organized as a SAM, the asymmetry that we would be able to observe would be larger. This required only minor modifications in the

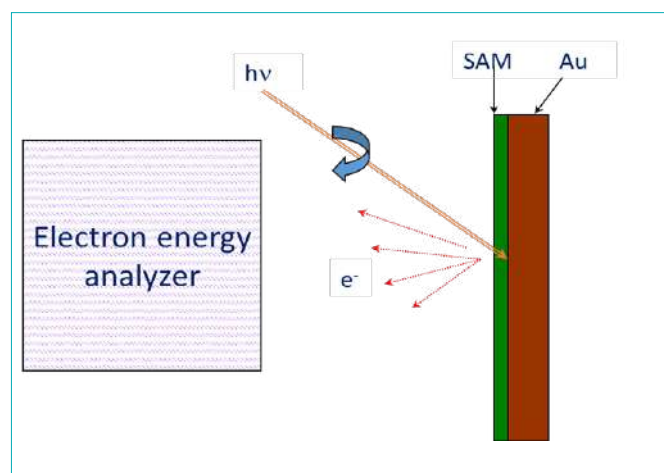


**Figure 1.** Spin-dependent photoelectron measurements. Electrons are ejected from a gold substrate coated with chiral molecules, using circular polarized light. The electron energy distribution and signal intensity are measured using a time-of-flight spectrometer.

experiment: instead of linear polarized light, we measured the photoelectrons as a function of circular polarized laser light. It is well established that photoelectrons ejected from a gold surface by circular polarized light are spin polarized and that the spin polarization correlates with the handedness of the circular polarized light. The spin polarization of photoelectrons ejected from pure gold, as measured before, is about 20%. When we performed the experiments on the monolayers of various chiral molecules adsorbed on gold, we found that there is about a 10% difference in the transmission

for electrons with one spin versus the other [4]. Which spin is preferred depended on the handedness of the chiral molecules. These results indicate that there is about 50% spin selectivity in the transmission, which is a very high value, especially since the experiments were carried out at room temperature. These studies, which were repeated with different molecules, established spin selectivity, only indirectly. We did not actually measure the spin of the electrons that passed through the monolayers but instead measured the difference in the transmission for electrons having two different spin states and inferred the spin polarization.

This situation changed when we collaborated with the group of Helmut Zacharias from Munster, Germany. The group in Munster was able to measure the spin of electrons after they passed through the monolayer, using a Mott scattering device which detects the electron spin by reflecting the electrons from a gold substrate and monitoring their angle of reflection. As in the case of a rotating Frisbee scattered from a wall, the Frisbee will scatter into different angles if it rotates clockwise or counter clockwise upon hitting the wall. In our joint study, we observed that indeed the spin polarization of electrons that passed through a monolayer of DNA exceeded 40% and that the polarization increases with the length of the DNA. Similar results were obtained later with oligopeptides that form helical structures [5].

In all the studies mentioned above, photoelectrons passed through the chiral molecules; thus, these electrons had energy above the vacuum level, namely, they were not bound to the molecules while passing through them. To verify that this effect also exists for bound electrons, we performed a spin-dependent conduction experiment, applying magnetic contact atomic force microscopy (mCAFM) as shown in Fig. 2 [6].

In this setup (Figure 2a), chiral molecules are adsorbed on a ferromagnetic substrate that can be magnetized with the north pole of the magnetic moment pointing towards the adsorbates (UP) or away from them (DOWN). The current versus voltage applied between the tip and the substrate is measured when the tip is in contact with the adsorbates. The measurements are carried out for substrates magnetized UP and DOWN. The spin polarization,  $P$ , is then defined as:  $P = \frac{I_{UP} - I_{DOWN}}{I_{UP} + I_{DOWN}}$ , where  $I_{UP}$  and  $I_{DOWN}$  are the currents measured when the magnetic pole of the substrate is pointing up or down, respectively. Figure 2b shows that the current through the chiral molecules depends on the electron spin. When presented on a semi-log graph (Figure 2c), it is evident that there is a voltage threshold; therefore, current can be observed only above a given voltage value. This threshold depends on the spin and differs by about a hundred meV (about 10 KJ/mole) for the two spins. Hence, there is a spin-dependent barrier for injecting electrons into chiral molecules.

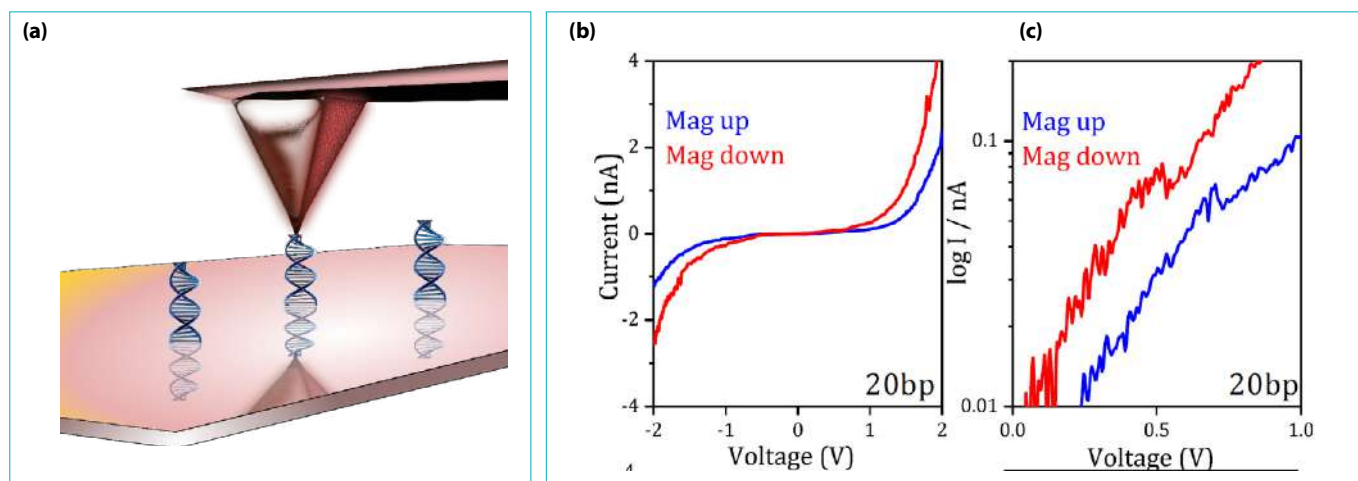


**Figure 2:** (a) The magnetic contact atomic force microscopy (mcAFM) setup and (b) the spin-dependent  $I$  vs.  $V$  curves obtained when the magnetic substrate is magnetized with the north pole pointing towards the adsorbed 20 bp DNA monolayer (Mag up is in blue) or with the south pole pointing towards the adsorbed layer (Mag down is in red). (c) The same results as in (b) plotted on a semi-log scale.

Interestingly, the spin polarization observed for photoelectrons and conducting electrons is very similar and is on the order of tens of percent at room temperature [7]. It was also found that for oligomers, like DNA and oligopeptides, the spin polarization increases almost linearly with the length of the oligomer [8]. In another important study it was shown that the chiral molecules do not act as a spin polarizer, but rather as a spin filter [9]. Namely, the electrons do not change their spin while under the influence of the chiral potential; rather, the electrons with the “wrong” spin are scattered back, whereas those with the “right” spin are transferred with high efficiency.

The CISS effect result in many new technological abilities. In the following, two examples of the impact of the CISS effect will be described, one in chemistry and the other in biology.

## The polarized electron’s spin as a chiral reagent

Commonly in chemistry it is assumed that an enantioselective reaction requires that either one of the reagents or the catalyst be in enantiomeric excess. Therefore, performing asymmetric reactions, when the product is mostly enantiopure, remains a challenge for synthetic chemists. In recent years, it has been found that spin-polarized electrons can enhance electrochemical redox reactions that involve oxygen, and it can induce asymmetric electrochemical reactions [10]. The studies performed to date can be divided into three categories:

### i) Multiple electron redox processes that involve oxygen.

Oxygen, unlike most molecules, has a triplet ground state that controls the spins involved in oxygen reduction or in oxygen evolution, which can enhance the reaction yield, reduce barriers, and eliminate byproducts such as hydrogen peroxide. The spin control can be achieved by either using magnetic electrodes or coating the electrodes with chiral layers. In recent years, many studies have been performed on this subject and, indeed, very large enhancement of the reaction yields was reported [11,12,13].

### ii) Spin-induced selective reaction of one enantiomer in a racemic mixture.

Usually, if there is no enantiomeric bias in a chemical reaction, the products are obtained as a racemic mixture. Since for applications related to biology and medicine, one must use as far as possible a single enantiomer, separation of a racemic mixture into its enantiomeric pure components is often a tedious process. Using spin-selective electrochemistry, it was shown that one can cause mainly one enantiomer in the racemic mixture to be oxidized or reduced [14].

### iii) Synthesis of enantiopure products using inexpensive and scalable methods.

Several Nobel prizes were awarded for the development of asymmetric catalysts that are themselves chiral and can synthesize the production of enantiopure products from achiral reagents. In recent studies, it was demonstrated that chiral enantiopure products can be synthesized by spin selective electrochemistry from achiral reagents. It was

suggested that the process occurs when the spin-polarized electron interacts with the chiral transition state of those reactions [15]. However, much more work is required to explore the mechanism of the process and then improve the enantiomeric excess in these reactions.

## CISS in biology

Many of the molecules that are essential for life, such as proteins, DNA, and sugars, are chiral. Interestingly, typically those molecules appear in all forms of life as one enantiomer. Despite the awareness to this homochirality, the question of why it is maintained throughout evolution so persistently is rarely discussed. The discovery of the CISS effect raised the question of whether the chirality in living organisms has specific functions, beyond being a structural motif. In this respect, it is interesting to note that electron transfer in biology typically occurs through proteins that are supposed to be insulators, and not through conjugated systems that are achiral and are better conductors.

Although studying the CISS effect in biology is still in its infancy, there are already several effects that have been investigated [16,17,18] and others that have been proposed. Next, some of the benefits that the CISS effect provides to living organisms will be discussed.

### i) Providing long-range electron transfer with high fidelity

In the CISS effect, the spin degree of freedom of the electron is coupled to the electron's linear momentum. Hence, within the helical electrostatic potential of a chiral system, an electron cannot scatter back without flipping its spin. Flipping spin is a low-probability event; hence, it is expected that the back scattering of electrons moving in a chiral system will be reduced, compared to an achiral system. This effect was indeed observed experimentally [19]. It is important to appreciate that, on average, the number of electrons transferred per second, through electron-conducting proteins, is about 500. Hence in biology it is not essential to have proteins with high conductivity; however, it is important that each electron entering the protein reaches its target. Otherwise, it may charge the protein, cause it to heat, and become damaged. Hence, the CISS effect and the chirality of the proteins well serve the needs of the bio-systems. Although the number of electrons that can be transferred through the protein is low, the electron transfer has a high fidelity due to the coupling of the spin with the electron's linear momentum because of the CISS effect.

### ii) Enhancing the selectivity of the reactions and interactions

It has been established that in chiral molecules charge polarization is accompanied by transient spin polarization. Since any interaction of chiral molecules with any object is accompanied by charge reorganization and polarization, it means that the interaction between chiral systems may involve a spin-exchange interaction. This interaction is short range and hence is relevant only when the two species are almost in contact; however, the interaction is on the order of ten times  $kT$  at room temperature and therefore dramatically affects interactions between biomolecules. The result of the spin-based interaction is that the enantioselectivity in bio-interactions is much higher than one would expect based on spatial configurations alone. Since most of the interactions in biology occur in crowded media, this spin-related interaction can play an important role in biorecognition [20].

## Conclusions and future perspectives

With time, the "secrets" behind the mechanism underlying the CISS effect will be revealed. The reason the CISS effect is so significant and robust is due to its immunity to all the elements that usually destroy spin selectivity in mesoscopic systems at room temperature. This effect exists only for moving electrons and it requires an exchange of momentum and energy between the moving electron and the molecular frame. Hence, electron vibrations and electron-electron interactions enhance the effective spin-orbit coupling (SOC) of systems that have a very small SOC in equilibrium. It is important to remember that despite CISS being related to moving charge and hence to the breaking of time-reversal symmetry, due to interactions with other spins (such as in metal substrates or ferromagnets), the spin polarization may be stabilized by the spin-exchange interaction. Another interesting result of CISS is that upon spin polarization in the chiral molecule, the entanglement of the singlet state is at least partially broken; therefore, one can associate a specific spin state with each electric pole. Indeed, it was observed that chiral molecules behave like magnetic impurities when adsorbed on a superconductor [21]. In general, the interplay between chirality, spin, and superconducting is an interesting field that we are just starting to explore [22]. Similarly, the relationship between the CISS effect and thermal conduction is very promising, from both a basic science perspective and for various applications [23].

The CISS effect has applications in many fields. It was observed and studied in inorganic chiral materials [24] and was demonstrated as an interesting way to enable spintronics. As previously mentioned, it is important in chemistry and can also be applied to separate enantiomers. In biology it

was demonstrated that due to the CISS effect, information in proteins can be transferred at long range and that the spin affects bio-recognition. In condensed matter physics and spintronics, chiral objects can replace ferromagnets for injecting highly polarized spin current and for constructing chiral interconnects that can transfer spins over relatively long distances at room temperature [25]. Recently it was suggested that CISS may play a role in the origin of life and may explain homochirality. It is expected that many more applications will be revealed and that the chiral effect will allow us to better understand Nature.

## References

1. R. Naaman, Y. Paltiel, D. H. Waldeck, *J. Phys. Chem. Lett.*, 2020, **11**, 3660–3666.
2. G. E. Uhlenbeck, S. Goudsmit, *Nature*, 1926, **117**, 264–265.
3. S. Mayer, J. Kessler, *Phys. Rev. Lett.* 1995, **74**, 4803.
4. K. Ray, S.P. Ananthavel, D.H. Waldeck, R. Naaman, *Science*, 1999, **283**, 814–816.
5. B. Göhler, V. Hamelbeck, T.Z. Markus, M. Kettner, G.F. Hanne, Z. Vager, R. Naaman, H. Zacharias, *Science*, 2011, **331**, 894–897.
6. Z. Xie, T. Z. Markus, S. R. Cohen, Z. Vager, R. Gutierrez, R. Naaman, *Nano Letters*, 2011, **11**, 4652–4655.
7. M. Kettner, B. Göhler, H. Zacharias, D. Mishra, V. Kiran, R. Naaman, C. Fontanesi, D. H. Waldeck, S. Şek, J. Pawłowski, J. Juhaniwicz, *J. Phys. Chem. C*, 2015, **119**, 14542–14547.
8. S. Mishra, A. K. Mondal, S. Pal, T. K. Das, E. Z. B. Smolinsky, G. Siligardi, R. Naaman, *JPC C* 2020, **124**, 10776–10782.
9. D. Nürenberg, H. Zacharias, *Phys.Chem.Chem.Phys.*, 2019, **21**, 3761.
10. R. Naaman, Y. Paltiel, D.H. Waldeck, *Acc. Chem. Res.*, 2020, **53**, 2659–2667.
11. W. Mtangi, V. Kiran, C. Fontanesi, R. Naaman, *J. Phys. Chem. Lett.*, 2015, **6**, 4916–4922.
12. Y. Liang, K. Banjac, K. Martin, N. Zigon, S. Lee, N. Vanthuyne, F. A. Garcés-Pineda, J. R. Galán-Mascarós, X. Hu, N. Avarvari, M. Lingenfelder, *Nat. Comm.* 2022, **13**, 3356.
13. J. Li, J. Ma, Z. Ma, E. Zhao, K. Du, J. Guo, T. Ling, *Adv. Energy Sustainability Res.* 2021, **2**, 2100.
14. T. S. Metzger, S. Mishra, B. P. Bloom, N. Goren, A. Neubauer, G. Shmul, J. Wei, S. Yochelis, F. Tassinari, C. Fontanesi, D. H. Waldeck, Y. Paltiel, R. Naaman, *Angew. Chemie*, 2020, **59**, 1653–1658.
15. D. K. Bhowmick, T. K. Das, K. Santra, A. K. Mondal, F. Tassinari, R. Schwarz, C. E. Diesendruck, R. Naaman, *Science Adv.*, 2022, **8**, eabq2727.
16. S. Mishra, S. Pirbadian, A. K. Mondal, M. Y. El-Naggar, R. Naaman, *J. Am. Chem. Soc.* 2019, **141**, 19198–19202.
17. K. Banerjee-Ghosh, S. Ghosh, H. Mazal, I. Riven, G. Haran, R. Naaman, *JACS*, 2020, **142**, 20456–20462.
18. S. Ghosh, K. Banerjee-Ghosh, D. Levy, D. Scheerer, I. Riven, J. Shin, H. B. Gray, R. Naaman, G. Haran, *PNAS*, 2022, **119**, e2204735119.
19. S. Mishra, A. K. Mondal, S. Pal, T. K. Das, E. Z. B. Smolinsky, G. Siligardi, R. Naaman, *JPC C*, 2020, **124**, 10776–10782.
20. A. Kumar, E. Capua, M. K. Kesharwani, J. M. L. Martin, E. Sitbon, D. H. Waldeck, R. Naaman, *PNAS*, 2017, **114**, 2474–2478.
21. H. Alpern, K. Yavilberg, T. Dvir, N. Sukenik, M. Klang, S. Yochelis, H. Cohen, E. Grosfeld, H. Steinberg, Y. Paltiel, O. Millo, *Nano Lett.* 2019, **19**, 5167–5175.
22. R. Nakajima, D. Hirobe, G. Kawaguchi, Y. Nabei, T. Sato, T. Narushima, H. Okamoto, H. M. Yamamoto, *Nature*, 2023, **613**, 479–484.
23. K. Kondou, M. Shiga, S. Sakamoto, H. Inuzuka, A. Nihonyanagi, F. Araoka, M. Kobayashi, S. Miwa, D. Miyajima, Y. C. Otani, *J. Am. Chem. Soc.* 2022, **144**, 7302–7307.
24. B. Bloom, Y. Paltiel, R. Naaman, D. Waldeck, *Chem. Rev.* 2024, **124**, 1950–1991.
25. K. Shiota, A. Inui, Y. Hosaka, R. Amano, Y. Ōnuki, M. Hedou, T. Nakama, D. Hirobe, J.-ichiro Ohe, J.-ichiro Kishine, H. M. Yamamoto, H. Shishido, Y. Togawa, *Phys. Rev. Lett.* 2021, **127**, 126602.

# Eugene Rabinowitch (1898-1973): A Voice of Conscience for the Atomic Age

## Bob Weintraub

POB 4562, Beersheva 8414402

Email: [bobweintraub@gmail.com](mailto:bobweintraub@gmail.com)

### Abstract:

Alexander Rabinowitch: "Eugene Rabinowitch, my father, was a world-class scientist and editor, as well as a talented teacher, journalist, and poet. Yet, he was much more than that. His life was forever changed by his service as a senior chemist and section chief on the Manhattan Project. Haunted to his final days by the threat to mankind posed by nuclear weapons, he became a voice of conscience for the atomic age" [*Bulletin of the Atomic Scientists*, 2005, **61** (1), 30].

## Eugene Rabinowitch

Eugene Rabinowitch was born to Jewish parents in St. Petersburg in 1898. He began his studies in 1916 at the new chemistry division of the Natural Sciences Faculty of the University of St. Petersburg. In 1918, two weeks before the start of the Red Terror against class enemies, he fled to Kiev, where he again started to study. In 1919, with the takeover in the Ukraine by the Bolsheviks, Rabinowitch fled first to Minsk and then to Warsaw. Here he tried again to study, but was distracted and worked as a Russian language journalist [1, 2], see Figure 1.

Rabinowitch moved to Berlin in 1921 where he took up his studies for a fourth time. He earned his PhD at the University under the supervision of Fritz Paneth. His thesis dealt with the preparation and properties of gaseous metal hydrides, in particular,  $\text{GeH}_4$  and  $\text{SnH}_4$ . In 1929 he accepted a research position in Göttingen. Here, he came under the influence of James Franck and learned to share Franck's fascination with photosynthesis.



**Figure 1.** Eugene Rabinowitch, circa 1950. Photograph courtesy of University of Illinois Archives.

**Bob Weintraub** was born in Brooklyn, New York and made aliyah in 1975 to Beer Sheva, where he remained. He earned the PhD in Physical Chemistry from MIT and the Diploma in Library Science from the Hebrew University of Jerusalem. He held positions in scientific and technical librarianship in industry, hospital and academic institutions. He is now retired. He has an interest in the history of chemistry.



In 1933, Rabinowitch fled Nazi Germany to Copenhagen, where he accepted a position with Niels Bohr. When his funding ended, he moved to University College London. In 1938, with the help of the British Academic Assistance Council (formed to assist displaced scientific teachers and investigators who by reason of race, religion or political views, were unable to carry on their work in their own country [3]), he found a position in the Chemistry Department of the Massachusetts Institute of Technology under the Solar Energy Project. During this time, he finished the first draft of his main piece of scientific writing, his 2000-page monograph published in three volumes, *Photosynthesis and Related Processes*.

## Manhattan Project

In 1943, Rabinowitch joined the Manhattan project, code name for the American project during World War II to design and build an atomic bomb, at the request of James Franck, who was then head of the Chemistry Division of the Metallurgical Laboratory. The Metallurgical Laboratory was the cover at the University of Chicago for work on the development of chain-reacting “piles” for plutonium production, to devise methods for extracting plutonium from the irradiated uranium, and to design a weapon. Rabinowitch joined the Information Division, headed by Robert Mulliken [4].

From the start of his work on the Manhattan project, Rabinowitch had deep ethical concerns about the uses of atomic energy and its international political implications. In 1944, he coauthored a report with Mulliken that stressed the need for combining nuclear energy with the effort to solve political problems worldwide. With the surrender of Germany, the issue as to whether or not the bomb should be used against Japan became an urgent matter.

In June 1945, Franck was appointed chairperson of a committee to discuss the social and political implications of atomic energy. The report, referred to as the *Franck Report*, was written mainly by Rabinowitch. The report was signed by J. Franck, D. Hughes, L. Szilard, physicists; T. Hogness, E. Rabinowitch, G. Seaborg, chemists; and a biologist, C. J. Nickson. Franck, Szilard, and Rabinowitch were deeply concerned about the lack of long-range planning and political implications of atomic energy. Due to differences of opinion about the use of the bomb, the report was issued not as a report of the committee, but rather as the opinion of the chairman and several of the committee members.

**Franck report:** “The scientists on this Project do not presume to speak authoritatively on problems of national and international policy. However, we found ourselves, by the force of events, during the last five years, in the position of a small group of citizens cognizant of a grave danger for

the safety of this country as well as for the future of all the other nations, of which, the rest of mankind is unaware. We therefore feel it is our duty to urge that political problems, arising from the mastering of nuclear power, be recognized in all their gravity, and that appropriate steps be taken for their study and the preparation of necessary decisions.” [5]

**Jungk:** “This passage was followed by an amazingly accurate forecast of the armaments race to be expected – as was later proved. In order to avoid such a contingency, the report continued, efforts should immediately be made to establish control of armaments on a basis of mutual trust. It was just this essential confidence which could be destroyed at the start if the United States were to make a surprise attack on Japan with a bomb which would be certain, like the German rocket missiles, to slaughter soldiers and civilians without distinction. The seven scientists warned the Secretary: ‘Thus, the military advantages and the saving of American lives achieved by the sudden use of atomic bombs against Japan may be outweighed by the ensuing loss of confidence and by a wave of horror and repulsion sweeping over the rest of the world and perhaps even dividing public opinion at home.’

“The Franck report proposed that, instead of the atomic bombardment of Japan as planned, demonstration of the new weapon might best be made, before the eyes of representatives of all the United Nations, in a desert or on a barren island. The report continued: ‘The best possible atmosphere for the achievement of an international agreement could be achieved if America could say to the world: ‘You see what sort of a weapon we had but did not use. We are ready to renounce its use in the future if other nations join us in this renunciation and agree to the establishment of an efficient international control.’” [6]

**A. Rabinowitch:** “Franck tried, but he was unable to deliver the report directly to the Secretary of War Henry Stimson. Eventually Stimson saw it but gave it only casual consideration.

“During many sleepless nights, waiting with mounting frustration for a response, my father thought about whether he had a moral obligation to leak the planning of the impending attacks on Japan to the media. But the thinking never went beyond sleepless nights. ‘The American War machine was in full swing, and no appeals to reason could stop it,’ he opined 25 years later in the *Bulletin*. Nevertheless, upon publication of the Pentagon Papers<sup>1</sup> in 1971, he remarked in a letter to the *New York Times*, ‘[I] would have been right to have done so.’

“President Harry S. Truman and Stimson were consumed with ending the war. They had little interest in long-term global issues and paid no heed to the ethical concerns of the

atomic scientists. On August 6, 1945, the bomb was dropped on Hiroshima, ushering in the atomic age. The second bomb was dropped three days later on Nagasaki, forcing the Japanese to surrender.

“It has been suggested that the atomic scientists were elated by the success of their work and that this response was only erased by use of the second bomb. This was certainly not the case for my father. I remember his reaction to Hiroshima well. He was completely devastated and devoted much of the rest of his professional life to preventing other *Hiroshimas*.” [1]

In 1947, Rabinowitch accepted the position as co-director of the Photosynthesis Research Laboratory in the Botany Department at the University of Illinois at Urbana-Champaign. S. S. Brody, a former student of Rabinowitch, listed the major scientific achievements of Rabinowitch and his co-workers: the ‘cage effect’ in photochemistry, first difference absorption spectroscopy in photochemistry, oxidizing capability of chlorophyll in solution, the ‘sieve effect’ in suspensions, photogalvanic effect, and the framework of the ‘Z’ scheme [7]. In 1945, Rabinowitch worked out all the kinetic possibilities whereby eight quanta gave rise to oxygen evolution – including the basics of the path accepted today [8].

## Bulletin of the Atomic Scientists

A. Rabinowitch: “My father founded the *Bulletin [of the Atomic Scientists]* in December 1945 with physicist Hyman Goldsmith. He served as the magazine’s editor-in-chief and guiding light from its inception until his death in 1973. ‘[The purpose of the *Bulletin* and the scientists’ movement it grew out of] was to awaken the public to full understanding of the horrendous reality of nuclear weapons,’ he explained in an editorial noting the twenty-fifth anniversary of the *Trinity Test* [code name of the first detonation of a nuclear device as part of the Manhattan Project], ‘and of their far reaching implications for the future of mankind; to warn of the inevitability of other nations acquiring nuclear weapons within a few years, and of the futility of relying on America’s possession of the ‘secret’ of the bomb.’

“From early on, my father viewed problems of arms control, the nuclear threat, and world security as connected to more fundamental issues. These included the division of the world into sovereign nations less concerned with global problems than with their own narrow self-interests; the economic and social disparity between technologically advanced and

technologically underdeveloped parts of the world; the population explosion, and global ecological degradation.

“Under his leadership, the *Bulletin* became a leading international forum for prominent thinkers from all over the world to discuss the issues related to the impact of recent scientific breakthroughs on society. At a time when the Cold War raged, the *Bulletin*, in its easy-to-understand layman’s language, brought the insights of leading Soviet scientists to Western readers. This was a reflection of my father’s immense respect for Russian science, as well as his conviction that all scientists, irrespective of national boundaries and international disputes, formed a community with shared values and critical perspectives, as well as a social responsibility to utilize them in the interest of human survival.” [1]

## Pugwash Conferences

Sir Joseph Rotblat and the *Pugwash Conferences on Science and World Affairs* were jointly honored by the award of the 1995 Nobel Peace Prize, “for their efforts to diminish the part played by nuclear arms in international politics and, in the longer run, to eliminate such arms.” [See endnotes 1 and 2.] Rotblat, in a tribute to Eugene Rabinowitch, “I have spent a large proportion of my time on the first ten years of the Pugwash history, for two reasons. First, these were the formative years of Pugwash, and laid the foundations for future activities. Second, because these were the years when Eugene Rabinowitch provided so much of our moral and ethical conceptions. His main endeavor was to ensure that Pugwash was not only a forum for informed debate on ongoing political/technological problems, but that it also had a mission: to serve as the social conscience of scientists, urging the scientific community to be accountable for the problems that have arisen from the advances of science.

“Let me conclude this talk with a few words about his philosophy, a philosophy much shared by me. Eugene was aware that to many of the so-called hard-nosed realists, his ideas would appear overtly romantic. In his [Pugwash] Presidential Address, at the 20th Annual Conference, in 1970, in Fontana, Illinois, he expressed the hope that society would adapt itself to the new technological habitat. He went on to say, ‘All this sounds like wishful dreaming – and will be undoubtedly dismissed as such, even by some Pugwash scientists. But yet, it represents the only realistically tenable evaluation of man’s existence on Earth in the age of science. Scientists are accustomed to serve common interests of

1 The Pentagon Papers was a top-secret US Department of Defense report leaked to the press on the history of US involvement in the Vietnam War. The study revealed that the administrations of Presidents Truman, Eisenhower, Kennedy, and Johnson had misled the public about the extent of the Nation’s involvement in Vietnam [18].

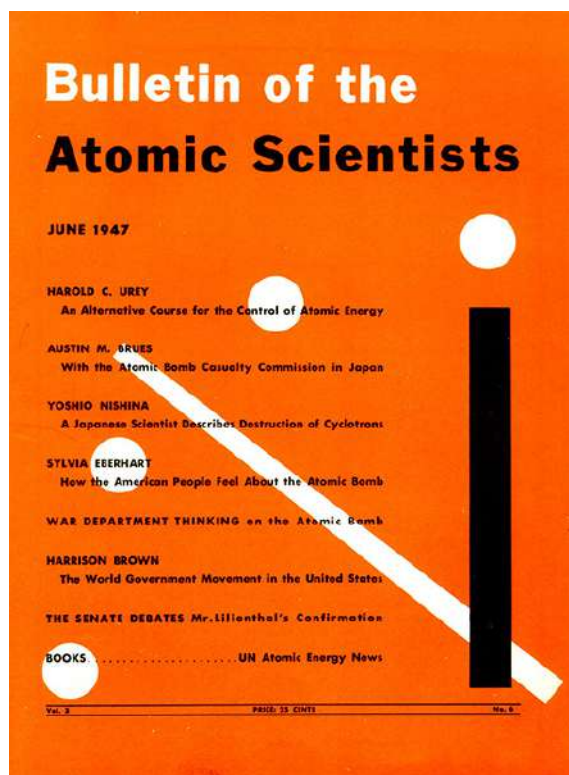


**Figure 2.** The cover of the June 1947 edition of the *Bulletin of the Atomic Scientists*, showing the Domsday Clock at 7 minutes to midnight. This was the first time the clock appeared. Artist, Martyl Langsdorf. Copyright notice follows references.

mankind, whatever their national or ideological commitment may be. Science is truly the first common enterprise of mankind. It is proper for scientists to accept responsibility for weaving this thread into the fabric of human society. What was once valid for a single society – united we stand, divided we fall – is becoming true of mankind as a whole.’

“Is all this Utopian, a pipe dream? If it were so then we are surely doomed, for there would be no escaping a nuclear holocaust. I would rather share Eugene’s beliefs, a blend of idealism and realism. For he was a giant of a man: his head was often in the clouds, but his feet were firmly planted on the ground.” [9]

## The Domsday Clock

The symbol of the *Bulletin of the Atomic Scientists*, the *Domsday Clock*, first appeared in 1947 (see Figure 2). Rabinowitch made the decisions about moving the clock’s settings until his death in 1973, after which the decisions were made by the *Bulletin’s* Science and Security Board. “The *Bulletin’s* clock measures the closeness of the world to

midnight – a nuclear war. It is intended to reflect basic changes in the level of continuous danger in which mankind lives in the nuclear age.” [10] With time the *Bulletin* expanded on the scope of threats that the clock was to represent. *Bulletin* (2021): “The Domsday Clock is a design that warns the public about how close we are to destroying our world with dangerous technologies of our own making. It is a metaphor, a reminder of the perils we must address if we are to survive on the planet. It expresses the countdown to *zero hour*.” [11]

## The Domsday Clock first set at 7 minutes to midnight

The Domsday Clock was first set at 7 minutes to midnight. It was moved for the first time in 1949 by Rabinowitch to three minutes to midnight after the Soviet Union successfully tested its first atomic bomb. In an editorial in the *Bulletin* in 1954, Rabinowitch expressed opinions on the stockpiling and use of nuclear weapons, “The only rationally defensible ground for the accumulation by the United States of ‘strategic’ atomic and hydrogen bombs is the deterrent effect of these stockpiles on whatever temptation the Soviet rulers might feel



**Figure 3.** First test of a hydrogen bomb at Eniwetok Atoll, Marshall Islands, November 1, 1952. Photo: US Army [16]. Following tests of the United States and Soviet Union of thermonuclear devices, in 1953 the hands of the Domsday Clock were moved back to 2 minutes to midnight. E. Rabinowitch: “The hands of the clock of doom have moved again. Only a few more swings of the pendulum, and, from Moscow to Chicago atomic explosions will strike midnight for Western Civilization. The achievement of a thermonuclear explosion by the Soviet Union, following on the heels of the development of ‘thermonuclear devices’ in America, means that the time, dreaded by scientists since 1945, when each major nation will hold the power of destroying, at will, the urban civilization of any other nation, is close at hand [17].”

to end the 'cold war' by an all-out onslaught on the 'capitalist' world. For this deterrent to be effective, the totalitarian rulers must be given no reason to believe that in the case of such an all-out aggression, atomic retaliation will not follow at once. For all other political or military emergencies, the non-Communist world should be equipped with means to defend itself wherever the aggression had occurred – even if this means leaving to the aggressor the choice of place and time. President Eisenhower's decision to release the film of the 1952 thermonuclear explosion at Eniwetok [site of the U.S. test of the first hydrogen bomb] is a first step in this direction. We hope it signifies the beginning of a new policy of letting the world face with open eyes the reality of an all-out future war. Full realization of this threat is, in our belief, the first prerequisite for a rational attempt to avoid it." [12], see Figure 3.

## Doomsday clock reset to 90 seconds in 2023

Over the years the minute hand has been reset by the *Bulletin* 25 times. It stands today (2023) at 90 seconds to midnight, the closest it has ever been set to midnight [13]\*.

In 1960 the clock was set back from 3 to 7 minutes to midnight. At that time Rabinowitch expressed "a few minutes" of optimism for the future. He saw new hopeful elements in the world picture. Rabinowitch: "The feeling seems justified that a turn of the road may have been reached, that mankind may have begun moving, however hesitantly, away from the dead end of its history." [14]

\* During the final stages of preparation of this manuscript, the Science and Security Board of the *Bulletin of the Atomic Scientists* announced that the hands of the Doomsday Clock for 2024 are unchanged at 90 seconds to midnight due to ominous trends that continue to point the world toward global catastrophe (PR, January 23, 2024).

### Endnotes:

**Endnote 1.** The participants from Israel to the 21 Pugwash Conferences held between 1957 and 1971 were: Dr. H. Boyko, Prof. A. de Shalit, Prof. M. Feldman, S. Freier, Prof. S. Friedlander, Prof. A. Keynan, Prof. S. Z. Lifson, Dr. Y. Peter, Prof. M. Sela, and Prof. G. Stein [15].

**Endnote 2.** In May 1967 the Continuing Committee of the Pugwash Conference sent a letter to Egypt and Israel offering assistance in arranging a private meeting between scientists of each of the two countries with a few members of the Continuing Committee with the intention of easing tension in the area. A response came quickly from President Shazar of Israel accepting the suggestion but no reply came

from President Nasser of Egypt [15]. The Six-Day War broke out on June 5, 1967.

## References

1. A. Rabinowitch, *Bull. At. Sci.*, 2005, **61** (1), 30–37.
2. T. T. Bannister, *Biophys. J.*, 1972, **12**, 707–18.
3. W. H. Beveridge, *Baron Beveridge, A Defense of Free Learning*, Oxford Univ. Pr., London, 1959.
4. "Manhattan Project Signature Facilities/atomicarchive.com," AJ Software & Multimedia, 1998–2020. <https://www.atomicarchive.com/history/sites/met-lab.html> .
5. E. Rabinowitch, *The Dawn of a New Age*, University of Chicago Press, Chicago, 1963.
6. R. Jungk, *Brighter Than a Thousand Suns*, Harcourt Brace, New York, 1958.
7. S. S. Brody, *Photosynth. Res.*, 1995, **43**, 67–74.
8. A. A. Krasnovsky, Jr., *Photosynth. Res.*, 2003, **76**, 389–403.
9. J. Rotblat, "Fifty Pugwash Conferences, A Tribute to Eugene Rabinowitch," *Pugwash Online*, Pugwash, Nova Scotia, 2000.
10. P. Findley, "Non-proliferation hearings. United States Senate. Hearings before the committee on foreign relations. Nineteenth Congress, second session," Washington, D. C.: U.S. Gov't Printing Office, 1968.
11. "What is the Doomsday Clock," *Bull. At. Sci.*, <https://thebulletin.org/doomsday-clock/faq/> .
12. E. Rabinowitch (editorial), *Bull. At. Sci.* 1954, **10** (5), 146–147 & 168.
13. "2023 Doomsday Clock Announcement," *Bull. At. Sci.*, 24 Jan. 2023. <https://thebulletin.org/doomsday-clock/>.
14. E. Rabinowitch (editorial), *Bull. At. Sci.*, 1960 **16** (1), 2–6.
15. J. Rotblat, *Scientists in the Quest for Peace*, Cambridge, MA.: MIT Press, 1972.
16. J. Lamm, "The Island is Missing!" U. S. Army, 28 Oct. 2010. [https://www.army.mil/article/47341/the\\_island\\_is\\_missing](https://www.army.mil/article/47341/the_island_is_missing) .
17. E. Rabinowitch, *Bull. At. Sci.*, **9** (8), 294–295 & 298, 1953.
18. "Richard Nixon Presidential Library and Museum," National Archives (US), 6 June 2022. Available: <https://www.nixonlibrary.gov/news/51st-anniversary-release-pentagon-papers>.

Front cover of the *Bulletin of the Atomic Scientists* (Figure 2) and quotes in text and abstract from Ref. 1 are copyright @ *Bulletin of the Atomic Scientists*, reprinted with permission of Taylor & Francis Ltd, <http://www.tandfonline.com> on behalf of the Atomic Scientists.

# Being a Patent Attorney (in Israel)

## Temira Sklarz

Neuroderm Ltd., 3 Pekeris Street, Rehovot 7670212, Israel

Email: [temira@neuroderm.com](mailto:temira@neuroderm.com)

The most basic requirement to become a patent attorney in Israel is to be a scientist, not an attorney. You learn the law aspects of the field along the way, during your two-year internship (and after), and are required to pass exams managed by the Ministry of Justice, focused on Intellectual Property Law. So, if you're an open-minded scientist, having some interest in law and business, this may be the field for you. But before we dive into what is required of you to become a patent attorney, let's describe what patents actually are.

As is well known, monopolies are frowned upon to the extent that in certain situations they are considered illegal. Governments around the world strive to enhance competition between various companies, leading to a thriving market, focused on the consumers' wellbeing. Patents are in essence the opposite to this – they provide the patent holder with a monopoly – they, and only they, are entitled to manufacture and sell whatever is covered by their patent, may it be a technological gadget or a drug able to save lives.

In the past decades the world has progressed so rapidly that we sometimes forget how hard it really is to achieve any type of innovation. But think of your laboratories – how many experiments do you need to run before succeeding? How many years might you work on something that, for a layman, would be considered, well, miniscule?

That's where patents come into play. You want innovation? You want drugs to be developed, technology to continue

to move forward? You must pay the price. Patents are that price. They provide the owner with a monopoly, allowing him to benefit financially from his invention, thus driving innovation in the first place – drug companies spend many millions on each drug being developed. Most of them fail along the way, and only a very few reach the endpoint. Overall expenses are enormous. As much as we'd like to think drug companies are in the business of curing patients, they are, for better or worse, in the business of making money. Their investments must be worth their while for them to stay in the business, and they do thanks to patents.

So, yes, the public loses from patents – the prices on products protected by patents are higher than they would be without the patents being in force; however, the public also benefits from patents, since many companies fund innovations thanks to the patents they hold to protect their “property”. Patents can therefore be viewed as a contract between governments (or the public) and innovators – you innovate, and I'll give you a monopoly on your innovation. In order to keep the balance, patents provide only a limited monopoly – mainly, they expire after 20 years and, at that time, the innovative knowledge becomes public knowledge, to be used by anyone desiring, allowing the prices to drop for the benefit of all (well, except for the company holding the patent...)

For this reason, by law, patent documents must describe the invention and the means by which one can reach it. That way, once the patent expires, the public actually holds the “recipe”

**Temira Sklarz** is an IL patent attorney and US patent agent. She has worked in the field since 2005, with experience in both law offices and industry. Temira studied chemistry at Bar-Ilan University, where she obtained a BSc (summa cum laude) and PhD in theoretical chemistry with Prof. Kenneth Kay.

<https://www.linkedin.com/in/temira-sklarz-036b41174/>



to the invention, which can be used directly, or built upon for further inventions (and possibly further patents as well). Without such disclosure, the patent is considered invalid and, if brought to court, the patent holder may lose the patent for not providing enough details for the public to be able to “follow” the invention.

This brings us back to the world of patent attorneys and the inventors they work with. Being a patent attorney gives you the unbelievable opportunity to be practically the first person to learn of any brand-new invention that is out there. Before publishing in *Science*, *Nature*, or elsewhere, the inventor comes to you to share his invention! But this is also one of the most sensitive parts of the job – who wants to share their newest development with you and, through you, with the entire public due to the disclosure requirement of patents?!? And this even before publishing in a scientific journal? What kind of scientist would want to do that?

So, other than being able to quickly grasp various scientific ideas, understanding the intricacies of the law, and being business minded, the patent attorney must have high emotional intelligence, needing to deal with people, who, to an extent at least, may be very reluctant to deal with the attorney. But even that is not it. On top of all of the above, first and foremost a patent attorney must be modest and even humble.

That’s not necessarily the first thing that comes to mind, but it should be – you just finished your PhD, but now, you’re starting a new field, and you sort of go back to square one. You may be bright, but everyone around you knows more than you do. Nothing in our scientific education teaches us the intricacies of intellectual property law. But even disregarding the law part of it, even on the science part you’ll be practically back in square one. Most, if not all, of the inventions you’ll encounter along the way will have little to do with your

advanced degree, and you’ll need to grasp new subjects as quickly and as thoroughly as possible.

Your modesty is essential for your work with the inventor – you must truly understand that the inventor will always, but always, know their invention better than you do. You have the job of asking the right questions and being able to use the answers to protect their invention, but always remember who the professional scientist is – and it’s not you.

On the flip side, inventors will do themselves a favor and listen to advice from the patent attorney – not in the field of science, but in the field of patents. If your attorney tells you something should be disclosed, if you want a patent to stand up in court, you should disclose, reluctant as you may be – remember – this disclosure is your deal with society – you get a monopoly in return. Your patent attorney may actually advise you not to file patents for certain inventions – you might be disclosing crucial information to your competitors, but getting little back for that disclosure. The breadth of the invention is also important – your patent attorney will probably try to focus the invention, seeing other things that have been published, while you may feel the patent should be broader. There’s always a give and take in any situation, but the bottom line is that each one of the parties should trust the other to be an expert in their field, allowing them to work harmoniously together.

On top of the above, you should have perfect English, good writing skills, an eye for detail, and an ability to work under strict deadlines. So, while any position requires various skills, that of a patent attorney requires an interesting combination of intellectual and personal skills, and it’s not necessarily easy to predict whether one will have what it takes. That being said, many patent attorneys (including myself), sort of “fell into” the field by chance or even “mistake”, but most of them will tell you that it’s one of the best “mistakes” they ever made.

# Interview with Ron Naaman – recipient of the 2022 ICS Gold Medal

## Arlene D. Wilson-Gordon

Chemistry Department, Bar-Ilan University, Ramat Gan 529002

Email: [gordon@biu.ac.il](mailto:gordon@biu.ac.il)



**Q:** Where were you born and where did your parents come from?

**A:** I was born in Israel as were both my parents. One of my grandfathers (Mintz) immigrated to Israel in the First Aliya. My other grandfather came in the Third Aliya about 1920 and was one of the founders of Moshav Yarkona, near the town of Hod Hasharon in central Israel where I and my brother still live. When my father Uri Naaman (Namenwirth) was asked in 1954 by the Mayor of Beer-Sheva, David Tuviahu, one of the founders of Moshav Yarkona, to establish the Departments of Youth and Culture in the Beer Sheva municipality, we moved there. Apart from two years in Munich, Germany, we lived in Beer Sheva until we moved to Haifa where I went to High School (Ironi Hei).

**Q:** What and who inspired you to study chemistry?

**A:** I had an excellent chemistry teacher at High School called Naama. My lifelong interest in physical chemistry began at high school. Whereas I appreciated the rigorous approach of physics, I was attracted by the intuitive thinking and artistic aspects of chemistry. Physical chemistry allows me to combine both of these approaches. The father of one of my classmates was a manager at the chemical company TAMI, now part of ICL. With his help, I worked there in the summers, at first distilling solvents but later involved in more interesting projects.

**Q:** Where did you study for your degrees?

**A:** After my army service, I began to study chemistry at Ben-Gurion University (BGU). This was the first year of undergraduate studies at Ben-Gurion and the degree in chemistry consisted of rigorous studies in chemistry, physics, and mathematics. Although it was a very challenging program, and many students dropped out, I greatly benefitted from obtaining such a solid background in mathematics and physics. I completed my BSc in 1973 on the eve of the outbreak of the Yom Kippur war and, after the war, began a direct PhD program at the Weizmann Institute and Ben-Gurion University. My advisers were Mendel Cohen of the Department of Structural Chemistry at Weizmann and Gad Fischer at BGU. After completing my PhD in 1978, I did postdocs at Stanford and Harvard.

In 1981, I joined the Department of Isotope Research (now Department of Chemical and Biological Physics) at the Weizmann Institute where I am now a Professor Emeritus.

**Q:** Why did you choose your particular field of chemistry?

**A:** It is a combination of experimental work and theoretical modelling.

**Q:** What do you consider to be your greatest scientific achievement, so far?

**Arlene Wilson-Gordon** was born in Glasgow, Scotland. She completed her BSc (Hons) at Glasgow University and her DPhil at Oxford University under the supervision of Peter Atkins. After a postdoc at the Hebrew University with Raphy Levine, she joined the faculty at the Department of Chemistry, Bar-Ilan University, where she rose to the rank of Professor and in 2015, Professor Emerita. Her research interests lie in the field of theoretical quantum and nonlinear optics. She is the editor of the Israel Chemist and Engineer, an online magazine for all who are interested in chemistry and chemical engineering.



**A:** Discovering the chiral induced spin selectivity (CISS) effect.

**Q:** Could you explain the phenomenon for those who are not familiar with your work.

**A:** According to the CISS effect, when electrons move within a chiral potential, their motion is spin-dependent; therefore, one spin state is preferred. Which spin is preferred depends on the handedness of the potential: for one handedness the spin is aligned parallel to the velocity, whereas for the other, the spin is aligned antiparallel to the velocity. The CISS effect has a wide range of implications in various disciplines.

**Physics:** When considering physics and electronic devices, the CISS effect presents chiral molecules as “nano devices” that produce spin-polarized electrons without the need to have a ferromagnet as a spin injector. The advantage here is the ability to miniaturize devices, since the reduction in the size of a regular ferromagnet is limited by the superparamagnetic-ferromagnetic transition. Namely, a small ferromagnet becomes superparamagnetic and therefore cannot function as a spin-selective source. However, chiral molecules or inorganic chiral materials are not limited by this size constraint. In addition, the CISS effect presents the chiral molecules as a new topological material.

**Chemistry:** In chemistry, the CISS effect was shown to allow the enhancement of multiple electron reactions, by controlling the relative orientation of the electron spins. An interesting example is the enhancement observed in the case of water splitting where, in addition, unwanted byproducts could also be eliminated. The CISS effect opened a new avenue towards efficient enantioseparation of chiral molecules by magnetic substrates and, as was recently shown, it allows for spin enantio-selective chemistry.

**Biology:** the CISS effect may provide the answers to several phenomena not completely understood so far. It explains how very long-range electron transfer occurs in biology and specifically, how it occurs through proteins. Apparently, the coupling between the spin and the electron’s linear momentum protects the electron from being back scattered. This property enhances the range of efficient electron transfer. The spin-dependent charge reorganization also explains the long-range allosteric control of protein association. In addition, the CISS effect increases the efficiency of multiple electron redox reactions that involve oxygen and may explain the efficient respiration process. Hence the CISS effect explains why chirality is preserved so persistently in Nature through evolution.

**Q:** What problems would you like to tackle in the near and far future?

**A:** To understand the role of the electron spin in biology and find ways to utilize it.

**Q:** Do you enjoy teaching and interacting with students?

**A:** Of course

**Q:** Would you recommend a career in academia to young scientists?

**A:** Yes, if the person is excited about discovering the unknown and prepared to work hard to do so.

**Q:** What are the main challenges facing Israeli science?

**A:** We need to transfer to the young generation the understanding that science is the key for prosperity and high quality of the life on earth and that we, as a country, can play an important role in it, providing that enough excellent young people join the scientific community in Israel. Sadly, in the current situation, there is no feeling of striving towards excellence by either the government or the public.

**Q:** What do you consider to be your greatest contribution to Israeli society?

**A:** My research should lead to various applications that can be commercialized. As scientist I am involved in science education in high schools. But my most important contribution is to serve as a role model to young scientists.

**Q:** If you had a magic wand, what would you change in Israeli society?

**A:** This is an impossible question. Right now, our country is falling apart and if the people of this country will not understand that our only hope to survive is to maintain society that is fair, open-minded, and values education, then we will become third world country in the Middle East.

**Q:** Do you have any advice for young people embarking on their career?

**A:** Go with your dreams and be ready to work hard to achieve them.

**Q:** How do you enjoy your free time?

**A:** I enjoy being with my family.

**Note:** Ron is married to a fellow chemist, Dr. Rachel Mamluk-Naaman, who contributed an article on “Women in Science” to the 8<sup>th</sup> issue of ICE <https://doi.org/10.51167/ice00011>

# The 87<sup>th</sup> Annual Meeting of the Israel Chemical Society: April 3, 2024, Smolarz Auditorium, Tel Aviv University

## Ehud Keinan

The Schulich Faculty of Chemistry, Technion-Israel Institute of Technology, Haifa, Israel

[E-mail: keinan@technion.ac.il](mailto:keinan@technion.ac.il)

## Introduction

The Annual Meeting of the Israel Chemical Society (ICS) has a long history since its establishment in 1933 and is a well-known event in the scientific landscape of the State of Israel. These colorful gatherings of Israeli chemists usually occur in mid-February, the inter-semester break for all Israeli universities. Unfortunately, the Meeting of 2021 fell victim to the global COVID-19 pandemic, forcing a gap of 2.5 years between the 85th Meeting of February 2020 at the International Conference Center, Jerusalem, and the 86th Meeting of September 2022 at the David Intercontinental Hotel, Tel Aviv. That disruption of our usual schedule and the consequences of the war in the Gaza Strip forced us to postpone the 87th meeting several times. Finally, the ICS Executive Board decided to hold the meeting on April 3, 2024, and reduce it to a single day rather than the traditional structure of two days.

The chosen venue was the Smolarz Auditorium, located on the southern section of the Tel Aviv University campus. The building, completed in 2003, offers 5,000 square meters for diverse activities. Its layout blends the two different urban grids that regulate the campus. The fusion between the two main volumes of the building, the foyer and auditorium, creates outstanding views, and the main hall, with its 1,200 convenient seats, could accommodate the planned meeting perfectly.

Following ICS tradition, the chemistry departments of the six major research universities share responsibility for organizing these meetings in a six-year cycle in a constant order: the Hebrew University of Jerusalem, Technion, Tel Aviv University, Bar-Ilan University, Ben-Gurion University of the Negev, and the Weizmann Institute of Science. Thus, looking back at the ICS history of the past two decades, the Technion, for example, has taken responsibility for organizing the 68th Meeting (2003), the 74th Meeting (2009), the 80th Meeting (2015), and the 86th Meeting (2022). This year, following a previous decision of the ICS Executive Board, Ariel University joined this cycle for the first time. Thus, the organizing Committee included four members from the Department

of Chemical Sciences, Ariel University: co-chairman Prof. Flavio Grynszpan, co-chairman Prof. Alex Schechter, Prof. Alex M. Szpilman, and Dr. Tomer Zidki, augmented by Prof. Norman Metanis of the Hebrew University of Jerusalem, and Prof. Micha Fridman of Tel Aviv University.

Another unique tradition the ICS has followed for over 25 years is hosting high-profile delegations of distinguished scientists from top academic institutions worldwide to deliver plenary and keynote lectures. This tradition has created outstanding opportunities for many Israeli scientists, particularly graduate students, to interact with world-renowned chemists, thus enhancing their prospects of networking and scientific collaboration. Unfortunately, the large delegation of 10 scientists and 20 graduate students from Denmark preferred to visit Israel when the war ends. The ICS Board decided to postpone their participation to a later year.

Nevertheless, with its ambitious program, the one-day event provided an excellent opportunity to gather together many students, postdoctoral fellows, and scientists from around Israel, 18 months after the 86th ICS meeting, even without a foreign delegation. Over 500 participants enjoyed a diverse scientific program that included 16 plenary and keynote lectures in the main hall and two technical lectures in another. The 230 posters, all displayed at a single poster session, required an extension of the foyer by an external tent. The organizing committee selected four posters for the Best Poster Prizes awarded at the Prize Ceremony, which was held in the evening.

In addition to the scientific program, the ICS held its traditional General Assembly in the early afternoon, discussing the past year's activities, plans for the next year, and financial issues. Mr. Shimon Nizrad, the ICS Accountant, provided an overview of the ICS's budget, legal status, and financial goals. A Gender Equality Power Hour occurred during the poster session, chaired by Mindy Levine of Ariel University. The prize ceremony, which took place in the evening, was preceded by a reception and light dinner for all participants.

The event attracted many sponsors, including the Weizmann Institute of Science, Tel Aviv University, Ben-Gurion University of the Negev, the Hebrew University of Jerusalem, Ariel University, the Technion, Bargal Analytical Instruments Ltd., Eldan Neopharm Group, and Tzamal D-Chem Laboratories.

The meeting featured a comprehensive commercial exhibition, with 13 providers showcasing a wide array of lab equipment, scientific instrumentation, chemicals, materials, analytical chemistry services, and publishing houses. The exhibitors included Arad-Ophir Information Specialists Ltd., Bargal Analytical Instruments Ltd., BioAnalytics Ltd., Bruker Scientific Israel Ltd., Labotal Scientific Equipment Ltd., LabSuit Projects Ltd., Rhenium Ltd., Tzamal D-Chem Laboratories Ltd., Gadot-Mercury, Eldan Neopharm Group, Medi-Fischer Engineering & Science Ltd., Merck, and Prime Lab Scientific Instruments Ltd.

The mix of excellent lectures, colorful poster sessions, exhibitions, and other activities created a vivid atmosphere with vibrant discussions, exchange of information, and social gathering, as reflected by the collage of photographs (Figure 1).

### Opening Ceremony

**Prof. Alex Schechter**, co-chairperson of the organizing committee, opened the meeting and greeted the guests and participants: “Good morning, everyone. On behalf of the other co-chairperson, Prof. Flavio Grynszpan, and the organizing committee, I am delighted to welcome you to the 87th meeting of the Israel Chemical Society in Tel Aviv. It has been a while since the previous meeting. Before fully recovering from the Covid pandemic, the war and resultant upheavals forced us to organize this annual meeting in a reduced format. Furthermore, the international delegation from Denmark postponed their arrival to quieter times.

“Nevertheless, our resilient academic community has shown remarkable strength in dealing with the changing conditions. We have found innovative ways to continue our scientific work, teaching, and meeting in workshops and conferences. Despite the difficulties, it is crucially important that we continue our longstanding tradition of ICS meetings. This celebration of Israeli chemistry is a unique opportunity to share our enthusiasm for science and to recognize excellence in research, teaching, and other aspects of academic life. I wish you all an enjoyable meeting.”

**Prof. Ehud Keinan**, president of the ICS, greeted the audience: “Good morning, everybody, and welcome to the 87th Meeting of the ICS. David Ben-Gurion once said that in Israel, ‘Anyone who doesn’t believe in miracles is not a realist.’

Indeed, seeing over 500 participants, 230 posters, and an extensive exhibition in these challenging times is no less than a miracle, certainly when most other scientific conferences in Israel were canceled, postponed to some unknown date, or transferred to another location abroad. Many members of our community are experiencing losses, grief, and stress, and many are still on active duty in the army. At the same time, the length and quality of the academic year still need to be determined. The ICS Board’s decision to take the risk and hold this meeting under the changing reality is a typical case of Israeli *hutzpah*. Condensing a two-day symposium into one day is non-trivial, and doing it for the first time without an organizing company is another miracle.

These achievements could only have happened with the coordinated effort and enthusiasm of many eager young people to meet friends and colleagues. I want to acknowledge them and all members of the organizing committee, most of them from Ariel University. It’s the first time Ariel University has joined the cycle, so now it includes seven universities. Next year, it will be the turn of Bar-Ilan University to organize the 88th ICS Meeting in February 2025, and we hope the environment will allow for the participation of an international delegation.

I want to acknowledge the main sponsors of this meeting, including all chemistry departments at the Israeli research universities and Bargal, Eldan, and Tzamal companies. I thank Rinat Avital and Lee Reider, who manage the Smolarz Auditorium, and Benny Bashan, who organized the commercial exhibition. I thank the exhibitors, lecturers, and poster presenters, and I encourage all of you to visit the posters and the exhibition. Above all, I would like to thank my right-hand, Ms. Tali Lidor, the administrative manager of the ICS, who served as the organizing company. Without her, this event would not be possible. Tali has done most of the work, and I joined her team. I want to thank the ICS Executive Board, with whom we have worked for many years.

The Israel Chemical Society is older than the State of Israel, and we now celebrate the 90th birthday of the ICS. The Establishment of the ICS and its history is a fascinating story that started in 1933, when a group of chemists, mainly chemistry professors who fled Nazi Germany, gathered in Tel Aviv and formed the Association of Chemists in Palestine, which later changed its name to the ICS. I’m proud to serve more than 15 years as ICS president. This year is particularly challenging for me as I started my role as the IUPAC president.

Later tonight, we’ll gather in this auditorium for an exciting evening, recognizing the achievements of 38 ICS Prize winners of the 2022 and 2023 cycles. Soon after the meeting, I’ll issue a call to nominate candidates for all 2024 ICS prizes, and I

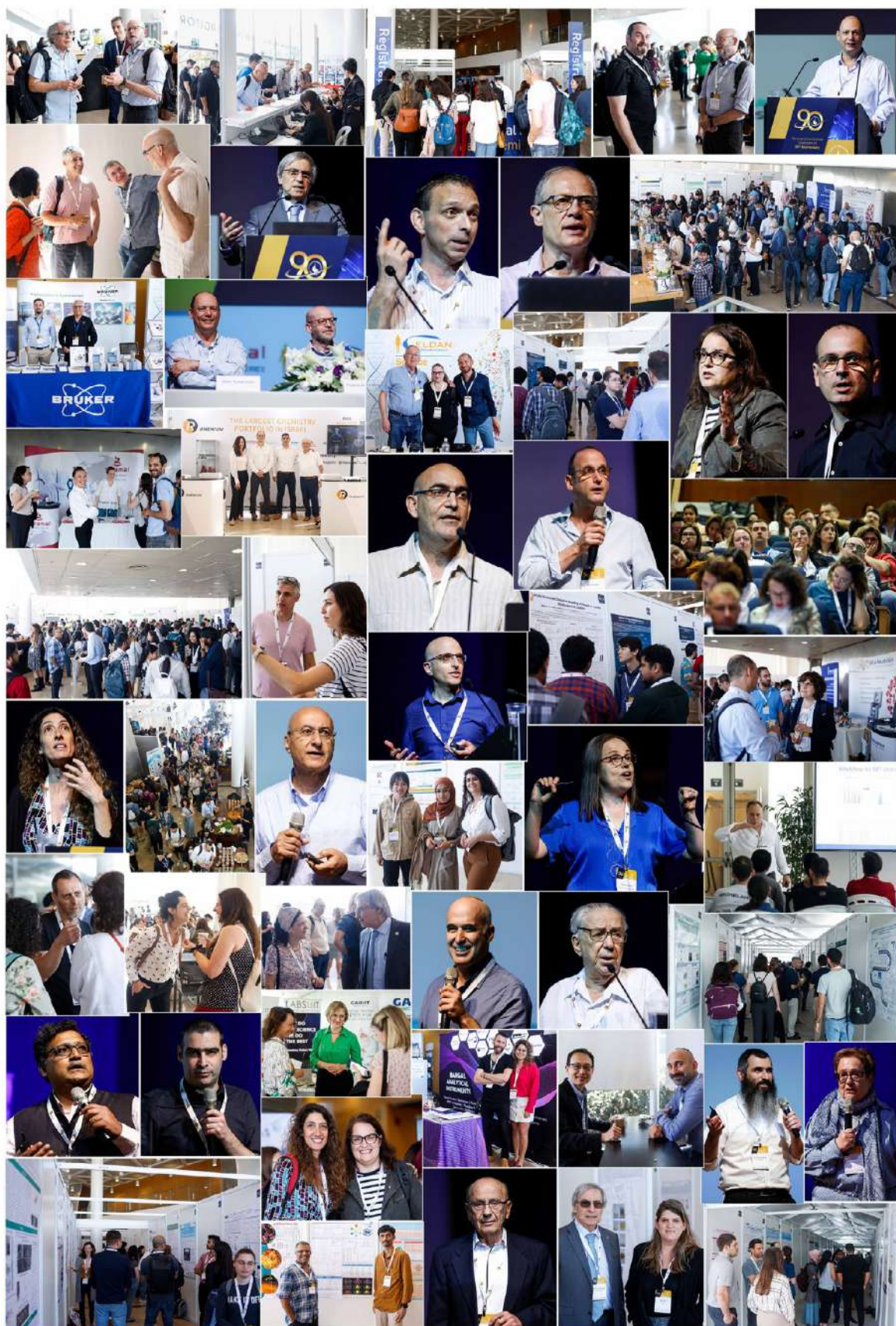


**Figure 1.** A collage of photos reflecting the general atmosphere throughout the 87th ICS meeting, including the lectures, posters, and commercial exhibition. Photos by Dror Sithakol.

will take this opportunity to focus on the gender issue. I am happy with the trend of steadily increasing gender equality in academia, although the list of ICS Prize laureates still needs to reflect this trend entirely. Although we cannot and should not influence the decision-making process of the specific prize juries, where gender equality exists, we must ensure that every gifted female scientist is nominated. And this responsibility goes to everybody because every registered ICS member can nominate other members as candidates.

Thanks again for participating in the 87th ICS Meeting; I wish you an enjoyable, highly fruitful experience!"

## Lectures

Unlike the traditional two-day ICS meeting programs, which included 4-5 parallel sessions, the one-day format, and the venue's structure led the organizing committee to build a program of 16 lectures in the main auditorium, two technical lectures in a separate hall, and 230 posters.

**Lucio Frydman** of the Weizmann Institute of Science, 2022 ICS Prize of Excellence winner, lectured on "Nuclear Magnetic Resonance or Magnetic Resonance Imaging? Let's take both."

**Oded Hod** of Tel Aviv University, 2022 ICS-Tenne Prize winner, spoke about "Layered Ferroelectricity: from Geometric Measures to First-Principles Calculations."

**Leeor Kronik** of the Weizmann Institute of Science spoke about "Understanding optical properties of biogenic and bio-inspired molecular crystals: a first-principles perspective."

**Sharon Ruthstein** of Bar-Ilan University lectured on "The correlation between the gating mechanism of the human copper transporter, Ctrl1, and the development of innovative biomarkers."

**Eylon Yavin** of the School of Pharmacy, The Hebrew University of Jerusalem, spoke about "FIT-PNAs as RNA sensors for Ovarian cancer diagnostics."

**Doron Pappo** of Ben-Gurion University of the Negev, 2023 ICS-Adama Prize winner, spoke about "Redox-Active 3rd-Transition Metal Catalysts for Dehydrogenative C-H Bond Coupling."

**Raya Sorkin** of Tel Aviv University spoke about "Membrane tension and membrane (hemi)fusion."

**Shlomo Magdassi** of The Hebrew University of Jerusalem, 2022 ICS Prize of Excellence winner, spoke about "From Gutenberg Bible to 4D printing."

**Galia Maayan** of the Technion lectured on "Bio-inspired electrocatalytic water oxidation."

**Dan Meyerstein** of Ariel University and Ben-Gurion University spoke about "The Mechanisms of the Fenton and Fenton-Like Reactions."

**Malachi Noked** of Bar Ilan University, 2023 ICS Young Scientist Prize winner, spoke about "Mitigating Electrode Material Degradation through Advanced Surface Modification Technique."

**David Eisenberg** of the Technion spoke about "Porous Materials: The Next Frontier in Energy Research."

**Emanuel Peled** of Tel Aviv University spoke about "Lithium and sodium metal batteries."

**Idan Hod** of Ben-Gurion University of the Negev, 2022 ICS Young Scientist Prize winner, spoke about "Molecular Manipulation of Heterogeneous Electrocatalysis Using Metal-Organic Frameworks."

**Abhishek Dey** of the Indian Association for the Cultivation of Science, West Bengal, India, spoke about "Factors Deciding the Selectivity of O<sub>2</sub>, NO, CO<sub>2</sub>, and SO<sub>2</sub> Reduction."

## The 2024 ICS Prize Ceremony

An extended audience gathered in the main auditorium for an exciting evening, where an unprecedented number of 38 prize winners of the 2022 and 2023 cycles were recognized for their achievements (Figure 2). A festive reception, which marked a delightful transition from the intense scientific lectures to the prize ceremony, allowed for a significant population change. The arrival of many family members of the prize winners, including young children and elderly grandparents, resulted in an atmosphere that transformed gradually from a solemn science-focused program to a more joyful social event (Figure 3). The 1.5-hour ceremony took place at the main auditorium in the presence of a heterogeneous audience.

## The 2022 ICS Prizes

The **2022 ICS Gold Medal** was awarded to **Prof. Ron Naaman** of the Department of Chemical Physics at the Weizmann Institute of Science for discovering the Chiral Induced Spin Selectivity (CISS) effect and explaining why nature preserved chirality persistently through evolution; and **Prof. Zeev Gross** of the Schulich Faculty of Chemistry, Technion, for pioneering the corrole chemistry, and impacting bio-inorganic chemistry, metal-based drug candidates and catalysis.

**Prof. James Y. Becker** of the Ben-Gurion University of the Negev became the **2022 Honorable Member of the ICS**





**Figure 3.** A collage of photos reflecting the general atmosphere in the evening reception preceding the ICS Prize Ceremony. Photos by Dror Sithakol.

for his extensive contributions to organic electro-synthesis and electro-catalysis and for outstanding contribution to chemistry education at all levels.

The **2022 ICS Prize of Excellence** was awarded to **Prof. Shlomo Magdassi** of The Hebrew University of Jerusalem for developing micro and nanomaterials and their applications in delivery systems and functional printing; and **Prof. Lucio Frydman** of the Weizmann Institute of Science for his long-standing, seminal contributions to Magnetic Resonance.

The **2022 ICS Excellent Young Scientist Prize** was awarded to **Prof. Ori Gidron** of The Hebrew University of Jerusalem

for his contribution to the fields of non-planar aromatic materials and macrocyclic chemistry and **Prof. Idan Hod** of Ben-Gurion University of the Negev for designing MOF-based platforms that manipulate heterogeneous electrocatalysis at the molecular level through secondary-sphere interactions.

The **2022 ICS-Dalia Cheshnovsky Prize for Excellence in Chemistry Teaching** was awarded to **Ms. Dafna Yam** of the Ohel-Shem High School, the Herzlia High School of Engineering in Tel Aviv, and the Ort High School for the Arts and Sciences, Ramla, for teaching chemistry with professionalism, dedication and creativity, and guiding chemistry teachers, while assimilating new teaching methods

and innovative pedagogy, giving attention to every student, at all times, with great patience and pleasant manners.

The **2022 ICS-Uri Golik Prize for an Excellent Graduate Student** was awarded to **Dr. Efrat Resnick** of the Weizmann Institute of Science for developing chemical probes for protein targets and a specific inhibitor against SARS-CoV-2 protease.

The **2022 ICS-Shahar Prize for the Excellent Administrative Assistant** was awarded to **Ms. Liat Presman**, Academic staff and Dean's office coordinator at the Schulich Faculty of Chemistry, Technion. She received the prize for her remarkable professional and creative management with passion and dedication, work ethic, human relations, and

outstanding organizational skills manifested by voluntarily expanding her contributions beyond the formally expected.

The **2022 Tenne Family Prize in memory of Lea Tenne for Nanoscale Sciences** was awarded to **Prof. Oded Hod** of the School of Chemistry at Tel Aviv University for predicting structural superlubricity in heterogeneous layered material contacts and developing simulation tools and geometric measures for nanoscale 2D materials.

The **2022 ICS-Adama Prize for Technological Innovation** was awarded to **Prof. Aharon Blank** of the Schulich Faculty of Chemistry, the Technion, for developing new methodologies in magnetic resonance and applying them to science, technology, and medicine.



**Figure 4.** Award ceremony of the 2022 ICS Prizes. First row from left: Excellent Graduate Students with their university representatives: David Azulay (with Shlomo Magdassi of The Hebrew University of Jerusalem), David Zitoun of Bar-Ilan University receives the award for Ariel Friedman, Itai Massad (with Aharon Blank of the Technion), Noy Nechmad (with Gabriel Lemcoff of Ben-Gurion University), Moshe Kol of Tel-Aviv University receives the award for Inbal Oz. Second row: Golokesh Santra (with Lucio Frydman of the Weizmann Institute of Science) and Alina Sermiagin (with Alex Szpilman of Ariel University). Lucio Frydman receives the ICS-Uri Golik award for Efrat Resnick of the Weizmann Institute (with Uri Golik, Eran Golik, and Moshe Cohen), Oded Hod receives the ICS-Tenne award (with Reshef Tenne), Resgef Tenne receives the ICS recognition for his extended support of the ICS). Third row: Aharon Blank receives the ICS-Adama Prize (with Efrat Lifshitz and Itsik Bar-Nahum of Adama), Liat Presman receives the ICS-Shahar Prize (with Efrat Lifshitz and Dani Shahar), Dafna Yam receives the ICS-Dalia Cheshnovsky Prize for Excellence in Chemistry Teaching (with Dorit Teitelbaum, Ori Cheshnovsky, and Dani Shahar), James Y. Becker becomes a Honorable Member of the ICS (with Gabriel Lemcoff), Ori Gidron receives ICS Excellent Young Scientist Prize. Fourth row: Ori Gidron receives the ICS Excellent Young Scientist Prize (with Gabriel Lemcoff), Lucio Frydman receives the ICS Prize of Excellence, Shlomo Magdassi receives the ICS Prize of Excellence, Ron Naaman receives the ICS Gold Medal, Zeev Gross receives the ICS Gold Medal. Photos by Dror Sithakol.

The 2022 ICS Prize for an Excellent Graduate Student was awarded to seven graduate students: **David Azulay** (The Hebrew University of Jerusalem), **Ariel Friedman** (Bar-Ilan University), **Itai Massad** (Technion), **Noy Nechmad** (Ben-Gurion University), **Inbal Oz** (Tel-Aviv University), **Golokesh Santra** (Weizmann Institute of Science), and **Alina Sermiagin** (Ariel University).

### The 2023 ICS Prizes

**Prof. Matityahu (Mati) Fridkin** of the Weizmann Institute of Science and **Prof. Chaim Gilon** of the Hebrew University of Jerusalem became **Honorable Members of the ICS** for their seminal contributions to the science of peptides and proteins from synthesis to therapeutic agents and for training many followers in academia and industry.

The **2023 ICS Excellent Young Scientist Prize** was awarded to **Prof. Malachi Noked** of Bar-Ilan University for his pioneering contributions to solid-state batteries, high-energy-density batteries, electromobility, thin functional films, and innovative materials; and **Prof. Nadav Amdursky** of the Schulich Faculty of Chemistry, the Technion, for developing new ways of studying and utilizing proton transfer reactions in biological materials, biopolymers, and dynamic systems.

The **2023 ICS-Dalia Cheshnovsky Prize for Excellence in Chemistry Teaching** was awarded to **Ms. Rachel Kelner** of the Amit Yeshurun Ulpanit, Petah Tikva, for four decades of excellence in chemistry teaching, for developing innovative teaching methods, educating students and teachers in different channels, and for evaluating and analyzing the matriculation exams in chemistry.

The **2023 ICS-Uri Golik Prize winner for an Excellent Graduate Student** was awarded to **Mr. Bar Cohn** of the Schulich Faculty of Chemistry, the Technion, for his outstanding contributions to ultrafast dynamics of the interaction between molecular vibrations and optical cavities at ambient conditions.

The winner of the **2023 ICS-Shahar Prize for Excellent Administrative Assistant** was awarded to **Ms. Elena Borodina**, administrative manager of the Department of Chemical Sciences at Ariel University, for her remarkable professional and creative management with passion and dedication, work ethic, human relations, and outstanding organizational skills.

The **2023 Tenne Family Prize for a young scientist in memory of Lea Tenne for Nanoscale Sciences** was awarded to **Dr. Benjamin Palmer** of the Department of Chemistry of Ben Gurion University for his outstanding work on the characterization of unique biogenic nanostructures and the

understanding of their structure-function relations in living organisms.

The **2023 ICS-Adama Prize for Technological Innovation** was awarded to **Prof. Doron Pappo** of the Ben-Gurion University of the Negev for developing innovative oxidative coupling methods based on abundant transition metal catalysts for practical synthesis of complex molecules.

The **2023 ICS Prize for an Excellent Graduate Student** was awarded to seven graduate students: **Itamar Liberman** (Ben-Gurion University), **Poulami Mukherjee** (Ariel University), **Ilan Shumilin** (The Hebrew University), **Benjamin Sorkin** (Tel-Aviv University), **Tamar Wolf** (Weizmann Institute of Science), **Anna Yucknovsky** (Technion), and **Shani Zev** (Bar-Ilan University).

The **2023 ICS award for the green chemical industry** was awarded to All Recycling and its CEO, **Gadi Reichman**, for applying advanced technology to recycle electronic waste and produce valuable raw materials, thus reducing the need to mine limited natural resources and lowering energy costs.

The **2023 ICS-Peled Prize for a high school graduate for an Excellent Chemistry Project** was awarded to **Yonatan Shapira** and **Ethan Amiran** of the Jerusalem's Israel Arts and Sciences Academy. Yonatan Shapira received the Prize for his research project "Production of atomic chips" under the supervision of Prof. Liraz Chai and Dr. David Azulay of the Institute of Chemistry, The Hebrew University of Jerusalem. Ethan Amiran received the Prize for his research project, "light-emitting perovskite nanoparticles after replacing halides and cations," supervised by Prof. Lioz Etgar and Mrs. Tal Binyamin of the Institute of Chemistry, The Hebrew University of Jerusalem.

**Prof. Reshef Tenne** was awarded recognition for his long-standing support of the ICS through the Tenne-family prize. Tenne responded, "I wish to congratulate the recipients, Prof. Oded Hod of Tel Aviv University and Dr. Ben Palmer of Ben-Gurion University, of the Tenne Family Prize in memory of Lea Tenne Z"l. Together with my family, we thank the Israel Chemical Society for hosting this prize. We are privileged to have such a list of excellent scientists to be chosen year after year (for the last 12 years) to receive this important recognition. This is the best way for me and my family to commemorate the legacy of my late first wife, Lea, who was not a scientist but was very attached to science. This prize is intended to recognize the contributions of Israeli scientists in this dynamic field of research, thereby promoting excellence in science in the country.



**Figure 5.** Award ceremony of the 2023 ICS Prizes. First row from left: Excellent Graduate Students with their university representatives: Itamar Liberman (with Idan Hod of Ben-Gurion University), Alex Szpilmán receives the award for Poulami Mukherjee of Ariel University, Ilan Shumilin (with Shlomo Magdassi of The Hebrew University), Benjamin Sorkin (with Moshe Kol of Tel-Aviv University), Tamar Wolf (with Lucio Frydman of the Weizmann Institute), Second row: Anna Yucknovsky (with Efrat Lifshitz of the Technion), and Shani Zev (with Dan Major of Bar-Ilan University), Bar Cohn receives the ICS-Uri Golik award (with Uri Golik, Efrat Lifshitz, Eran Golik and Moshe Cohen), Benjamin Palmer receives the ICS-Tenne award (with Reshef Tenne), Doron Pappo receives the ICS-Adama Prize (with Itsik Bar-Nahum of Adama), Third row: Elena Borodina receives the ICS-Shahar Prize (with Dani Shahar), Rachel Kelner receives the ICS-Dalia Cheshnovsky Prize for Excellence in Chemistry Teaching (with Dorit Teitelbaum, Ori Cheshnovsky, Dani Shahar, and Dafna Yam), Yonatan Shapira (left) and Ethan Amiran (right) receive the ICS-Peled Prize for a high school graduate for an Excellent Chemistry Project (with Dorit Teitelbaum, Nehama Peled, and Michael Peled), Nehama and Michael Peled receive the ICS recognition for their extended support of the ICS, Gadi Reichman of All Recycling receives the ICS award for the green chemical industry. Fourth row: Chaim Gilon becomes an Honorable Member of the ICS, Matityahu Fridkin becomes an Honorable Member of the ICS, Matityahu Fridkin, Emma Fridkin, Noemi Gilon, and Chaim Gilon, Malachi Noked receives the ICS Excellent Young Scientist Prize (with David Zitoun), Efrat Lifshitz of the Technion receives the ICS Excellent Young Scientist Prize for Nadav Amdursky. Photos by Dror Sithakol.

## POSTER PRIZES

The organizing committee selected four posters for the Best Poster Prizes awarded at the evening Prize Ceremony.

Poster ICN-18 “Enhancing Stability and Solar Cell Efficiency of CsPbBr<sub>3</sub> Nanowire Arrays Grown on Anodized Aluminum Oxide: Insights into Light-Matter Interactions,” by **Neena Prasad** and Lena Yadgarov of the Department of Chemical Engineering, Ariel University.

Poster OOC-05, “Stereoselective synthesis of 1,n dicarbonyl compounds through palladium catalyzed ring opening/isomerization of densely substituted cyclopropanols,” by **Charlotte S. Teschers**, Anthony Cohen, and Ilan Marek of the

Schulich Faculty of Chemistry and the Resnick Sustainability Center for Catalysis, Technion.

Poster PC-15, “Investigating Radical Chemistry With Synchrotron Radiation,” by **Nadav Genossar-Dan** and Joshua H. Baraban of the Department of Chemistry, Ben Gurion University.

Poster EC-19, “Nitrate Reduction to Ammonia: Assessing the Electrocatalytic Behavior of Cu<sub>3</sub>N,” by **Paz Stein**, Ronen Bar-Ziv, and Maya Bar-Sadan of the Department of Chemistry, Ben Gurion University, and Department of Chemistry, Nuclear Research Center Negev.

The [full report](#) was published in the Israel Journal of Chemistry.



The Israel Chemical Society  
(ICS: [www.chemistry.org.il](http://www.chemistry.org.il))